

**Adaptive Signal Control and Coordination in Connected Vehicle Environment**

by

Jiangchen Li

A thesis submitted in partial fulfillment of the requirements for the degree of

Doctor of Philosophy

In

Transportation Engineering

Department of Civil and Environmental Engineering  
University of Alberta

© Jiangchen Li, 2021

# ABSTRACT

Existing signal control systems are usually based on traffic flow data from fixed location detectors. Because of rapid advances in the emerging vehicular communication, connected vehicle (CV)-based signal control demonstrates significant improvements over existing conventional signal control systems. Though various CV-based signal control systems have been investigated in the past few years, these approaches still have issues to overcome. These issues include sub-optimal results in low market penetration conditions, underperformance in both under-saturated and saturated traffic conditions, a lack of consideration for rapidly changing demand uncertainties, and expensive complex signal control systems architecture.

With this in mind, this thesis contributes to current research from three essential perspectives, including data, traffic model, and control strategy. More specifically, the contributions can be defined in the following ways: firstly, the issue of data quality is addressed with a proposed enhanced dynamic segmentation approach for the low penetration rate to obtain accurate traffic data; secondly, the traffic model is addressed by proposing a virtual cycle-based store and forward model (Vi-SFM) in addition to a dynamic parametric dispersion model for intersection and corridor level modeling, respectively; thirdly, the control strategy is addressed by proposing a model predictive control (MPC)-based framework for adaptive signal control and coordination, as well as a stability method, for a considerable scalable capability and good performance; finally, CV-centric in-the-loop testing prototypes for adaptive signal control and coordination are implemented.

Both field and simulation results from implemented CV-centric in-the-loop testing then validate the efficiency of these proposed methods in the CV environment, in which the proposed methods have shorter travel times for different approaches, different demands, and different

penetration rates than typical existing conventional signal control methods. In addition, both semi-closed loop control in 23 Ave. and closed-loop control in the South Campus are more efficient with lower travel times than non-CV-based open-loop control. Besides, simulation results of the proposed stable method indicate that high-frequency communication helps the MPC controller be more efficient with a faster convergency speed.

# PREFACE

## a. Refereed journal papers (published/accepted)

- [J5] **J. Li\***, C. Qiu\*(\*co-first author), M. Seraj, L. Peng, and T. Qiu: Platoon Priority Visualization Modeling and Optimization for Signal Coordination in Connected Vehicle Environment. *Transportation Research Record*, 2673(5): 36-48, 2019.
- [J4] **J. Li**, J. Gao, H. Zhang, and T. Qiu: RSE-Assisted Lane-Level Positioning Method for a Connected Vehicle Environment. *IEEE Transactions on Intelligent Transportation Systems*, 20(7): 2644-2656, 2019.
- [J3] **J. Li**, C. Qiu, L. Peng, and T. Qiu: Signal Priority Request Delay Modeling and Mitigation for Emergency Vehicles in Connected Vehicle Environment. *Transportation Research Record*, 2672(18): 45-57, 2018.
- [J2] S. He, **J. Li**, and T. Qiu: Vehicle-to-Pedestrian Communication Modeling and Collision Avoiding Method in Connected Vehicle Environment. *Transportation Research Record*, 2621(1): 21-30, 2017.
- [J1] M. Seraj, **J. Li**, and T. Qiu: Modeling Microscopic Car Following Strategy of Mixed Traffic to Identify Optimal Platoon Configurations for Multi-Objective Decision-Making. *Journal of Advanced Transportation*, p.7835010, 2018.

## b. Refereed conference papers in Transportation Research Board (TRB) annual meeting and World Congress on Intelligent Transport Systems (ITSWC) series (published/accepted)

- [C11] **J. Li**, L. Peng, and T. Qiu: *Real-time Predictive Signal Coordination based on Single-vehicle-triggered Platoon Dispersion in a Low Penetration Connected Vehicle Environment*. The TRB Annual Meeting, Washington, USA; 2021.
- [C10] **J. Li\***, C. Qiu\*(\*co-first author), M. Seraj, L. Peng, and T. Qiu: *Platoon Priority Visualization Modeling and Optimization for Signal Coordination in Connected Vehicle Environment*. The TRB Annual Meeting, Washington, USA; 2019.
- [C9] **J. Li**, and T. Qiu: *An Extended Time-Delayed V2X-Based Bi-Directional Looking Car-Following Model and Its Linear Stability Analysis*. The TRB Annual Meeting, Washington, USA; 2018.
- [C8] **J. Li**, C. Qiu, L. Peng, and T. Qiu: *Signal Priority Request Delay Modeling and Mitigation for Emergency Vehicles in Connected Vehicle Environment*. The TRB Annual Meeting, Washington, USA; 2018.
- [C7] **J. Li**, and T. Qiu: *Improving Throughput of a Signalized Intersection in a Connected Vehicle Environment*. The TRB Annual Meeting, Washington, USA; 2017.
- [C6] S. He, **J. Li**, and T. Qiu: *Vehicle-to-Pedestrian Communication Modeling and Collision Avoiding Method in Connected Vehicle Environment*. The TRB Annual Meeting, Washington, USA; 2017.
- [C5] M. Seraj, **J. Li**, and T. Qiu: *Real-Time Driving Behavior Recognition of Connected Vehicles for Advanced*

*Driver Assistance System: A Data-Driven Approach on Safety Pilot Model Deployment Program*. The TRB Annual Meeting, Washington, USA; 2019.

[C4] **J. Li**, J. Gao, H. Zhang, and T. Qiu: *A RSE-Assisted GPS-RSS Hybrid Lane-Level Positioning System for Connected Vehicles*. (Lectern), The TRB Annual Meeting, Washington, USA; 2016.

[C3]. **J. Li**, and T. Qiu. *Real-Time Predictive Signal Coordination Embedding Dynamic Platoon Dispersion in a Connected Vehicle Environment*. 27<sup>th</sup> World Congress on Intelligent Transport Systems, Los Angeles, USA, 2020.

[C2] **J. Li**, D. He, J. Zhang, and T. Qiu: *Leveraging the general transit feed specification real-time for traffic signal coordination in a connected vehicle environment*. 26<sup>th</sup> World Congress on Intelligent Transport Systems, Singapore, 2019.

[C1]. **J. Li**, and T. Qiu. *Improving throughput of an isolated signalized intersection in a connected vehicle environment*. 24<sup>th</sup> World Congress on Intelligent Transport Systems, Montreal, Canada, 2017.

### **c. Under review in refereed journals**

[J8] **J. Li**, K. Hou, L. Peng, and T. Qiu: *RSE Overlap-assisted Coordination Preservation for Emergency Vehicles along a Connected Vehicle-enabled Arterial Corridor*. *submitted*.

[J7] **J. Li** and T. Qiu: *Real-time Predictive Signal Coordination embedding Dynamic Platoon Dispersion in a Connected Vehicle Environment*. *submitted*.

[J6] **J. Li** and T. Qiu: *Fast Adaptive Signal Control for High-frequency Connectivity in Connected Vehicle Environments*. *submitted*.

### **d. Participation in selected important projects**

[P2] Tony Qiu. Clean Tech Connected Vehicle Applications with ACTIVE-AURORA. 2018.

[P1] Tony Qiu. ACTIVE Component in Edmonton of ACTIVE-AURORA Test Bed, Phase one and two. 2015.

# ACKNOWLEDGEMENTS

First and foremost, I owe my deepest gratitude and sincere appreciation to my advisor, Dr. Tony Z. Qiu, for his careful supervision, guidance, patience, and encouragement on my research during the past several years. He is not only skilled at identifying essential and challenging theoretical research problems, but also an expert at his mastery of how the new theoretical models and methods can be implemented in the field to change real-world transportation systems. His wise guidance places great emphasis on extreme preciseness, attention to detail, sharp and distinct insights, hard work, and organization and provides deeply inspiring insight that has helped shape my research philosophy. In addition, I extend my genuine thankfulness to Dr. Qiu for providing financial support throughout my Ph.D. study program. He truly is a great advisor and an excellent life counselor.

I would also like to thank Dr. Tony Qiu, Dr. Karim El-Basyouny, Dr. Amy Kim, Dr. Jinfeng Liu, and Dr. Michael Buro for participating in my candidacy exam, and Dr. Tony Qiu, Dr. Karim El-Basyouny, Dr. Amy Kim, Dr. Jinfeng Liu, Dr. Michael Buro, Dr. Wei Victor Liu, and Dr. Behrouz Far for participating in my final exam. Their suggestions were extremely insightful, and their comments upon reviewing the thesis were highly constructive.

My thanks are also extended to my graduate colleagues and friends at the Centre for Smart Transportation at the University of Alberta for their support and help, especially Dr. Jie Gao, Dr. Liqun Peng, Dr. Kasra Rezaee, Dr. Hui Zhang, Dr. Xu Wang, and Dr. Gang Liu for research and project discussions and collaborations, to Chen Qiu, Mudasser Seraj, Kaizhe Hou, Xiangdong Kong, Fan Wu, Jerry Chen, Jerry Zhang, and Vishal Vadhada for their superior technical teamwork on many projects and field implementations, to Chenhao Wang, Difei He, Yuwei Bie, Huiyu Chen, Can Zhang, Andres Rosales, Mohammed Ahmed, Ai Teng, Hongzhi Miao, Shuxian

He, Dr. Yang (Naomi) Li, and Yunzhuang Zheng for daily study discussions and feedback, and finally to Dr. Sharon Harper, Aalyssa Atley, Alice da Silva, and Brant Coghlan for project communication and writing support. Their input at all levels has made my graduate experience a pleasurable and rewarding one.

Finally, I would like to own my most enormous love for my parents and younger brother, who have continually encouraged and supported me over the past several years. Without their endless encouragement and support, this thesis could not have reached completion.

# TABLE OF CONTENTS

<b>ABSTRACT</b> .....	<b>II</b>
<b>PREFACE</b> .....	<b>IV</b>
<b>ACKNOWLEDGEMENTS</b> .....	<b>VI</b>
<b>TABLE OF CONTENTS</b> .....	<b>VIII</b>
<b>LIST OF TABLES</b> .....	<b>XI</b>
<b>LIST OF FIGURES</b> .....	<b>XIII</b>
<b>LIST OF ABBREVIATIONS</b> .....	<b>XV</b>
<b>CHAPTER 1.INTRODUCTION</b> .....	<b>1</b>
<b>1.1 BACKGROUND</b> .....	<b>1</b>
<i>1.1.1 Connected Vehicles</i> .....	<b>3</b>
<i>1.1.2 Adaptive Signal Control</i> .....	<b>4</b>
<i>1.1.3 Traffic Signal Coordination</i> .....	<b>5</b>
<i>1.1.4 CV-based Adaptive Signal Control and Signal Coordination</i> .....	<b>6</b>
<b>1.2 PROBLEM DEFINITION</b> .....	<b>6</b>
<b>1.3 RESEARCH OBJECTIVES AND SCOPES</b> .....	<b>10</b>
<b>1.4 RESEARCH CONTRIBUTIONS</b> .....	<b>15</b>
<b>1.5 ORGANIZATION OF THE THESIS</b> .....	<b>17</b>
<b>CHAPTER 2.LITERATURE REVIEW</b> .....	<b>19</b>
<b>2.1 ADAPTIVE SIGNAL CONTROL</b> .....	<b>19</b>
<b>2.2 TRAFFIC SIGNAL COORDINATION</b> .....	<b>24</b>
<b>2.3 CONNECTED VEHICLE-BASED ADAPTIVE SIGNAL CONTROL</b> .....	<b>27</b>
<b>2.4 CONNECTED VEHICLE-BASED TRAFFIC SIGNAL COORDINATION</b> .....	<b>32</b>
<b>2.5 BIBLIOGRAPHIC ANALYSIS OF LITERATURE</b> .....	<b>36</b>
<b>2.6 DETAILED COMPARISON AND LIMITATION ANALYSIS</b> .....	<b>39</b>
<i>2.6.1 Data Comparison and Limitation Analysis</i> .....	<b>42</b>
<i>2.6.2 Model Comparison and Limitation Analysis</i> .....	<b>47</b>
<i>2.6.3 Control Strategy Investigations and Limitation Analysis</i> .....	<b>53</b>
<b>2.7 SUMMARY OF ISSUES</b> .....	<b>62</b>
<b>CHAPTER 3.METHODOLOGY</b> .....	<b>66</b>

<b>3.1 OVERVIEW .....</b>	<b>66</b>
<b>3.2 IMPROVED PLATOON-BASED HYBRID MODEL FOR CV-BASED TRAFFIC DYNAMIC MODELING .....</b>	<b>68</b>
3.2.1 <i>Enhanced Platoon-based Hybrid Model via Spatial Dynamic Segmentation .....</i>	69
3.2.2 <i>Dynamic Parametric Platoon Dispersion Model in Free-flow Region .....</i>	76
3.2.3 <i>Updated Merging Process in Slow-down Region via the Real-time Priority Request .....</i>	79
3.2.4 <i>State Evolution in the CV Environment.....</i>	80
3.2.5 <i>Priority-augmented Signal Dynamic Model.....</i>	82
3.2.6 <i>Updated Node Model based on Vacation Queueing Model .....</i>	84
<b>3.3 INTERSECTION-LEVEL PERFORMANCE FUNCTION FOR ASC AND CORRIDOR-LEVEL PERFORMANCE FUNCTION FOR COORDINATION .....</b>	<b>87</b>
3.3.1 <i>Extended Delay Function for the Adaptive Signal Control.....</i>	87
3.3.2 <i>Extended Performance Function considering Tuning Flows for Coordination .....</i>	88
<b>3.4 MPC-BASED REAL-TIME ASC AND COORDINATION .....</b>	<b>92</b>
3.4.1 <i>Proposed Framework of the MPC-based ASC and Coordination.....</i>	92
3.4.2 <i>Cycle Length and Split Optimization Module.....</i>	94
3.4.3 <i>Common Cycle Length Calculation .....</i>	95
3.4.4 <i>Offset Optimization Module with and without Identical Common Cycle Length.....</i>	96
<b>3.5 STABILITY SYNTHESIS OF THE MPC-BASED SIGNAL CONTROL .....</b>	<b>99</b>
3.5.1 <i>Abstract Model of the System Dynamics and the MPC Controller .....</i>	99
3.5.2 <i>Qualitative Synthesis: Infinite Horizon Optimization (IHO) Approximation .....</i>	100
3.5.3 <i>Stabilizing Control Scheme.....</i>	103
<b>CHAPTER 4.CONNECTED VEHICLE-BASED SIGNAL CONTROL IMPLEMENTATION AND EVALUATION PLATFORM .....</b>	<b>110</b>
<b>4.1 ACTIVE CONNECTED VEHICLE ENVIRONMENT .....</b>	<b>110</b>
<b>4.2 ON-SITE EVALUATION ENVIRONMENT FOR IN-THE-LOOP TESTS.....</b>	<b>114</b>
<b>4.3 DESIGN AND IMPLEMENTATION OF IN-THE-LOOP TESTS.....</b>	<b>117</b>
4.3.1 <i>An Overview of the In-the-loop Testing Prototypes.....</i>	117
4.3.2 <i>Laboratory Hardware-in-the-loop Platform for Basic Functioning Tests (Scenario A) .....</i>	118
4.3.3 <i>Field Hardware-in-the-loop Platform for One Major Approach Tests (Scenario B) .....</i>	120
4.3.4 <i>Complex Software-in-the-loop Platform for Comprehensive Traffic Tests (Scenario C)....</i>	124
<b>4.4 FIELD CV DATA DESIGN AND COLLECTION.....</b>	<b>126</b>
<b>CHAPTER 5.EVALUATION RESULTS AND ANALYSIS .....</b>	<b>129</b>

<b>5.1 RESULTS OF THE BASIC FUNCTIONING TESTS (SCENARIO A)</b> .....	<b>129</b>
<b>5.2 FIELD RESULTS OF ONE MAJOR APPROACH TESTS (SCENARIO B)</b> .....	<b>133</b>
<b>5.3 COMPREHENSIVE RESULTS OF COMPLEX CONDITIONS (SCENARIO C)</b> .....	<b>138</b>
<i>5.3.1 Results of the Proposed Adaptive Signal Control</i> .....	138
<i>5.3.2 Results of the Proposed Signal Coordination</i> .....	145
<i>5.3.3 Stability Synthesis Results</i> .....	149
<b>CHAPTER 6.CONCLUSION AND FUTURE WORKS</b> .....	<b>156</b>
<b>6.1 CONCLUSION</b> .....	<b>156</b>
<b>6.2 FUTURE WORKS</b> .....	<b>158</b>
<b>REFERENCES</b> .....	<b>160</b>

# LIST OF TABLES

TABLE 1-1. Summary of three conventional signal control systems.....	4
TABLE 1-2. Summary of research contributions and corresponding questions, chapters, and papers.....	17
TABLE 2-1. Fine classifications of adaptive signal control (ASC).....	22
TABLE 2-2. Classifications of signal coordinations in UTCSs.....	25
TABLE 2-3. Summary of the objective functions in the existing CV-based ASCs .....	29
TABLE 2-4. Fine classifications of the CV-based ASC.....	31
TABLE 2-5. Summary of the CV-based advanced signal coordination systems' research teams and outputs.....	33
TABLE 2-6. Fine classifications of the CV-based advanced signal coordination systems .....	34
TABLE 2-7. Summary of the CV-based ASC and advanced signal coordination systems.....	37
TABLE 2-8. Fine classifications of traditional (non-CV-based) and CV-based ASC.....	40
TABLE 2-9. Fine classifications of traditional (non-CV-based) and CV-based signal coordination.....	41
TABLE 2-10. Summary of the data comparisons and limitations for both the static and mobile sensor data.....	45
TABLE 2-11. Summary of studies targeting the low-penetration issue.....	47
TABLE 2-12. Summary of traditional UTCSs applied different traffic models.....	50
TABLE 2-13. Summary of traditional UTCSs using rolling horizon approach.....	57
TABLE 2-14. Summary of CV-based signal control systems.....	61
TABLE 3-1. Summary of the contributions corresponding to three basic components.....	67
TABLE 4-1. Summary of the collected field data.....	127

TABLE 5-1. Vehicle delay in the semi-closed-loop control ( 23 <sup>rd</sup> Ave.) .....	135
TABLE 5-2. Vehicle delay in the closed-loop control ( South Campus ).....	136
TABLE 5-3. Comparison of vehicle delays for fixed timing control, actuation control, and MPC-ASC (CV-mASC) in different penetration rate conditions, with demand type I: typical demand.....	143
TABLE 5-4. Comparison of vehicle delays for fixed timing control, actuation control, and MPC-ASC (CV-mASC) in different penetration rate conditions, with demand type II: large demand.....	144
TABLE 5-5. Comparison of vehicle delays for fixed timing control, actuation control, and MPC-Coordination (CV-mCoordination) in different penetration rates conditions, with demand type I: typical demand.....	146
TABLE 5-6. Comparison of vehicle delays for fixed timing control, actuation control, and MPC-Coordination (CV-mCoordination) in different penetration rates conditions, with demand type II: large demand.....	147

# LIST OF FIGURES

FIGURE 1-1. Three basic components of urban traffic control systems (UTCSs).....	3
FIGURE 1-2. A graphical statement for the signal control in a mixed CV environment, where there is an urban road segment with two adjacent signalized intersections.....	7
FIGURE 1-3. Research flow for the real-time adaptive signal control and coordination in the CV environment.....	13
FIGURE 3-1. Proposed CV-based adaptive signal control (CV-ASC) and coordination (CV-Coordination) framework in the CV environment.....	67
FIGURE 3-2. Dynamic segmentation-based improved hybrid model.....	68
FIGURE 3-3. (a) Rectangular platoon-based hybrid model (b) Vehicle dynamic when a phase at a boundary intersection is green.....	69
FIGURE 3-4. Platoon identification via the proposed single Bi-PCD.....	74
FIGURE 3-5. Dynamic parametric platoon dispersion model.....	77
FIGURE 3-6. Priority-augmented signal model for signal controllers in the CV environment....	83
FIGURE 3-7. The proposed vacation queueing model .....	85
FIGURE 3-8. Minimum platoon delay when the platoon encounters residual queue .....	89
FIGURE 3-9. Proposed framework of the basic MPC-based ASC and coordination.....	93
FIGURE 3-10. The offset variable between two adjacent signalized intersections.....	97
FIGURE 3-11. Different prediction horizon ranges of the FHO and IHO problems.....	101
FIGURE 3-12. Strategies for the infinite horizon optimization approximation.....	103
FIGURE 3-13. Principles of a two-step quasi-infinite horizon stabilizing scheme.....	106
FIGURE 4-1. Connected vehicle environment in the ACTIVE testbed .....	112
FIGURE 4-2. Locations of connected infrastructure along the test roads .....	116

FIGURE 4-3. An overview of the in-the-loop testing prototypes in the CV environment.....	117
FIGURE 4-4. An in-lab hardware-in-the-loop (HIL) prototype .....	119
FIGURE 4-5. Field implementation and closed-loop test in South Campus (Scenario B1).....	121
FIGURE 4-6. Field implementation and semi-closed-loop test in 23 <sup>rd</sup> Ave (Scenario B2).....	123
FIGURE 4-7. Complex software-in-the-loop prototype for comprehensive traffic scenarios....	124
FIGURE 4-8. Scenario design using the SIL test prototype.....	125
FIGURE 4-9. Standard communication message sets for field implementations.....	126
FIGURE 4-10. Practical flow and turning rates profiles.....	128
FIGURE 5-1. The connectivity performance of the study areas.....	129
FIGURE 5-2. Functioning results of the trajectories and phase intervals .....	130
FIGURE 5-3. Basic functioning test results.....	131
FIGURE 5-4. Field trajectory results ( 23 <sup>rd</sup> Ave. and South Campus )......	134
FIGURE 5-5. Simulation setup for complex conditions.....	138
FIGURE 5-6. Boundary estimations of the slow-down region for one approaching vehicle stream in one lane at three timestamps during a red phase.....	140
FIGURE 5-7. Results of delay comparisons for CV-mASC, where smaller is better.....	142
FIGURE 5-8. Simulation setup for the signal coordination in the ACTIVE testbed .....	145
FIGURE 5-9. The simulation scenario setup for the target intersection.....	149
FIGURE 5-10. Numerical results of the stabilizing synthesis algorithm.....	151
FIGURE 5-11. Performance comparison between the basic and stable MPC for different sampling times.....	152
FIGURE 5-12. Terminal regions and state trajectories for different sampling times.....	153
FIGURE 5-13. The faster convergence results enabled by the faster sampling frequency .....	155

# LIST OF ABBREVIATIONS

---

<b>Acronym</b>	<b>Definition</b>
AAWDT	Annual Average Weekday Traffic
ACS	Adaptive Control Software
ACTIVE	Alberta Cooperative Transportation Infrastructure and Vehicular Environment
AMBAND	Asymmetrical Multi-band
API	Application Programming Interface
ASC	Adaptive Signal Control
BSM	Basic Safety Message
CTM	Cell Transmission Model
CV	Connected Vehicle
CV-ASC	Connected Vehicle-based Adaptive Signal Control
DL	Deep Learning
DP	Dynamic Programming
DSM	Dispersion-and-Store Model
DSRC	Dedicated Short-Range Communications
FHO	Finite Horizon Optimization
GPS	Global Positioning System
HIL	Hardware-In-the-Loop
HMI	Human-Machine Interface
HZ	Hertz
IHO	Infinite Horizon Optimization
LP	Linear Programming
MAP	Map
MAXBAND	Max-band
MILP	Mixed Integer Linear Programming
MITROP	Mixed-Integer Traffic Optimization Program
MPC	Model Predictive Control
MULTIBAND	Multi-band

---

<b>Acronym</b>	<b>Definition</b>
NCHRP	National Cooperative Highway Research Program
NEMA	National Electrical Manufacturers Association
OBE	Onboard Equipment
OPAC	Optimization Policies for Adaptive Control
PAMSCOD	Platoon-based Arterial Multi-modal Signal Control with Online Data
PMSA	Predictive Microscopic Simulation Algorithm
RHODES	Real-time Hierarchical Optimized Distributed Effective System
RSE	Roadside Equipment
SAE	Society of Automotive Engineering
SCATS	Sydney Coordinated Adaptive Traffic System
SCOOT	Split, Cycle, and Offset Optimization Technique
SFM	Store and Forward Model
SIL	Software-In-the-Loop
SPaT	Signal Phasing and Timing
SRM	Signal Request Message
SUMO	Simulation of Urban MObility
TMC	Traffic Management Center
TOD	Time-of-Day
TraCI	Traffic Control Interface
TUC	Traffic-responsive Urban Control
UTCS	Urban Traffic Control System
V2I	Vehicle-to-Infrastructure
V2V	Vehicle-to-Vehicle
V2X	Vehicle-to-Everything

# CHAPTER 1. INTRODUCTION

## 1.1 BACKGROUND

The emerging improvements in recent wireless communication technology that have enabled vehicles to communicate with roadway infrastructure and with each other are collectively known as connected vehicle (CV) technology (*1*). CV technology features low latency, real-time data, high reliability, and high security in a high-mobility environment (*1*). It has developed rapidly for its potential to improve the mobility, safety, and environmental impact of traffic systems over the past few years (*2–9*). These three challenges, i.e., safety, mobility, and environment, are significant issues faced by modern transportation systems. The impact of these three issues includes significant economic loss, heavy casualties, as well as long-term adverse environmental damage in large urban areas (*10*).

To tackle these serious problems, urban transportation systems have relied heavily on various proposed urban traffic control systems (UTCSSs) over the last few decades (*1, 11–16*). Considering the complexity of urban transportation networks and performance dependency on different control types, both the choice and design of proper traffic signal control systems are important. Thus, there is a large body of literature that has investigated developments of the conventional traffic signal control systems, and most of their methods can be categorized into three strategies: fixed-time, actuated, and adaptive control (*1, 17*).

Within the current practice, fixed-time control systems typically create best-suited timing settings for different times of the day (TOD) determined by the

historical traffic data. This method assumes that the traffic demand remains fairly constant during the entire period of a particular timing plan. However, this assumption is seldom valid in realistic scenarios, causing the fixed-time strategy to demonstrate weak control performance (1).

Actuated control systems collect real-time traffic flows from fixed infrastructure-based detectors, e.g., loop detectors, and apply simple logics, including phase calls, green extension, and max out, to change the timing plans. However, these systems have proven to be sub-optimal because the simple logic is based on a set of pre-defined and static parameters (17, 18).

The existing adaptive signal control methods use real-time traffic data to predict future traffic flows and obtain optimal signal timing settings. Subsequent control decisions are based on defined maximal or minimal objective functions (1, 17). The adaptive signal control has been widely applied to urban arterial networks.

Furthermore, to provide smooth traffic flows and reduce the number of stops and delays along an urban corridor or multiple intersections, signal coordination systems have been proposed and implemented by synchronizing traffic signals along a corridor (19).

In summary, the existing literature (12–16) examines existing UTCSSs that generally consist of three essential components: data, traffic model, and control strategy, graphically represented in Figure 1-1 below.

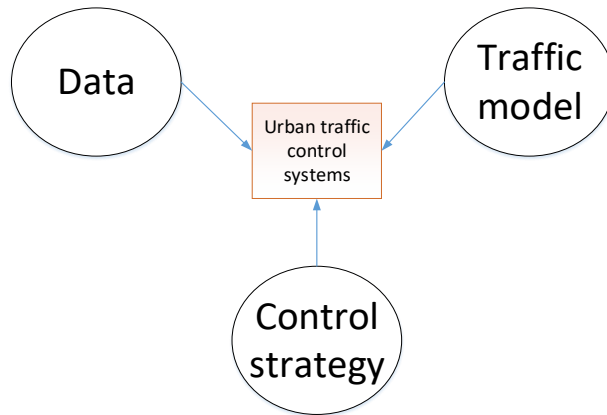


**FIGURE 1-1. Three basic components of urban traffic control systems (UTCSs).**

The data describes the spatial and temporal characteristics of the acquired data as input. The traffic model depicts the dynamics of traffic on the road links. The control strategy utilizes various timing plans to control traffic dynamics, for which standard signal variables include cycle length, split, and offset. Generally, every UTCS includes these three basic components, although not always in some of the early developed products.

Before discussing further details of the three basic UTCS components in the literature review, a brief background of different traffic control technologies is outlined here, thus introducing traditional and widely implemented traffic control systems in current transportation systems, i.e., adaptive signal control and traffic signal coordination. Also, briefly outlined in this chapter is the emerging CV technology, as well as updates of both enhanced adaptive signal control and coordination in the CV environment.

### **1.1.1 Connected Vehicles**

CV technology leverages vehicle-to-vehicle (V2V) and vehicle-to-infrastructure (V2I) communications based on dedicated short-range communication (DSRC). It

has been developing rapidly over the past few years, improving its efficiency, safety, and environmental benefits for traffic systems (2–9).

In addition, CV technology features low latency, real-time data, high reliability, and large security in a fast-mobility condition, which provides a new control dimension in solving the issues of signal control. For example, new real-time CV data, including connectivity indications, signal phase and timings, and vehicle trajectories, all extracted from basic safety messages (BSMs), are providing the potential for significant performance improvements.

### 1.1.2 Adaptive Signal Control

Conventional traffic signal control systems are classified into three strategies: fixed-time, actuated, and adaptive control (1, 17). Characteristics of these three signal control systems are summarized in the following Table 1-1:

Signal control	Data type	Traffic prediction	Control strategy
Fixed-time	Historical	N/A	Pre-defined timing plans
Actuated	Real-time	N/A	Simple logics
Adaptive	Real-time	Predictions by traffic models	Signal optimizations

**TABLE 1-1. Summary of three conventional signal control systems.**

Compared with both fixed-time and actuated signal control systems, the current adaptive signal control system utilizes real-time traffic data to forecast near-future traffic flow conditions. Subsequently, an optimal signal timing setting is obtained to make control decisions based on defined performance-based objective functions (2, 4). The adaptive traffic control system has been widely applied to urban arterial networks around the world since the 1970s because of its capability to respond to changes in traffic demand.

Different system architectures and algorithms for the adaptive traffic control system have been proposed and implemented during the last several decades. Typical examples of the adaptive signal control systems include SCOOT (Split, Cycle, and Offset Optimization Technique) (20), SCATS (the Sydney Coordinated Adaptive Traffic System) (21), OPAC (Optimization Policies for Adaptive Control) (22), RHODES (Real-time Hierarchical Optimized Distributed Effective System) (23), ACS-lite (15), and the recent MOTION system (24).

### **1.1.3 Traffic Signal Coordination**

Among various signal control strategies, traffic signal coordination is another significant and widely implemented strategy with enhanced performance measures (19, 25) to improve the mobility of arterial roads. Usually, the coordination system synchronizes traffic signals over the span of a corridor to provide signal progression for the approaching vehicle, thus reducing the number of stops and delays (19). Since the signal coordination control is recognized to perform better than other control strategies for corridors, a focus on coordination improvement is essential, indeed critical, for current urban transportation systems.

To enhance coordination systems, various methods have been proposed to achieve better performance (19) (26) (27). These approaches can be classified into two major types of optimization methodology (19): 1) advancement of the quality of progression, like the classical MAXBAND (26), and 2) optimization of a performance index, like the mixed-integer traffic optimization program (MITROP) method (27). For the former methodology, the objective is to maximize the green bandwidth along a particular arterial roadway. For the latter methodology, different

objectives are formulated to minimize performance indices like the number of stops, total delays, average travel times, or a combination thereof.

#### **1.1.4 CV-based Adaptive Signal Control and Signal Coordination**

Existing signal control systems are usually based on traffic flow data from fixed location detectors (1, 17, 19). Due to the rapid advances in the emerging vehicular communication, the CV-based signal control demonstrates significant improvements as compared to existing conventional signal control systems (1, 19, 28, 29). As a result, several CV-based adaptive signal control methods (1, 28, 30–32) and coordination approaches (19, 25, 33–37), aimed at improving the efficiency of adaptive and coordination systems, have been introduced in the past few years. They can be summarized into several categories: adaptive signal control methods aiming for an isolated signalized intersection, adaptive signal control methods for multiple signalized intersections, and signal coordination for multiple signalized intersections. Typical examples include PAMSCOD (35) and its variants (38), proposed in 2012 and 2014, respectively.

However, existing works on CV-based adaptive signal control and coordination methods still have outstanding issues (17, 19, 36, 39), and, therefore, the potential of CV technology in this domain warrants further study.

## **1.2 PROBLEM DEFINITION**

In this section, the problem definition of a real-time signal control consisting of both adaptive signal control (ASC) and signal coordination in the CV

environment is described in detail. The section also includes a research flow to provide the logic of an efficient solution for the problem.

As depicted in Figure 1-2, a vehicle platoon approaches a corridor with two signalized intersections and then passes through it. The vehicle platoon might encounter red lights at the signalized intersections and thus experience potential stop delays, thus increasing total travel time significantly. To mitigate stop delays, a CV-based adaptive signal control and coordination framework is deployed as a real-time and, therefore, efficient method.

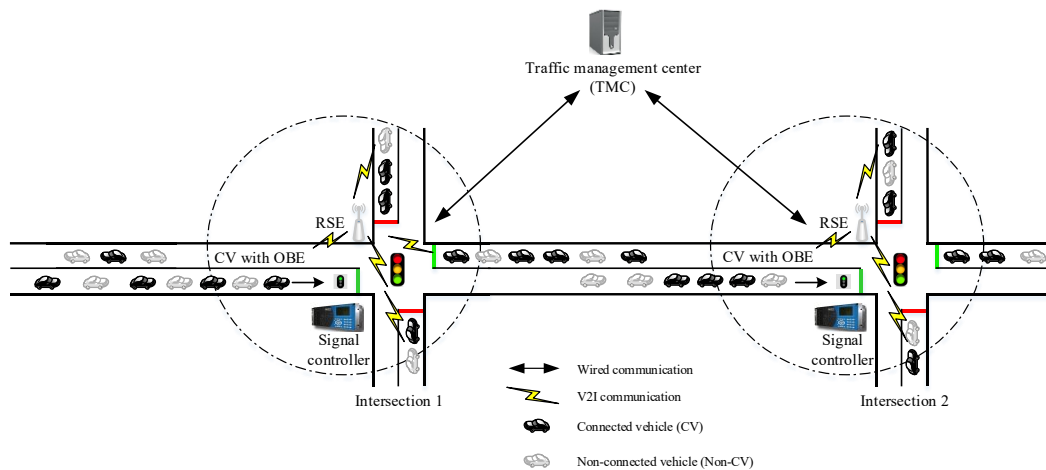


**FIGURE 1-2. A graphical statement of signal control in a mixed CV environment, with an urban road segment with two adjacent signalized intersections.**

In such a CV-based signal control framework, including both adaptive signal control and coordination, the critical real-time data transmission between the CVs and the connected roadside infrastructure, as well as the real-time control strategy, improves traffic control performance to be more flexible and efficient (19). These data generated from the CV technology can be categorized into two fundamental classes (25). The first class is the real-time CV data, including trajectories, motion data, and signal priority request data. The second class is the real-time infrastructure-based data providing signal phasing and timing (SPaT), the

roadway geometry, and current priority status data. These real-time data offer an opportunity to develop a new generation signal control using these real-time CV data. Thus, the full utilization of this highly valuable data could be further exploited to decrease the total travel time in the CV-based signal control framework.

In addition, with the rapid development of CV technology, an increasing number of vehicles will be equipped with On-board Equipment (OBE) and can operate the vehicle to infrastructure (V2I) technology. However, there will be a transition period over the next few decades where many existing and newly released vehicles will continue to lack OBE (40). Thus, the mixed traffic composition of CVs and non-CVs must continue to be assessed, and the potential negative impact of mixed traffic composition should be mitigated. Based on the literature review, key issues and corresponding questions requiring answers are summarized from three fundamental component perspectives as follows:

***(a) Data***

For data quality, two issues are apparent:

- 1) The low penetration rate condition will continue for many years before a critical threshold rate is reached that can take the use of CV technology to the next level of benefit (e.g., 20%-30% for traffic signal control (40)). This low penetration rate issue will continue to cause the loss of CV data and degrade the performance of the CV-based signal control framework (19, 36, 36, 41, 42). (Question 1, i.e., Q1)
- 2) The presence of a large number of non-CVs causes incomplete information, accumulates disturbances, and increases uncertainty when obtaining

optimal signal timings (17). Moreover, there are few proposed methods (1, 40) to estimate the state of non-connected vehicles from different perspectives (e.g., location, speed, acceleration). (Question 2, i.e., Q2)

The existing techniques that are aimed at solving these two issues in low-penetration conditions continue to demonstrate performance drawbacks.

***(b) Model***

3) Microscopic models in the existing CV-based ASC (1, 29, 43–55) and signal coordination (19, 25, 33–35, 39, 56) systems are suffering high computational costs with limited utility when the information is incomplete. (Question 3, i.e., Q3)

4) Though hybrid models combine advantages of two or more levels of the other models, none of the existing CV-based ASC and coordination systems are based on hybrid models. (Question 4, i.e., Q4)

***(c) Control strategy***

As for control strategies in a CV environment, the existing deployed control strategies usually use either the static or the dynamic optimization-based control strategy. There are several problems with these strategies, outlined below.

5) The existing CV-based signal control systems suffer from the original drawbacks of static and dynamic optimization-based control strategies. There are no existing CV-based ASC and signal coordination techniques based on the model predictive control (MPC) method. In particular, there are no existing designed

MPCs for non-congested arterials in the CV environment. (Question 5, i.e., Q5)

6) The low-penetration issue, the high frequency of data exchange, and the issues of microscopic models increase disturbances and fluctuations, which further cause more complexity when designing an MPC in the CV environment. For example, slow timing plan revision capability of the existing MPC-based control is not compatible with rapid, high-frequency data communication by V2V and V2I communication in the CV environment. (Question 6, i.e., Q6)

7) The performance of MPC-based traffic control systems can still be degraded by unpredictable demand variations and traffic disturbances on the road when using an open-loop optimization model of the MPC. (Question 7, i.e., Q7)

### **1.3 RESEARCH OBJECTIVES AND SCOPES**

In order to provide an efficient real-time CV-based adaptive signal control and coordination framework and resolve the outlined existing issues, several research objectives are investigated in this work. Those objectives are as follows:

#### ***(a) Data***

1) develop an updated CV-based data acquisition method for low penetration rates that feature broader spatial coverages, more detailed spatial and temporal data types, and lower installation and maintenance costs. The enhanced CV-based data acquisition method for low penetration rates can present enough spatial-temporal traffic characteristics and phenomena; (Scope 1-S1, corresponding to Question 1)

2) develop an enhanced estimation to capture the complexity of microscopic driving behaviours in urban areas and utilize this enhanced model to estimate the state of non-CVs from different perspectives (e.g., travel time, queue, lane, acceleration, speed, and location). The estimation method is a compensated data source to improve the performance of the CV-based ASC further and signal coordination. (Scope 2-S2, corresponding to Question 2)

***(b) Model***

3) design an updated traffic dynamic model for the intersection link level to decrease the sizeable computational effort and increase the availability of signal dynamics for adaptive signal control in the CV environment. (Scope 3-S3, corresponding to Question 1, Question 3, and Question 4)

4) design an extended traffic dynamic model for the corridor coordination level to decrease the sizeable computational effort and add the availability of signal dynamics for signal coordination in the CV environment. (Scope 4-S4, corresponding to Question 1, Question 3, and Question 4)

***(c) Control strategy***

5) propose a model predictive control (MPC)-based adaptive signal control and signal coordination for non-congested arterials in the CV environment. (Scope 5-S5, corresponding to Question 5 and Question 6)

6) develop an enhanced MPC-based signal control system in the CV environment, compatible with the rapid, high-frequency data communication in the

low penetration rate condition and have a stable performance in the short communication interval condition in the CV environment. (Scope 6-S6, corresponding to Questions 6 and 7)

7) the corresponding adaptive signal and coordination control-based prototype will be developed to implement and validate the efficiency of the proposed techniques. (Scope 7-S7, is corresponding to Question 1-7 here)

These research categories are shown in Figure 1-3, where three different categories are listed: 1) the objective on the left, marked in green, 2) research methodology down the middle, marked in blue, 3) and the corresponding CV technology component on the right, marked in purple. The details of these categories are further described in the next sections.

The objective category is abstracted to two points: one is the arterial performance monitoring, and the other is the adaptive signal control and coordination improvements. To achieve these objectives, real-time data, including typical SPaT, and vehicle trajectories, will be used as microscopic data input. Also, detector placement, actuation detection, and trajectory control techniques are involved in achieving final performance monitoring and improvements.

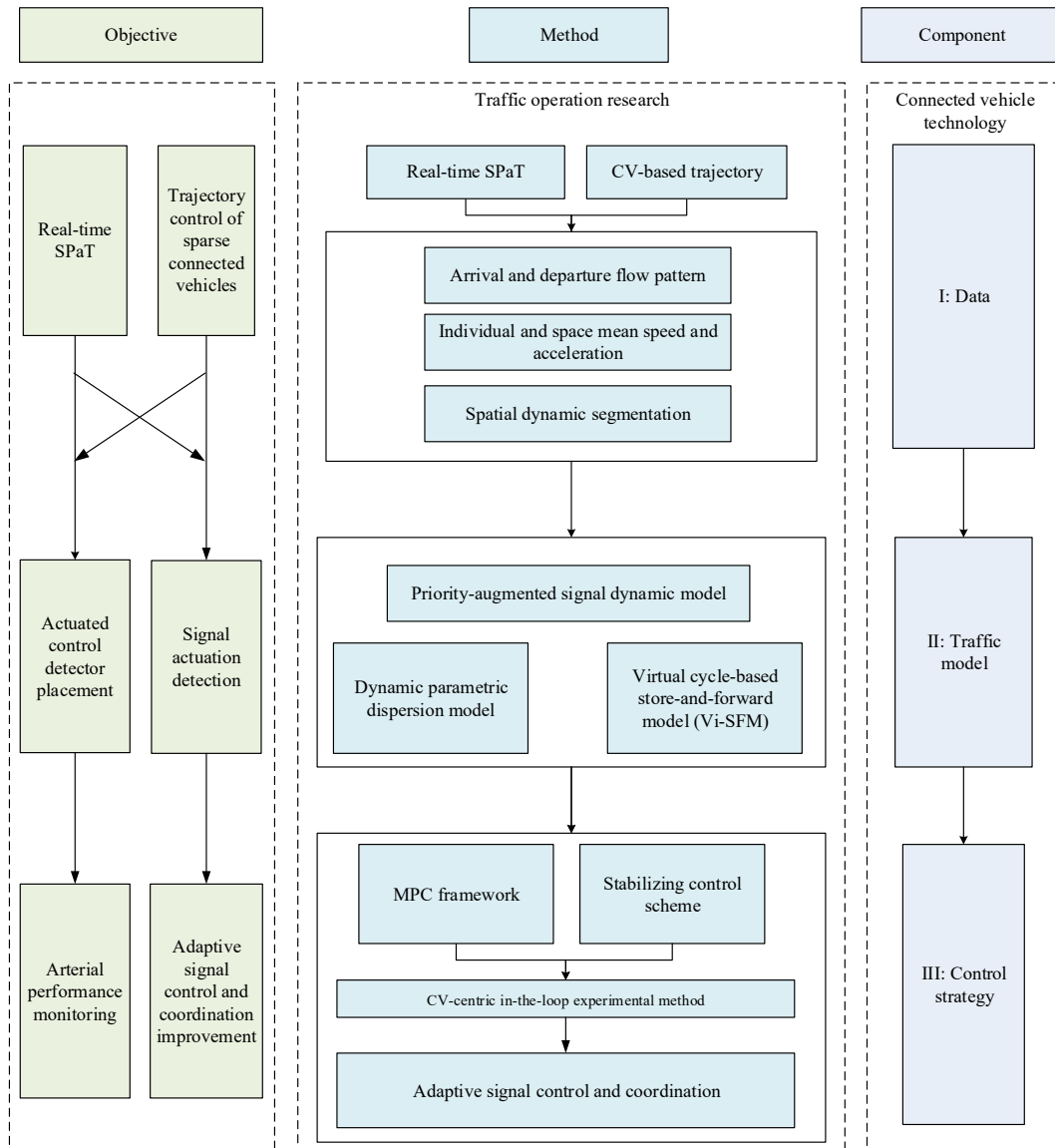


**FIGURE 1-3. Research flow for the real-time adaptive signal control and coordination in the CV environment.**

These three CV technology components: data, traffic model, and control strategy are marked as the purple boxes in Figure 1-3. With these CV technology components, the traditional corridor, associated infrastructure, and vehicles are connected with each other, resulting in the creation of a fully connected corridor. This full connectivity is obtained with the rapid implementations of CV technology.

The key is the research methodology shown in the middle of Figure 1-3. It has several steps: 1) real-time data acquisition and accurate traffic state estimation, 2) traffic prediction of flow dynamics by a hybrid traffic model, and 3) a control strategy for adaptive signal control and signal coordination.

Using data acquisition and state estimation, the complex traffic states are obtained using limited and incomplete information in low market penetration rate conditions. First, the real-time SPaT, roadway geometry (MAP), and vehicle trajectory data are obtained by V2I communication between a particular vehicle and the infrastructure. Then, this data is used to estimate the vehicle and traffic status, e.g., dense time-space diagram, arrival flow pattern, location, space mean speed, etc. (corresponding to CHAPTER 3.2.1 here).

After the estimation of the vehicle and traffic state, the traffic flow dynamics and interactions of different participators in this complex urban traffic system is apprehended through the hybrid traffic model. In this step, extended traffic models for intersection and corridor levels are developed to quantify the traffic flow dynamics along the whole corridor (corresponding to CHAPTER 3.2 and CHAPTER 3.3 here).

Then, the MPC-based control strategy for ASC and signal coordination is developed to minimize one or several performance indices, or a combination of them, in both under-saturated and saturated traffic conditions. Three major timing parameters are optimized: cycle, split, and offset for adaptive signal control and traffic signal coordination. (corresponding to CHAPTER 3.4 here)

Last, the corresponding CV-centric in-the-loop test prototypes are developed to implement and justify the efficiency of the proposed adaptive signal control and coordination in the CV environment. (corresponding to CHAPTER 4.2 and CHAPTER 4.3 here)

## **1.4 RESEARCH CONTRIBUTIONS**

The research contributions and the corresponding parts of the thesis presenting these contributions are shown as follows:

### ***(a) Data***

1) develop an enhanced dynamic segmentation approach in low penetration rate conditions by dividing the current approaching roadway into different smaller stretches. This approach helps to estimate the arrival flow pattern more accurately and in a timely fashion. (corresponding to CHAPTER 3.2.1, and Question 1 and Question 2 here)

### ***(b) Traffic model***

2) develop a virtual cycle-based store-and-forward model at the intersection level to reduce the high computational cost for the adaptive signal control. (corresponding to CHAPTER 3.2 and CHAPTER 3.3, corresponding to Question 1, Question 3, and Question 4 here)

3) develop a priority-augmented signal model at the intersection level to increase the availability of signal dynamics. (corresponding to CHAPTER 3.2 and CHAPTER 3.3, corresponding to Question 1, Question 3, and Question 4 here)

4) develop a dynamic parametric dispersion model at the corridor level to increase the availability of flow and signal dynamics in low penetration conditions. (corresponding to CHAPTER 3.2 and CHAPTER 3.3, corresponding to Question 1, Question 3, and Question 4 here)

***(c) Control strategy***

5) propose a MPC-based ASC and signal coordination for non-congested arterials in the CV environment. A framework of MPC-based ASC and coordination is proposed to optimize the signal control for multiple intersections. The CV sends real-time vehicle data, including the trajectories and motion data, to the roadside equipment (RSE). Then, RSE operation work includes two essential components: the intersection-level adaptive signal control and corridor-level coordination. After that, the traffic controller receives the final optimal signal output commands from the traffic controller interface to activate the optimal timings. (corresponding to CHAPTER 3.4, and Question 5 here)

6) develop an enhanced MPC-based signal control system in the CV environment, compatible with rapid, high-frequency data communication in low penetration rate conditions. A stability method is proposed to have a good scalable capability and performance. (corresponding to CHAPTER 3.4, and solving Question 1, Questions 6 and 7 here)

7) design and implement the CV-centric in-the-loop testing prototypes to validate the efficiency of the MPC-based adaptive signal control (ASC) and coordination in a CV environment. (corresponding to CHAPTER 4 and solving Questions 1-7 here)

These contributions are summarized in Table 1-2.

Component	Contributions	Related questions	Corresponding chapters	Related publications
Data	R1: A spatial dynamic segmentation	Q1, Q2	Ch. 3.2.1	J5, J6
Traffic model	R2: Virtual cycle-based store-and-forward model	Q3, Q4	Ch.3.2 and 3.3	J6, J2, J4,
	R3: Priority-augmented signal dynamic model	Q3, Q4	Ch.3.2 and 3.3	J6
	R4: Dynamic parametric dispersion model	Q3, Q4	Ch.3.2 and 3.3	J7, J3, J8
Control strategy	R5: Proposed MPC-based ASC and coordination	Q5, Q6	Ch.3.4	J6, J7
	R6: Stabilizing control scheme	Q6, Q7	Ch.3.4	J6
	R7: CV-centric in-the-loop experimental method	Q1-Q7	Ch.4.2 and 4.3	J6, J7, J8

**TABLE 1-2. Summary of research contributions and corresponding questions, chapters, and papers.**

## 1.5 ORGANIZATION OF THE THESIS

The remainder of this proposal is organized into five additional chapters, not including the introductory chapter. Chapter 2 shows a comprehensive review of the research literature on adaptive signal control, signal coordination, CV-based adaptive signal control, and CV-based signal coordination. Chapter 3 outlines the

proposed methodology with a two-level dynamic modeling and control strategy framework outlined in sub-chapters. Sub-chapter 3.2 presents improved intersection and corridor levels modeling of traffic dynamics. Sub-chapter 3.3 demonstrates the model's performance functions. Sub-chapter 3.4 introduces an MPC-based control strategy. Chapter 4 charts field setups, in-the-loop testing prototype designs, and implementations. Chapter 5 presents field and simulation results as well as the corresponding analysis. Chapter 6 discusses the conclusions and suggested future work.

## **CHAPTER 2. LITERATURE REVIEW**

This chapter engages in a comprehensive review of existing urban traffic signal control methods, including the following points:

1. Adaptive signal control,
2. Traffic signal coordination,
3. Connected vehicle-based adaptive signal control,
4. Connected vehicle-based traffic signal coordination,
5. Detailed limitation analysis of existing traditional ( non-CV- ) and connected vehicle- ( CV- ) based signal control systems that considers three fundamental components. These three components are data, traffic model, and control strategy, previously outlined in Figure 1-1.

A summary of issues closes this chapter.

### **2.1 ADAPTIVE SIGNAL CONTROL**

The adaptive signal control uses real-time traffic flow data to predict future traffic flow conditions, then generates an optimal signal timing plan. There have been numerous adaptive signal control systems proposed and developed over the past several decades. From the surveys in Stevanovic (15, 16), there are more than 20 implemented urban adaptive traffic control systems. Ten of the most widely implemented urban traffic control systems (UTCSs) are reviewed and analyzed in detail in the published NCHRP (National Cooperative Highway Research Program) report (15).

In the following discussion, various ASC systems, including SCOOT (20), SCATS (21), are examined in detail to understand their system architectures and algorithms based on performance indices. Then a summary of these systems is given in a table to distinguish them using several different metrics.

The SCATS (21) utilizes a subsystem consisting of several adjacent intersections that is a centralized signal control system. Each near subsystem can be joined together to build one larger subsystem, or divided to build smaller subsystems. Each intersection of one subsystem is controlled by an actuated signal control system. The changes in the cycle, split, and offset are based on heuristic algorithms without traffic models. The heuristic algorithm chooses one timing plan from several pre-defined timing plans to balance the saturation degree on each traffic approach. Only stop-bar detectors are required to record traffic occupancy and volume data when obtaining the saturation data.

SCOOT (20) utilizes a platoon dispersion model and an online optimization method to obtain a proper real-time signal timing setting, which is a hierarchical traffic control system. The delay minimization is implemented to change the current timing plan, in which three parameters are optimized: split, cycle, and offset. Before adjusting the current signal timing plan, the signal timing is used as a fixed timing plan. Upstream and advanced detectors are required to obtain traffic counts, residual queues, and lower bounds of queues, respectively.

Other UTCSs worth mentioning include the following. OPAC (22) is a real-time signal optimization system based on dynamic programming (DP). The

deployed DP-based optimization model minimizes delays over a finite future prediction horizon and eventually can be used for a coordinated network (57).

RHODES (23) is based on a hierarchical framework, where it has both an upper level determining the network flow control and a lower level minimizing the intersection level's performance indices. In the lower level, a rolling horizon scheme-based DP is proposed to achieve performance optimizations (58, 59). Both stop-bar and advanced detectors are required to predict an arrival table for an intersection-level control at the lower level.

ACS-lite (15) focuses on developing lower maintenance and installation costs and a deployable adaptive signal control system. The ACS lite system is composed of three control algorithms: a time-of-day (TOD) planner, a run-time refiner, and a transition controller (57). The TOD planner changes the current timing plan for different TODs and is responsive to existing traffic conditions. The run-time refiner determines the optimal time to change one timing plan to another. The transition controller determines the optimal transition strategy during the transition period.

Other recent adaptive signal controls include the MOTION system proposed by Brilon and Wietholt in 2013 (24), the FITS system introduced by Jin et al. in 2017 (60), and the Deep Learning (DL)-based system proposed by Gao et al. in 2017 (61). The MOTION ASC system (24) possesses typical architecture, and the system itself determines optimal timing plans at the global network level and utilizes the actuated signal control at the local intersection level (60). The FITS system (60) introduced an intelligent control system based on fuzzy logics to

optimize timing plan parameters. The DL-based system (61) proposed a deep reinforcement learning method-based system to automatically distill useful flow features from raw traffic condition data to obtain optimal timing plans. Considering the differences with respect to three key components discussed here, these ASC systems can be summarized into three categories: adjusted control, responsive control, advanced adaptive control (14)(15)(16)(62). This classification is shown in Table 2-1.

Category	Adjusted control	Responsive control	Advanced adaptive control
<sup>a</sup> Data quality: sensor density level (L)	L1 & L1.5, less than one sensor up to one sensor per link	static sensor data L2, one sensor per link up to one per lane	L3, two sensors per lane
<sup>a</sup> Responsive to demand variations	<b>slow reactive</b> response based on pre-calculated historical traffic flow	<b>prompt reactive</b> response based on changes in regularly disrupted traffic	<b>very rapid proactive</b> response based on short-term predicted movements
<sup>a</sup> Change frequency in control plan (HZ)	minimum of <b>15</b> minutes, usually several times at a rush period, (< 1/900 HZ)	minimum of <b>5-15</b> minutes, <b>per several cycles,</b> (< 1/300 HZ)	<b>continuous</b> adjustments are made to all timing parameters, <b>per several seconds</b> (< 1/5 HZ)
<sup>c</sup> Control strategy	pattern matching from pre-stored plans by <b>static optimization</b>	cyclic timing plan generating and matching via <b>static/dynamic optimization</b>	real-time timing adjusting via <b>dynamic optimization</b> and <b>optimal control</b>
<sup>a,b</sup> Generations of UTCSs (G)	G1 & G1.5 <sup>a</sup> , e.g., SCATS (21)	G2 <sup>a</sup> , e.g., SCOOT (20)	G3 <sup>b</sup> , e.g., OPAC(22), RHODES(23), ACS Lite (63)
Coordination included	mostly yes	mostly yes	yes

**TABLE 2-1. Fine classifications of adaptive signal control (ASC) (14) (15) (16) (62).**

<sup>a</sup> adopted from Klein et al. (14) and Stevanovic (15),

<sup>b</sup> summarized from Gartner et al. (62) and Wang et al. (16),

<sup>c</sup> identified in this report drawn from across a number of studies.

As shown in Table 2-1, all existing UTCSs are divided into the three outlined categories (14)(15)(16)(62). The more advanced the control system, the

higher the sensor density level and UTCS generation. At the same time, the responsive change frequency and control strategy are faster, higher, and more comprehensive. A detailed analysis of this is shown in the following Chapter ‘2.6 limitation analysis’.

As shown in Table 2-1, the traffic adjusted control uses both L1 and L1.5 sensor density levels, which means there is less than one sensor and up to one sensor per link. The responsiveness to demand is a slow reactive response with a minimum of a 15-minute change frequency. This kind of control system is categorized as UTCS G1 and G1.5. A typical, widely implemented example is SCATS.

Second, the traffic responsive control uses L2 sensor density level, which means there is one sensor per link up to one sensor per lane. The responsiveness to demand is prompt and reactive, with a minimum of a 5 to 15-minute change frequency. This type of control system is categorized as UTCS G2. A typical example is SCOOT.

Lastly, the advanced adaptive control utilizes L3 sensor density level, which means that there are **two** sensors per lane. The responsiveness to demand is rapid and proactive, with a several-seconds-level change frequency. This type of control system is categorized as UTCS G3. Typical examples include OPAC, RHODES, and ACS Lite.

However, there are two significant limitations related to data quality and sensor costs because the current ASC systems are mostly utilizing data from infrastructure-based sensors (17, 23) that include video-based and pavement-based

loop detectors. First, these infrastructure-based sensors are fixed-location sensors that are only providing the instantaneous individual vehicle data when a vehicle passes over the installation location. There is no spatial vehicle status, such as location, speed, and acceleration, provided by these point sensors. Second, the installation and maintenance costs of these point loop detectors are high. If any detectors are not working correctly, the performance of implemented ASC systems significantly degrades (17, 23). The additional disadvantages of control strategies are given in sub-chapter 2.6. Thus, a significant need to develop new advanced approaches to fix the two limitations is still present.

## 2.2 TRAFFIC SIGNAL COORDINATION

Among various signal control strategies, traffic signal coordination is another important and widely implemented strategy with enhanced performance (19, 25). Usually, the coordination system synchronizes traffic signals over the span of a corridor to provide signal progressions for approaching vehicles to reduce the number of stops and delays (19). Even though the coordination control performs better than other control strategies for corridors, it still needs improvement.

To enhance the performance of the signal coordination, various methods (27)(26, 64, 65)(66–71)(72–76)(77)(78)(79)(80)(81, 82)(83)(84) are proposed to achieve better performance measures. These approaches are classified into two categories of optimization methodology (19): **advancement of quality of progression**, like the classical MAXBAND (26), and **optimization of a performance index**, like using the mixed-integer traffic optimization program (MITROP) method (27). This is shown in Table 2-2.

Category	Adjusted control	Responsive control	Advanced adaptive control
<sup>a</sup> <b>Data</b> quality: sensor density level (L)			
<sup>a</sup> Responsive to demand variations			
<sup>a</sup> Change frequency in control plan		Same to Table 2-1	
<sup>c</sup> <b>Control strategy</b>			
<sup>a,b</sup> Generations of UTCSSs (G)			
Specific <b>control strategy</b> for <b>Coordination</b>	advancement of quality of progression, e.g., classical MAXBAND (26) and recent AMBAND (77)	optimization of a performance index, e.g., MITROP (27)	

**TABLE 2-2. Classifications of signal coordinations in UTCSSs (19).**

Regarding the first class, **improving the quality of progression**, many optimization methods have been tried by researchers to maximize green bandwidth along a corridor (26, 64, 65) (66–71) (72–76) (77). Little et al. (1964, 1966, 1981) proposed several mixed integer linear programming (MILP)-based models to synchronize traffic signals for maximizing the bandwidth along a corridor; these proposed methods were called the MAXBAND series (26, 64, 65). Many extensions of the MAXBAND were then proposed considering more traffic variables and phenomena. Two classes that showed significant improvement are MULTIBAND (66–71) and PASSER series (72–76). The MULTIBAND series was designed by Gartner and Stamatiadis et al. (1990, 1991, 1996, 1999, 2002, 2004) (66–71) to introduce the variable bandwidth progression considering dynamic changes in traffic volumes along a target corridor (19), while the PASSER series (progression analysis and signal system evaluation routine) proposed by Messer, Chang, and Chaudhary (1973, 1988, 1991, 1996) (72–76) further considered a

phase sequence optimization method and a queue clearance method for the bandwidth maximization via heuristic algorithms. Recently, an asymmetrical multi-BAND ( AMBAND ) model proposed by Zhang et al. (2015) extended the MULTIBAND to achieve a broader bandwidth by relaxing the requirement of the symmetrical progression band (77).

Regarding the second category, **optimization of a performance index**, various algorithms have been proposed to improve one or more performance measures (27)(78)(79)(80)(81, 82)(83)(84). These performance indices include delay, travel time, number of stops, and their combinations. Several examples of these methods are described below in order to illustrate their effectiveness and usefulness.

Early on, Gartner et al. (1975) developed the mixed integer traffic optimization program (MITROP) to minimize the platoon's average delays using a proposed platoon flow model and link performance function. The optimal offset values are determined by a piece-wise linear approximation of the platoon delay model (27). Then, the faster computation was achieved by Köhler et al. (2005) using an extended, simplified formulation of the original model (78). Hu and Liu (2013) recently developed an improved offset optimization method to minimize total delays using high-resolution loop detector data (79). Also, an individual vehicle travel times data-based method was presented by Shoup and Bullock (1999) to achieve optimal offset settings using vehicle re-identification equipment (80). Furthermore, a weighted combination function of the number of stops and the delay

is used by several widely recognized signal optimization tools to obtain optimal coordination plans (19) (81, 82) (83) (84).

However, since existing coordination systems are mostly based on fixed-location-based detectors and sensors, these sensors have two limitations related to data quality and sensor costs, as introduced above in sub-chapter 2.1 (19). Also, the limitations of traffic prediction models and control strategies are given in sub-chapter 2.6. Thus, improving signal coordination is crucial.

### **2.3 CONNECTED VEHICLE-BASED ADAPTIVE SIGNAL CONTROL**

Most of the existing ASC systems rely on traffic conditions from fixed-location-based detectors (1, 17, 19). Because of rapid advancements in emerging vehicular communication, CV-based signal control demonstrates significant improvements over existing conventional signal control systems (1, 19, 28, 29). As already highlighted, CV technology features low latency, real-time data, high reliability, and large security in a fast-mobility condition, thereby providing a new perspective to solve the issues of signal controls. The real-time data includes connectivity indication, transmitted SPaT data, and vehicle status data extracted from the BSM and other data. Thus, by utilizing the CV-based data, traffic signal control strategies are more dynamically reactive to real-time fluctuations and changes in traffic conditions.

Various CV-based adaptive signal control approaches have been proposed, and they are divided into two types regarding their applied scopes: one type applies to a single isolated signalized intersection, and the other type applies to multiple signalized intersections.

In terms of methods aimed at an isolated signalized intersection, they (1) (29) (43) (44) (45) (46) (47) (48) (49) (50) (51) (52) (53) (54) (55) are categorized into different types according to their different performance indices. These performance indices include delay, queue length, waiting time, travel time, or a combination of them.

Gradinescu et al. in 2007 (43) proposed an ASC based on an optimization model to decrease the average delay. Chou et al. in 2012 (44) presented a passenger feeling-based ASC to minimize passenger delays, as well as vehicle delays and stops. Nafi and Khan in 2012 (45) introduced an ASC to minimize average waiting time. Chang and Park in 2013 (46) proposed an ASC to reduce junction waiting times and queue lengths. Ahmane et al. in 2013 (47) presented an ASC to minimize queue lengths. Cai et al. in 2013 (48) developed a travel-time-based ASC using approximate dynamic programming (ADP) to reduce travel times. Pandit et al. in 2013 (49) proposed an ASC based on the oldest arrival first algorithm to minimize delays. Lee et al. in 2013 (50) presented a cumulative travel-time-based ASC to minimize cumulative travel times. Kari et al. in 2014 (51) developed an agent-based online ASC to minimize travel delays via the time of arrival prediction. Guler et al. in 2014 (29) proposed an ASC based on a discharging sequence to decrease the total delay and number of stops. Tiaprasert et al. in 2015 (52) presented a queue length estimation-based ASC to minimize queue lengths for both saturated and under-saturated conditions. Feng et al. in 2015 (1) proposed an ASC using an enhanced controlled optimization of phases algorithm (COP) and an Estimation of Location and Speed (ELVS) method of unequipped vehicles to minimize vehicle

delays or queue lengths. Younes and Boukerche in 2016 (53) presented a new ASC to minimize delays. Cheng et al. in 2017 (54) developed a Fuzzy group-based ASC to minimize average waiting time.

Author, year	Objective functions				
	delay	queue length	waiting time	stop	travel time
Gradinescu et al. in 2007 (43)	average delay				
Chou et al. in 2012 (44)	vehicle and passenger delay			stops	
Nafi and Khan in 2012 (45)			average waiting time		
Chang and Park in 2013 (46)		queue length	junction waiting time		
Ahmane et al. in 2013 (47)		queue length			
Cai et al. in 2013 (48)					travel time
Pandit et al. in 2013 (49)	delay				
Lee et al. in 2013 (50)					cumulative travel time
Kari et al. in 2014 (51)	travel delay				
Guler et al. in 2014 (29)	total delay			stops	
Tiapraser et al. in 2015 (52)		queue length			
Feng et al. in 2015 (1)	vehicle delay	queue length			
Younes and Boukerche in 2016 (53)	delay				
Feng et al. (25) in 2016	vehicle delay				
Islam et al. in 2017 (85)		queue length			
Liu et al. in 2017 (32)			average waiting time		
Cheng et al. in 2017 (54)			average waiting time		
Feng et al. in 2018 (55)	total delay				
Ban et al. (86) in 2018	delay				

**TABLE 2-3. Summary of the objective functions in the existing CV-based ASCs applied to both the isolated intersection and multiple intersections.**

Regarding proposed methods applied to multiple signalized intersections, they are described as follows (28) (40) (30): In 2013, Goodall et al. (28) proposed a

predictive microscopic simulation algorithm (PMSA) for the ASC. The algorithm obtains vehicle status data from CVs and inputs them into a microscopic-level simulation model to forecast near-future traffic flows. Then, a rolling horizon scheme with a 15s interval was deployed to optimize a combination of several performance indices, such as delays, stops, and accelerations. The status of unequipped vehicles was estimated based on the status of the CV (40). Considering the high computational costs of parallel simulations for the prediction process, this method cannot be used in real-time conditions (1). Also, the performance degraded in undersaturated conditions. In 2013, Maslekar et al. (30) presented a clustering algorithm to obtain optimal cycle lengths, green intervals, and other parameters by estimating the density of approaching vehicles. A modified Webster's model was deployed to calculate cycle length. Simulations presented that the proposed method reduced the average waiting times and the number of stops.

Also, though several research projects evaluated their models in both under-saturated and saturated traffic conditions in a CV environment (28, 35, 52), their performances could significantly decrease in both under-saturated and saturated conditions. To address saturated conditions, Christofa et al. (2013) (87) proposed queue spillback detection based on CV data then mitigated the queue spillbacks. In 2011, Venkatanarayana et al. (31) presented a signal control method using location and speed in the CV environment. The control strategy detected the real-time queue length at the downstream to responsively change splits at the upstream intersection. However, the method was only evaluated in a simple network.

Also, the use of recent machine learning and agent techniques to develop ASC for multiple intersections was demonstrated by Xiang and Chen in 2016 (88). Xiang et al. presented a multi-agent-based ASC. The intersection was modeled as an agent and was modeled by a Markov decision process. The signal control was optimized based on vehicle status, actions, and other parameters. However, this method did not consider the offset optimization in the CV environment, thus decreasing the effectiveness. Liu et al. (32) and Yang et al. in 2017 (89) developed reinforcement learning-based ASC systems to obtain optimal timing plans. However, both systems still require a proper coordination to run along a corridor.

According to differences with respect to three components, the existing CV-ASC systems are classified in Table 2-4.

Category	CV-based basic ASC	CV-based advanced ASC
	mobile sensor data	
<sup>a, c</sup> <b>Data</b> quality: sensor density level (L) and market penetration rate ( $P_{cv}$ )	L4 <sup>a</sup> , $P_{cv} = 100\%$ , i.e., 100 % market penetration rate	L3.5 <sup>c</sup> & L4 <sup>a</sup> , $P_{cv} < 100\%$ & $P_{cv} = 100\%$ , i.e., both non-full and full market penetration rate
	each connected vehicle (CV) regularly reports its location, speed, and possibly its destination <sup>a</sup>	
<sup>b</sup> Responsive to demand variations	<b>very rapid proactive</b> response based on short-term traffic predictions	
<sup>b</sup> Change frequency in control plan (HZ)	<b>continuous</b> adjustments, <b>per several seconds to per second (&lt; 1 HZ)</b>	
<sup>c</sup> <b>Control Strategy</b>	real-time timing adjustment via static optimization, dynamic optimization, and optimal control	
<sup>c</sup> Generations of UTCSS (G)	G4 <sup>c</sup> , e.g., work by Gradinescu et al. (43)	G4.5 <sup>c</sup> , e.g., PAMSCOD (35) and detector-free ASC (55)

**TABLE 2-4. Fine classifications of the CV-based ASC (14) (15) (62) (16).**

<sup>a</sup> adopted from Klein et al. (14), Stevanovic (15),

<sup>b</sup> summarized from Gartner et al. (62), and Wang et al. (16),

<sup>c</sup> identified in this report.

As shown in Table 2-4, the first significant difference of CV-based ASC as compared to previous traditional ASC systems is the emergence of mobile sensor data introduced by CV technology. The second difference is that the CV-ASC has a higher change frequency (i.e., less than 1 HZ) in the control plan because of recently developed control strategies. This higher change frequency gives the CV-ASC systems faster response times to the demand variations.

According to the differences of the data types, i.e., different market penetration rates, these existing CV-based ASC systems are classified into two types: 1) basic CV-ASC, and 2) advanced CV-ASC. The basic CV-ASC system can only work in 100% market penetration rate conditions, while the advanced CV-ASC system can perform well in both partial and full market penetration rate conditions. However, a significant issue is that the real-time ASC performance degrades in low market penetration conditions. In addition, there are limitations to the prediction models and control strategies, as given in sub-chapter 2.6.

## **2.4 CONNECTED VEHICLE-BASED TRAFFIC SIGNAL COORDINATION**

The limitations caused by the infrastructure-based detectors (19), coupled with the substantial benefits of CV technology, have prompted the rapid development of both the CV-based ASC and CV-based signal coordination.

Several recent CV-based coordination approaches (19) (25) (56, 33, 34, 39) (35) (36) (90) have been introduced, aimed at improving the efficiency of the coordination systems. These approaches are briefly outlined in Table 2-5 by author, country/region, and institution.

<b>Author, year</b>	<b>Country/region</b>	<b>Institution</b>
He et al. (35) in 2012	USA	University of Arizona
C.M. Day et al. (33) in 2016	USA	Purdue University
Li et al. (34) in 2016	USA	Purdue University
Feng et al. (25) in 2016	USA	University of Arizona
Beak et al. (19) in 2017	USA	University of Arizona and University of Michigan
C.M. Day et al. (56) in 2017	USA	Purdue University
Remias et al. (39) in 2018	USA	Purdue University
Zheng et al. (90) in 2018	USA, China	University of Michigan, Didi Chuxing LLC

**TABLE 2-5. Summary of the CV-based advanced signal coordination systems' research teams and outputs.**

Further, these proposed approaches can be classified into two types, **offline “detector-free” offset optimization method** and **online priority-based coordination**, shown in Table 2-6 below.

Category	CV-based advanced signal coordination systems	
	mobile sensor data	
<sup>a, c</sup> <b>Data quality:</b> sensor density level (L) and market penetration rate ( $P_{cv}$ )	L3.5 <sup>c</sup> & L4 <sup>a</sup> , $P_{cv} < 100\%$ & $P_{cv} = 100\%$ , i.e., both non-full and full market penetration rate	
<sup>b</sup> Responsive to demand variations	<b>slow reactive</b> response based on historic traffic flows	<b>rapid proactive</b> response based on short-term predicted movements
<sup>b</sup> Change frequency in control plan (HZ)	minimum of <b>15 min-3h</b> , ( $< 1/900$ HZ)	<b>continuous</b> adjustments, usually <b>per cycle</b> ( $< 1/100$ HZ)
Minimum $P_{cv\_min}$	0.1% for per 3 hrs change, 5% for per 15 mins change	25% for per cycle change
<b>Specific control strategy</b> of coordination	<i>offline</i> offset method, e.g., detector-free method (56, 33, 34, 39)	<i>online</i> priority-based method, e.g., adaptive coordination method (19) (25) (35)
<sup>c</sup> Generations of UTCSS (G)	UTCS G4.5 <sup>c</sup>	

**TABLE 2-6. Fine classifications of the CV-based advanced signal coordination systems (56, 33, 34), (19) (25) (35) (36).**

<sup>a</sup> adopted from Klein et al. (14), Stevanovic (15),

<sup>b</sup> summarized from Gartner et al. (62), and Wang et al. (16),

<sup>c</sup> identified in this report.

As shown above (Table 2-6), the first type is the so-called **offline “detector-free” offset optimization method** originated from C. M. Day et al. (56, 33, 34, 39). These researchers presented detector-free offset optimization studies, where CV data-based trajectories were used to generate “virtual detections”. Then, arrival profiles created by virtual detections were used to obtain signal offset optimization for signal coordination. Later, an extension model of this method was proposed to better determine coordination plans under low penetration rate conditions (36) by integrating similar historical automated vehicle location data. In 2018, Zheng et al. (90) proposed a method to utilize CV-based trajectory data to assess signal coordination quality, thus optimizing the traffic signals. However, the

current detector-free methods are not capable of real-time signal coordination control use (91), which means they do not feature CVs' real-time data.

The second type is an *online priority-based method*, which is shown in Table 2-6. This method has a higher frequency response to demand variations but requires a high market penetration, i.e.,  $P_{cv\_min} = 25\%$ . Feng et al. (2015) evaluated an online coordination with fixed offset values in a CV environment, where the coordination was integrated with an adaptive control algorithm in a high penetration rate situation (25). The model was then extended to optimize offsets along a corridor using a CV-based corridor-level optimization (19). However, the optimal common cycle length was determined offline by average flow data, which degenerates optimal effectiveness. Also, He et al. (2012) tested a platoon-based arterial signal control using the CV technology that included the dynamic signal coordination for both under-saturated and saturated traffic conditions (35). Within their method, they tried to obtain a multi-modal dynamical progression for significant platoons by considering existing queue delays. However, CV penetration rates significantly influence the positive performances of those CV-based algorithms discussed above, which presents a challenge (19)(25)(35). The prediction results are sensitive to market penetration rates because variations are largely yielded in low penetration rate conditions (19, 35).

Consequently, one problem is that the real-time coordination performance degrades with incomplete information in low market penetration conditions. In other words, achieving progressive improvements in online CV-based coordination methods with higher response frequencies in lower penetration rate conditions is

critical. Also, the limitations of prediction models and control strategies are given in sub-chapter 2.6.

## **2.5 BIBLIOGRAPHIC ANALYSIS OF LITERATURE**

In this subchapter, a bibliographic analysis of published papers is presented from the aspects of authors, institutions, and countries/regions. The results of this analysis are given in Table 2-7.

<b>Authors</b>	<b>Year</b>	<b>Country/ region</b>	<b>Institution</b>	<b>CV application</b>
Gradinescu et al. (43)	2007	USA	Rutgers University	CV-ASC
Chou et al. (44)	2012	China	National Central University	
Nafi and Khanin (45)	2012	Australia	The University of Newcastle	
Chang and Parkin (46)	2013	Korea	Korea University	
Ahmane et al. (47)	2013	France	Université de Technologie de Belfort-Montbeliard	
Cai et al. (48)	2013	Australia	University of New South Wales	
Pandit et al. (49)	2013	USA	University of California, Davis	
Lee et al. (50)	2013	USA	University of Virginia	
Kari et al. (51)	2014	USA	University of California, Riverside	
Guler et al. (29)	2014	Switzerland	ETH Zurich	
Tiapraseret et al. (52)	2015	USA	Texas A&M University	
Feng et al. (1)	2015	USA	University of Arizona	
Younes et al. (53)	2016	Canada	University of Ottawa	
Feng et al. (25)	2016	USA	University of Arizona	
Islam et al. (85)	2017	USA	Washington State University	
Liu et al. (32)	2017	China	Central South University	
Cheng et al. (54)	2017	China	Sun Yat-sen University	
Feng et al. (55)	2018	USA	University of Michigan	
Ban et al. (86)	2018	USA	University of Washington	
He et al. (35)	2012	USA	University of Arizona	
C.M. Day et al. (33)	2016	USA	Purdue University	
Li et al. (34)	2016	USA	Purdue University	
Feng et al. (25)	2016	USA	University of Arizona	
Beak et al. (19)	2017	USA	University of Arizona and University of Michigan	
C.M. Day et al. (56)	2017	USA	Purdue University	
Remias et al. (39)	2018	USA	Purdue University	
Zheng et al. (90)	2018	USA, China	University of Michigan, Didi Chuxing	

**TABLE 2-7. Summary of the CV-based ASC and advanced signal coordination systems \*.**

\* summarized from previous Table 2-3 and Table 2-5, where further details of the above notations are available.

The results in Table 2-7 are analyzed to express general research productivity information in three ways: 1) by year, 2) by country/region, 3) by institution.

1) *Year*. From Table 2-7, the paper count in the past three years is the largest, indicating that CV-based ASC and signal coordination systems have attracted significant interest from scholars who have produced substantial and positive developments in this area.

2) *Country/Region*. Table 2-7 shows the country/region statistics according to the paper count. The United States (USA) ranks at the top with the highest number of published research papers in this field. From this, it can be concluded that the USA is leading the research development of the CV-based signal control systems. Overall, there are nine countries/regions that have recently published research developments in this area, thus indicating that the interest in the CV-based signal control systems is developing in a broader international context.

3) *Institution*. Table 2-7 also reports the institutional affiliation with the literature outlined in this subsection. Remarkably, the top four institutions are all in the USA, including University of Arizona, Purdue University, University of Michigan, and the University of Washington. This result reinforces the conclusion that the leading role in developing the CV-based signal control systems is occupied by the USA.

## **2.6 DETAILED COMPARISON AND LIMITATION ANALYSIS**

As was shown in Figure 1-1, there are three basic components in the existing traditional (non-CV-) and CV-based (CV-) ASC and coordination systems:

1) data quality, 2) traffic model, and 3) control strategy.

Several of the previous tables are put together now to clarify significant differences among different non-CV- and CV-based ASC and signal coordination systems. The summarized tables are shown in Table 2-8 and Table 2-9.

Some rough descriptions for these existing systems from the three perspectives are given. After that, a detailed limitation analysis is presented.

Category	Non-CV-based Adjusted control	Non-CV-based Responsive control	Non-CV-based Advanced adaptive control	CV-based Basic ASC	CV-based Advanced ASC
	static sensor data			mobile sensor data	
<sup>a</sup> Data quality: sensor density level (L)	L1 & L1.5, less than one sensor up to one sensor per link	L2, one sensor per link up to one per lane	L3, two sensors per lane	L4 <sup>a</sup> , $P_{cv} = 100\%$ , i.e., 100 % market penetration rate	L3.5 <sup>c</sup> & L4 <sup>a</sup> , $P_{cv} < 100\%$ & $P_{cv} = 100\%$ , i.e., both non-full and full market penetration rate
<sup>a</sup> Responsive to demand variations	<b>slow reactive</b> response based on pre-calculated historical traffic flow	<b>prompt reactive</b> response based on changes in regularly disrupted traffic	<b>very rapid proactive</b> response based on short-term predicted movements	<b>very rapid proactive</b> response based on short-term traffic predictions	
<sup>a</sup> Change frequency in control plan (HZ)	minimum of <b>15</b> minutes, usually several times at a rush period, (< 1/900 HZ)	minimum of <b>5-15</b> minutes, <b>per several cycles, (&lt; 1/300 HZ)</b>	<b>continuous</b> adjustments are made to all timing parameters, <b>per several seconds (&lt; 1/5 HZ)</b>	<b>continuous</b> adjustments, <b>per several seconds to per second (&lt; 1 HZ)</b>	
<sup>c</sup> Control strategy	pattern matching from pre-stored plans by <b>static optimization</b>	cyclic timing plan generating and matching via <b>static/dynamic optimization</b>	real-time timing adjustment via <b>dynamic optimization and optimal control</b>	real-time timing adjustment via static optimization, dynamic optimization and optimal control	
<sup>a,b</sup> Generations of UTCSs (G)	G1 & G1.5 <sup>a</sup> , e.g., SCATS (21)	G2 <sup>a</sup> , e.g., SCOOT (20)	G3 <sup>b</sup> , e.g., OPAC (22), RHODES (23), ACS Lite(63)	G4 <sup>c</sup> , e.g., the work by Gradinescu et al. (43)	G4.5 <sup>c</sup> , e.g., PAMSCOD (35) and detector-free ASC (55)
Coordination included	mostly yes	mostly yes	yes	mostly yes	mostly yes
<b>Traffic model</b>	microscopic/ macroscopic/ mesoscopic models			mostly microscopic models	

**TABLE 2-8. Fine classifications of traditional (non-CV-based) and CV-based ASC \*.**

\* summarized from previous Table 2-1 and Table 2-4, where further details of the above notations are available.

Category	Non-CV-based Adjusted control	Non-CV-based Responsive control	Non-CV-based Advanced adaptive control	CV-based Advanced signal coordination systems
<sup>a</sup> Data quality: sensor density level (L)	L1 & L1.5,	L2,	L3,	mobile sensor data L3.5 <sup>c</sup> & L4 <sup>a</sup> , $P_{cv} < 100\%$ & $P_{cv} = 100\%$ , i.e., both non-full and full market penetration rate
<sup>a</sup> Responsive to demand variations				<b>slow reactive</b> response based on historical traffic flows
<sup>a</sup> Change frequency in control plan (HZ)		Same to Table 2-8		<b>rapid, proactive</b> response based on short-term predicted movements
<sup>c</sup> Minimum $P_{cv\_min}$				minimum of <b>15 min-3h</b> , ( < 1/900 HZ)
<sup>a,b</sup> Generations of UTCSs (G)				<b>continuous</b> adjustments, usually <b>per cycle</b> ( < 1/100 HZ)
Specific control strategy for Coordination	advancement of quality of progression, e.g., classical MAXBAND (26) and recent AMBAND (77)		optimization of a performance index, e.g., MITROP (27)	0.1% for per 3 hrs change, 5% for per 15 mins change
Traffic model	microscopic/ macroscopic/ mesoscopic models			25% for per cycle change
				G4.5 <sup>c</sup> ,
				<i>offline</i> offset method, e.g., detector-free method (56, 33, 34, 39)
				<i>online</i> priority-based method, e.g., adaptive coordination method (25) (19) (35)
				mostly microscopic models

TABLE 2-9. Fine classifications of traditional (non-CV-based) and CV-based signal coordination \*.

\* summarized from previous Table 2-2 and Table 2-6, where further details of the above notations are available.

There are several preliminary observations from these two tables. First, a data paradigm shift appears; the mobile sensor data almost replaces the traditional static sensor data. Also, new issues related to data quality emerge in the data paradigm shift when switching to the new mobile sensor data basis.

Second, the control strategies feature fewer delays and better real-time and efficient response performance over time, but they are becoming more complex. For example, the most advanced control methods are always adopted in the most recent CV-based signal control systems.

Lastly, various traffic models are widely used in both traditional ASC and signal coordination systems. These models include different major micro-/meso-/macroscopic models. On the other hand, traffic models included in the emerging CV-based ASC and signal coordination systems are mostly dependent on microscopic models.

The above discussions are summary descriptions of the existing systems from three perspectives: data, traffic model, and control strategy. A further detailed comparison and limitation analysis of them is given in the following sub-chapters.

## **2.6.1 Data Comparison and Limitation Analysis**

### ***(1) Analysis and limitation of static (fixed) sensor data***

As shown in Table 2-8 and Table 2-9, the traditional ASC and signal coordination systems are based on fixed location-based detectors with different sensor density levels (17, 23). These fixed location-based sensors include

video-based and pavement-based loop detectors. They generate static sensor data, including occupancy, flow data, and speed profiles.

However, there are several limitations to traditional fixed detector-based static sensor data related to data quality and sensor costs. First, these sensors are fixed-location detectors that only give instantaneous individual vehicle data when a vehicle passes through the installation location. There is no direct spatial vehicle data provided by these point sensors, such as location, speed, and acceleration.

Second, the installation and maintenance costs of these sensors are significantly high. These high installation and maintenance costs make re-installations and functional operations of detectors inefficient. Thus, if any detectors are operating inefficiently or incorrectly, the performance of the implemented urban signal control systems can significantly degrade to low levels (17, 23). Additionally, proactive information, like signal priority request commands, cannot be integrated into the static sensor data. This limitation can incur additional device installation and maintenance costs when implementing a priority-based traffic control, like transit priority control.

## ***(2) Analysis and limitation of mobile ( CV-based ) sensor data***

CV technology features low latency, real-time data, high reliability, and high security in a high-mobility environment. Each CV regularly broadcasts its position, speed, and possible destination. Thus, when compared to the static sensor's data quality and costs, it avoids the previous two limitations by its advantages of real-time spatial motion reports and low installation and maintenance

costs. More importantly, CV technology enables a vehicle to acquire SPaT data from signal controllers and issue a signal priority request to signal controllers, something beyond the capability of fixed sensors.

However, during the initial implementation stage of CV technology, not every vehicle is a CV. Consequently, the initial stage is characterized by a low market penetration rate situation that possesses two major drawbacks.

First, during the initial deployment stage, there are limited numbers of CVs on the road generating limited amounts of CV data. Consequently, the **limited CV data** volume degrades the performance of the CV-based signal control system (19, 36, 36, 41, 42).

Second, there are large numbers of non-CVs on the road at the same time. They are not connected, and their motion information is missing. This lack of **non-CV data** creates uncertainties for performance quality as well as large fluctuations and disturbances within the road traffic thereby increasing computation complexity when obtaining optimal timings (17). In addition, the high frequency of data exchange also increases data disturbances and fluctuations, thus adding to the complexity of the CV environment.

A summary of the above comparisons and limitations are given in the following table:

Data Type		Spatial-temporal property of traffic data	Cost*	Extra proactive data	Pros/Cons
Static sensor data		<b>instantaneous</b> data at fixed location	high	No	Cons
Mobile sensor (CV) data	Full penetration	complete spatial and temporal CV data, high frequency of data exchange	low	Yes, e.g., priority request data	Pros
	Low penetration	<b>limited</b> CV data large <b>missing</b> of non-CV data			Cons

**TABLE 2-10. Summary of the data comparisons and limitations for both the static and mobile sensor data.**

\* usually considering the installation and maintenance cost.

As shown in Table 2-10, the mobile sensor data outperforms the traditional static sensor data in three respects: 1) spatial-temporal property, 2) cost, and 3) the capability to provide extra proactive data. However, it still has two issues in low penetration conditions, which are the limited CV data and the missing non-CV data. These two issues need to be resolved in order to provide better control performance. Additionally, an exploration of the new method is also needed to utilize the extra proactive data fully.

### ***(3) Analysis and limitations of CV-based signal control systems in low penetration rate conditions***

Low penetration conditions cause two critical issues: 1) the limitations on CV data and 2) missing non-CV data. Some current research work aims to solve these issues in the CV environment and are discussed below.

*(a) Limited CV data.* Most of the existing CV-based ASC and signal coordination methods do not design unique methods to overcome this issue. Thus,

these widely accepted practical studies can only perform well with sufficient CVs, i.e., when the penetration rate is above a minimum penetration rate. Results of different minimum penetration rates ( $P_{cv\_min}$ ) are identified in many studies (33, 40, 55). There are few studies (19) (56, 33, 34, 39) (55) that worked at solving this problem. From 2016 to 2018, C. M. Day et al. (56, 33, 34, 39) proposed a detector-free coordination series based on historical limited CV data. However, their work was not implemented in real-time conditions. In 2017, Beak et al. (19) tested a stop-bar detector-assisted method to achieve adaptive coordination. In 2018, Feng et al. (55) presented a real-time detector-free CV-ASC using a probabilistic estimation model based on both a prior arrival distribution assumption and historical CV data. Thus, there is no applied method to solve this issue in low penetration conditions when considering real-time.

(b) *Missing non-CV data.* Similar to the concern of limited CV data, most of the existing CV-based ASC and signal coordination systems do not design specific methods to overcome this issue. A few researchers (1, 40) have tried methods that estimate the status of unequipped vehicles. In 2014, Goodall et al. (40) utilized a micro-simulation-based method to estimate non-CV locations, but it could not be applied in real-time. In 2015, Feng et al. (1) extended Goodall's method by proposing an estimation algorithm of the vehicle location and speed (EVLS) based on Wiedemann's model. However, Wiedemann's model still needs further extensions, and there is no field validation for this proposed method.

A summary of the existing contributed methods for these two issues is shown in Table 2-11.

Low penetration rate issue	Limited CV data issue	Missing of non-CV data issue	CV applications	Min $P_{cv}$
	Proposed methods			
Goodall et al. (40) in 2014	n/a	Micro-simulation-based estimation of the non-CV position	CV-ASC	10-25%
Feng et al. (1) in 2015	n/a	EVLS algorithm	CV-ASC	25-50%
C.M. Day et al. (56, 33, 34, 39) from 2016 to 2018	Historical limited CV data-based aggregation	n/a	detector-free coordination	5%, 15mins change
Beak et al. (19) in 2017	Stop-bar detector assisted method	n/a	adaptive coordination	25%
Feng et al. (55) in 2018	Probabilistic model based on both prior arrival distribution and historical CV data	n/a	CV-ASC	10%

**TABLE 2-11. Summary of studies targeting the low-penetration issue.**

In conclusion, the existing studies that are aiming at solving two issues in low penetration rate conditions have their drawbacks. Thus, research on this topic is still needed.

### 2.6.2 Model Comparison and Limitation Analysis

As shown in Table 2-8 and Table 2-9, the second observation is that various traffic models are used in the traditional ASC and signal coordination systems. These models include different micro-/meso-/macroscopic models.

However, models included in the emerging CV-based ASC and signal coordination systems are based mostly on microscopic models. The following contents give a brief review of existing traditional and CV-based signal control systems.

### ***(1) Microscopic models***

Microscopic models describe details of various components' behaviour that makeup moving traffic streams on the road (92–94). These components include vehicles, roadside controllers, static detectors, road geometry, and so on. The most widely used microscopic models are various car-following models and lane-change models.

However, there are several limitations to microscopic simulation models (92–94). First, the microscopic modeling of large participated components like vehicles introduces a large computational cost when simulating large arterial networks. The second is that the digital coding of the road surface network incurs substantial complexity and financial cost. Third, there is limited availability of the real-time control plans from modern controllers when requiring complete information. In particular, there is a lack of SPaT data dynamic descriptions. Last, it is challenging to obtain details of the fluctuations and disturbances from the surrounding traffic demands and traffic streams.

### ***(2) Mesoscopic models***

Mesoscopic models are usually identified to fill the gap between high-level aggregations of macroscopic models and high-level disaggregations of microscopic models and work at an intermediate level of detail (92–94). Typically, these popular mesoscopic models are classified into three types (92–94). The first type is the queuing approach for both freeways and signalized arterial roads. In this method, the queuing theory is introduced to model interaction between arrival

patterns and signal status. The second form is the cellular automata-based method. In this method, the road is discretized into cells that each vehicle can occupy based on specific rules. The last alternative groups individual vehicles into packets or cells. The packet or cell controls the aggregate individual vehicles.

However, due to high-level aggregated representations of traffic streams and road geometry in these mesoscopic models, dynamic behaviour of facilities cannot be accurately analyzed or replicated (92–94). Mainly, it lacks dynamic descriptions of the SPaT data. Also, large participating components like vehicles introduce huge computational costs when simulating big arterial networks.

### ***(3) Macroscopic models***

There are various macroscopic models that describe the moving traffic stream at a high level of aggregation as traffic flow (92–94). Macroscopic models are a widely used strategy within many UTCSSs. Various typical UTCSSs (15, 95–97) that applied different macroscopic traffic models from 1960s to 2010s are shown in following Table 2-12. These macroscopic models can be classified into three generalized as well as typical types: dispersion-and-store model (DSM), cell transmission model (CTM), and store-and-forward model (SFM).

Decade	Typical UTCSSs	Data <sup>a</sup>	Global optimization formulation and/or solution algorithm	Traffic model
1960s	TRANSYT in UK in 1968	Loop data	Domain-constrained optimization	DSM model (15)
	SCATS in Australia in 1979	SL, Loop data	Strategic and tactical control	Flow-delay profiles (15)
1970s	SCOOT in UK in 1979	US, Loop data	Domain-constrained optimization	Flow-occupancy profiles, DSM model (15)
	DYPIC in UK in 1974 (95)	US, Loop data	Backward dynamic programming (95), Rolling horizon approach	DSM model
1980s -1990s	OPAC in US in 1983 (15)	MB & SL, Loop data	Complete enumeration / exhaustive enumeration (98, 99), Rolling horizon approach	DSM model (15)
	RHODES in US in 1992 (15)	MB & SL, Loop data	Dynamic programming (98, 99), Rolling horizon approach (23)	DSM model (15)
	UTOPIA /SPOT in Italy in 1985 (15)	US & SL, Loop data	Online dynamic optimization and off-line optimization (95), Rolling horizon approach (100)	DSM model
	PRODYN in France in 1984 (95)	US, Loop data	Forward dynamic programming (98, 99), Rolling horizon approach (96)	DSM model
2000s	ACS-lite in US in 2003 (15)	US, Loop data	Domain-constrained optimization, three levels of optimization methodology	DSM model
	Aboudolas et al. in 2010 (96)	AL, Loop data	Quadratic programming, Rolling horizon approach	SFM model
	Liu and Qiu in 2016 (97)	US & SL, Loop data	Multi-objective optimization problem and an evolutionary algorithm	Extended SFM model
2010s	Hao et al. in 2018 (101, 102)	US, Loop data	Model predictive control-based method integrating optimizations	CTM model
	Han et al. in 2018 (103)	n/a	Linear quadratic model predictive control	Extended CTM model
	Lu et al. in 2019 (104)	n/a	Explicit model predictive control	SFM model

**TABLE 2-12. Summary of traditional UTCSSs applied different traffic models.**

<sup>a</sup> SL = stop-line, MB = mid-block, US = upstream, AL = arbitrary location, adopted from Stevanovic (15) and Aboudolas et al. (96).

(a) *Dispersion-and-store model (DSM) (105, 106)*. The DSM, originally proposed by Pacey in 1956 and Robertson in 1969 (105, 106), is an empirical observation mimicking both the platoon dispersion behaviour during a green signal

and platoon storage during a red signal. Usually, two forms are used for this modeling: a normal distribution form and a geometric distribution form. The geometric distribution form is also called Robertson's Platoon Dispersion Model (RPDM) and has been widely incorporated in many UTCSs, e.g., SCOOT (105, 106). However, the DSM cannot model real-time precise complex queue formulation and dissipation since the road segment between any two adjacent intersections is considered as one link. In addition, its adaptiveness to traffic fluctuations is difficult to calibrate (107).

(b) *Cell transmission model (CTM)*. The CTM proposed by Daganzo in 1994 (108) discretized the continuum of Lighthill and Witham's kinematic model (LWR) into multiple cells. In this case, the road network is represented by many small cells. One cell's vehicle dynamics are based on a transition process between two consecutive cells. In 2018, Hao et al. extended the CTM to an extended urban cell transmission model (UCTM) to obtain the average travel delays of the vehicles in the upstream approaches of each intersection (101, 102). However, the major disadvantage of CTM is that the fine discretization of the arterial network requires substantial computational complexity and sensor density. A shortage of sensors and limited computational capability significantly degrade the performance of CTM-based control methods (107).

(c) *Store-and-forward model (SFM)*. Gazis et al. originated the SFM model in 1965, which was extended by Aboudolas, Papageorgiou, and Kosmatopoulos in 2009 to model traffic dynamics in congested arterials (99). Similar to CTM, vehicles in the SFM model are either stored within the current link

in the red signal or forwarded to the next link in the green signal. The link dynamic is given by the conservation law. The most significant characteristic of the SFM is that the discrete time step  $T_k$  is equal to cycle length  $C$ , i.e.,  $T_k = C$  (107). This leads the model to describe a continuous (uninterrupted) average outflow from each link outside of the consideration for a queuing formulation or for dissipation due to a green-red switching mechanism (99). In other words, SFM has difficulty modeling real-time accurate complex queue formulations and dissipations, similar to the disadvantage of the DSM. This model only provides an efficient representation of the dynamics in congested networks.

In conclusion, the dynamics of facilities are not accurately analyzed and replicated (93, 94, 109), similar to the disadvantages of mesoscopic models with the high-level aggregated representation of the traffic streams and road geometry. For example, macroscopic models lack dynamic descriptions of the SPaT data. Also, DSM, CTM, and SFM have the difficulty with modeling real-time accurate complex queue formulations and dissipations. In other words, there is a problematic level of performance degradation because of queuing uncertainties.

#### ***(4) Hybrid models***

The hybrid models that combine advantages of two or more levels of the individual models, emerge as possible solutions (110). There are two major types: mesoscopic–microscopic models and macroscopic–microscopic models (94, 111). Usually, researchers aim to integrate the strengths of macroscopic or mesoscopic models (better modeling of large networks and easier calibrations) with

microscopic models (greater details and modeling control strategies capability) (94, 111). However, all of these studies are based on simulations that have extraordinary computational complexity. Consequently, existing research studies (94, 111) (110) are only suitable for offline verification and evaluation of different ITS and signal strategies rather than for real-time signal control use.

### ***(5) Models in CV-based ASC and coordination systems***

Most of the existing CV-based ASC (1) (29) (43) (44) (45) (46) (47) (48) (49) (50) (51) (52) (53) (54) (55) and signal coordination (19) (25) (56, 33, 34, 39), (35) (36) systems depend on microscopic models. Thus, they suffer the problems described above in the sub-chapter '*Microscopic models*'. One major issue is that performances degrade because of a shortage of sensors and computational capability.

To the best of our knowledge, none of the existing CV-based ASC and signal control systems are based on hybrid models. Thus, they cannot benefit from the advantages of the hybrid models.

### **2.6.3 Control Strategy Investigations and Limitation Analysis**

The second observation, as summarized in Table 2-8 and Table 2-9, is that the control strategies feature fewer delays, and better real-time and more efficient response performance over time whilst, at the same time, are becoming more complex. The responsiveness to demand has upgraded from a slow reactive response to rapid proactive response. The change frequency of the control plan is

evaluated to around 1 HZ for traditional advanced ASC and CV-based advanced ASC. As for the CV-based signal coordination, the offset is quickly adjusted at per cycle level.

What is apparent is that these adopted control strategies are becoming more complex over time. In this study, these control strategies are divided into three types: (1) static optimization-based basic control strategy (112), (2) dynamic optimization-based intermediate control strategy (112), and (3) model predictive control (MPC)-based advanced control strategy (113).

### ***(1) Static optimization***

A static optimization-based basic method refers to a method where a signal control system achieves an optimal timing plan by solving a static optimization problem. The word ‘*static*’ used in the term ‘static optimization’ means that objective functions and constraints are time-independent, where they are focusing on the current time step. Most of the existing methods (15) utilizing static optimization omit the word ‘*static*’. However, this thesis uses the term ‘static optimization’ to clarify and claim the time-independent characteristics of these methods. Usually, mathematical programming, e.g., linear programming (LP), mixed integer linear programming, is used for solving this static optimization.

This static optimization-based basic control strategy is used in various traditional adjusted control and responsive control systems, e.g., SCATS. Details of these systems can be found in the descriptions in sub-chapter 2.1. Furthermore, if no other feedback control methods ( e.g., rolling horizon method (96) ) are added, the static optimization-based method is an open-loop system without a feedforward

control. Consequently, it causes these control systems to have slow reactive responses with a slow change frequency to demand variations. This means that these systems are readily affected by traffic demand fluctuations and traffic stream disturbances.

Thus, the static optimization-based method has limited capability to optimize timing plans in high-dynamic conditions. The control performance is significantly affected by traffic demand fluctuations and traffic stream disturbances.

## ***(2) Dynamic optimization***

Compared to the basic control strategy using ‘*static optimization*’, ‘*dynamic optimization*’ is widely used in the intermediate control strategy and is a method whereby the decision variables of constraints involve sequences of decisions over time or multiple periods (112). In other words, it has a dynamic model, i.e., traffic model, as a constraint to describe traffic dynamics, whereby the traffic model can be either a microscopic, a mesoscopic, or a macroscopic model. The deployed traffic model predicts the future status of the traffic system. Usually, this type of control system is labeled as a *model-based control*.

Without adding other feedback control strategies (e.g., rolling horizon method (96)), this dynamic optimization causes the intermediate control strategy to be an open-loop system with a feedforward control. Thus, this intermediate control strategy performs better than the basic control strategy since it has a *prior* feedforward control and is adopted in most responsive control systems and

advanced adaptive control systems, as shown in tables 2-8 and 2-9. Typical examples include SCOOT (20), MOTION (24), BALANCE (15), ACS Lite (63), MOVE(15), OPAC (15), RHODES (15), UTOPIA (15), PYODYN (15), DYPIC (15), and Aboudolas et al. (96) amongst others.

In order to solve dynamic optimization problems, there are several proposed methods: (a) dynamic programming (DP), (b) rolling horizon approach, and (c) other intelligent approaches.

(a) *Dynamic programming (DP)*. Dynamic programming is a technique that can be used for solving many optimization issues over time (i.e., dynamic optimization) (107, 112). In most applications, DP breaks the original large-scale and complex problem into a series of small, solvable problems by Bellman's equation. DP has been used in some signal control systems, including OPAC V1 (15) and studies by Caceres et al. (114–117). However, the DP method has problems to overcome for the real-time control (95). In detail, the DP method requires complete future information for the optimization horizon, which is very hard to achieve in the real-time operation since the upstream sensor may only provide 5-10s future vehicle arrival data.

(b) *Rolling horizon approach*. The rolling horizon approach refers to a 'rolling planning horizon' that has a rolling mechanism with a planning horizon consisting of  $K_p$  time intervals (95, 107). The planning horizon has two portions: a head portion with first  $K_H$  time intervals and a remaining tail portion with next ( $K_p - K_H$ ) time intervals. The traffic status is updated by measured data during the head portion and predicted by traffic models during the tail portion. The dynamic

optimization is then solved during the whole planning horizon with the measured and predicted traffic status. Thus, a sequence of optimal control actions (e.g., split, offset) over the whole planning horizon is obtained. In practice, only the first optimal control action (95, 107) or a sequence of control actions over the head portion (98) is implemented. After that, a rolling mechanism is applied, in which the planning horizon moves forward into the future by one rolling period, and the above routine is repeated. Moreover, the rolling horizon approach introduces a feedback loop that further increases the system’s performance. Various traditional UTCSSs (15) (95) (96) (97) that have applied the rolling horizon approach are shown in Table 2-13.

Typical UTCSSs	Data <sup>a</sup>	Rolling horizon Approach	Global optimization formulation and/or solution algorithm
OPAC (15)	MB & SL, Loop data	Yes (15)	Complete enumeration (CE) / exhaustive enumeration (98, 99)
RHODES (15)	MB & SL, Loop data	Yes (23)	Dynamic programming (98, 99)
UTOPIA /SPOT (15)	US & SL, Loop data	Yes (100)	Online dynamic optimization and off-line optimization (95)
PRODYN (95)	US, Loop data	Yes (96)	Forward dynamic programming (98, 99)
DYPIC (95)	US, Loop data	Yes (95)	Backward dynamic programming (95)
Aboudolas et al. (96) in 2010	AL, Loop data	Yes	Quadratic programming
Liu and Qiu (97) in 2016	US & SL, Loop data	Yes	Multi-objective optimization problem and an evolutionary algorithm
Hao et al. in 2018 (101, 102)	US, Loop data	Yes	MPC-based method integrating optimizations, CTM model
Lu et al in 2019 (104)	Loop data	Yes	Explicit model predictive control (EMPC), SFM model
Jamshidnejad et al. in 2018 (118)	Loop data	Yes	Sustainable model-predictive control, S-model
Han et al. in 2018 (103)	Loop data	Yes	LQ-MPC, extended CTM, corridor

**TABLE 2-13. Summary of traditional UTCSSs using the rolling horizon approach.**

<sup>a</sup> SL = stop-line, MB = mid-block, US = upstream, AL = arbitrary location, adopted from Stevanovic (15) and Aboudolas et al. (96).

However, there is a concern that the rolling horizon approach does not always abide by the optimality principle if the parameter design (e.g., length of the projection horizon) is not well devised (107). The concern is that the rolling horizon approach causes a disadvantage where it degrades its performance in highly dynamic environments, especially in CV environments.

(c) *Intelligent approaches*. Intelligent approaches use other models that are not traffic models to update timing plans. There are two typical examples: the Fuzzy logic-based FITS system introduced by Jin et al. in 2017 (60), and the Deep Learning (DL)-based system proposed by Gao et al. in 2017 (61).

### ***(3) Model predictive control (MPC)***

A special advanced model-based control strategy called model predictive control (MPC) is considered in this section (100, 113). MPC is the most widely accepted modern control strategy to offer a compromise between optimality and computation speed (113). Generally speaking, MPC-based traffic control utilizes both a traffic model and the current traffic state to predict the dynamic evolution of traffic states, then applied to obtain optimal signals. An MPC controller includes several basic components, including a state estimation module, a state evolution model, and an optimization module (100), with further details of MPC outlined by Kouvaritakis and Cannon (113). It is widely recognized that MPC can further decrease the adverse effects of traffic disturbances (119).

Traffic controls that explicitly use MPC were originally proposed by Bellemans in 2003 (120) and Hegyi et al. in 2005 (121) for both ramp metering

(RM) and the variable speed limit (VSL) studies on freeways. In recent years, Hegyi et al. (100, 122), Papageorgiou et al. (119, 123), and Wang and Qiu et al. (124–127) further summarized, extended, and validated the MPC-based RM and VSL studies on freeways. Studies that focus on traffic signal controls that explicitly employ MPC focus on congested arterial networks include Dotoli et al. (128), Aboudolas et al. (99), Lin et al. (129), Liu and Qiu (107, 130), and Baldi et al. (131). Only few works explored performance in non-congested arterials (101, 102).

There are other traffic control systems (15) (95) that use similar schemes, shown in Table 2-13. These systems also obtain optimal signals by applying predictions and models, but they are not formulated and implemented explicitly to the MPC structure correspondingly (100). Thus, these systems cannot feature the benefits of MP without simultaneously solving their problems.

Although MPC shows good performance ability in RM and VSL control on freeways and signal control on congested arterials, several concerns arise concerning its capability on non-congested arterials. First, the traffic dynamic and signal mechanism are more involved in under-saturated arterials without a simplified traffic model, causing a lack of computational tractability. Second, the performance of traffic control systems can degrade from unpredictable demand variations and traffic disturbances on the road when using an open-loop prediction model of the MPC. The reason for the open-loop structure is that the nominal future demand and signal control variables are still functions of time.

#### ***(4) Control strategies in the CV environment***

Corresponding to the above classification, the existing control strategies in various CV-based signal control systems are categorized into the following approaches: (1) static optimization-based control, (2a) dynamic optimization-based control with the DP, (2b) dynamic optimization-based control with the rolling horizon scheme, (2c) dynamic optimization-based control with other intelligent approaches, and (3) MPC-based control. This classification is shown in Table 2-14.

Authors	Data	Rolling horizon Approach	Global optimization formulation and/or solution algorithm *	CV Applications
Gradinescu et al. (43) in 2007	online CV data	No	static optimization <sup>1</sup>	CV-ASC
Priemer et al. (132) in 2009		No	dynamic optimization with DP & Complete enumeration <sup>2a</sup>	CV-ASC
Lee et al. (50) in 2013		No	static optimization <sup>1</sup>	CV-ASC
Cai et al. (48) in 2013		No	dynamic optimization <sup>2c</sup>	CV-ASC
Pandit et al. (49) in 2013		No	dynamic optimization <sup>2c</sup>	CV-ASC
Kari et al.(51) in 2014		No	static optimization <sup>1</sup>	CV-ASC
Guler et al. (29) in 2014		No	dynamic optimization <sup>2c</sup>	CV-ASC
Younes et al. (53) in 2016		No	scheduling algorithm <sup>2c</sup>	CV-ASC
Islam et al. (85) in 2017		No	modified MILP <sup>1</sup>	CV-ASC
Liu et al. (32) in 2017		No	reinforcement learning <sup>2c</sup>	CV-ASC
PAMSCOD (35) and its variant (38) in 2012 and 2014, respectively		Yes	MILP <sup>2b</sup>	CV-ASC
Goodall et al. (28) in 2013		Yes (16)	dynamic optimization with rolling horizon <sup>2b</sup>	CV-ASC
Feng et al. (1) and its variant (55) in 2015 and 2018, respectively		Yes	hybrid structure <sup>2b</sup>	CV-ASC
C.M. Day et al. (56, 33, 34, 39) from 2016 to 2018	offline CV data	No	static optimization <sup>1</sup>	CV-based coordination
Priority-based method (25) (35) in 2016	online CV data	No	static optimization <sup>1</sup>	CV-based coordination
Beak et al. (19) in 2017	online CV data	No	static optimization <sup>1</sup>	CV-based coordination

**TABLE 2-14. Summary of CV-based signal control systems.**

\* 1 = static optimization-based control, 2a = dynamic optimization-based control with the DP, 2b = dynamic optimization-based control with the rolling horizon scheme, 2c = dynamic optimization-based control with other intelligent approaches.

From Table 2-14, the existing control strategies usually fall into the static

and dynamic optimization-based option. There are no existing studies based on the MPC. Therefore, the existing CV-based signal control systems suffer from the original drawbacks of these two control types, as outlined in subsection 2.6.3 (1) and (2). Furthermore, it cannot draw upon the benefits of the MPC. Finally, the high frequency of data exchange and the low penetration issue increases data disturbances and fluctuations. This causes more complexity when designing an MPC in the CV environment. In particular, the slow revision of timing plans in existing MPC-based controls is not compatible with the rapid, high-frequency data communication in the CV environment.

## **2.7 SUMMARY OF ISSUES**

Although there are many non-CV and CV-based ASC and signal coordination systems, problems, and issues arise in all. These issues are summarized as two types: 1) new issues introduced by the CV technology and 2) inherent drawbacks of the traditional signal control methods.

The above sub-sections gave a detailed analysis of these existing non-CV and CV-based ASC and signal coordination systems. For the sake of clarity, this thesis now provides a comprehensive summary of these systems.

### **□ A. Data**

There are three major limitations of the static sensor data obtained by the traditional fixed loop detectors.

(1) It only provides instant individual vehicle data when a vehicle travels through the fixed sensors and does not capture the spatial data.

(2) The maintenance and installation costs of the fixed-location sensors are significantly large. Also, unstable operation causes notably degraded performances.

(3) Proactive information, such as signal priority request commands, cannot be integrated into static sensor data.

There are several new issues of the CV-based mobile sensor data. Most significantly, the issues are caused by low market penetration.

(1) Limited amounts of CV data degrade system performance (19, 36, 36, 41, 42).

(2) Large amounts of missing non-CV data cause incomplete information and increase computational complexity (17).

(3) The high frequency of data exchange increases data disturbances and fluctuations, thus causing more computational complexity.

#### □ ***B. Traffic model***

Microscopic models introduce considerable computational complexity, and they have limited availability when requiring complete information. Specifically, they lack a dynamic description of signal status.

Macroscopic and mesoscopic models provide limited details due to the high-level aggregate representations when modeling the control and information systems. Most of the existing CV-based ASC (1, 29, 43–55) and signal (56, 33, 34, 39, 25, 19, 35) systems depend on microscopic models. Thus, they do suffer from

substantial computational complexity and provide limited information. And, although hybrid models combine the advantages of two or more levels of models, none of the existing CV-based ASC and signal coordination systems are based on hybrid models.

### □ *C. Control strategy*

Static optimization has limited capability to optimize the high-dynamic signals.

The dynamic programming-based control creates a real-time operation problem of complex dynamic systems, where it is tough to achieve in the real-time operation since the upstream sensor may only provide 5-10s future vehicle arrival data.

There is a concern that the rolling horizon method-based control does not always abide by the optimality principle if the parameter design (e.g., length of the projection horizon) is not well-conceived (107). That the rolling horizon approach degrades in performance within the high-dynamic environment, especially in the CV environment, is considered a disadvantage.

As for the MPC, there are several concerns about the capability of the MPC as applied to non-congested arterials.

(1) The traffic dynamic and signal mechanism are more complex in under-saturated arterials without a simplified traffic model than that in over-saturated traffic conditions.

(2) The performances of traffic control systems can degrade through unpredictable demand variations and traffic disturbances on the road when using an open-loop prediction model of the MPC. This is because the nominal future demands and signal control variables are still functions of time.

As for the control strategies in the CV environment, the deployed control methods usually fall into the static and dynamic optimization-based control strategies, as shown in Table 2-14. There are several problems with them:

(1) The existing CV-based signal control systems suffer the original drawbacks of these two control types.

(2) There are no existing studies based on the MPC in the CV environment, which means they cannot feature the benefits of the MPC. Currently, there are no MPC designed for non-congested arterials in the CV environment that are evident in the literature.

(3) The low penetration issue, high frequency of data exchange, and issues of microscopic models increase disturbances and fluctuations. They then cause further complexity when designing an MPC in the CV environment. For example, the slow timing plan revision capability of the existing MPC-based control is not compatible with high-frequency data communication in the CV environment.

Thus, considering that existing non-CV- and CV-based ASC and coordination systems continue to have issues to overcome, the potential of CV technology needs further study.

# CHAPTER 3. METHODOLOGY

## 3.1 OVERVIEW

As described in the above chapters, the proposed methodology has three components: 1) data acquirement, 2) traffic models for obtaining flow dynamics, and 4) control strategy using model predictive control (MPC) framework. Consequently, the proposed methodology includes two major parts, 1) traffic dynamic modeling, and 2) MPC-based traffic control strategy. This proposed methodology aims to solve the previously outlined Questions 1 to Question 7 that correspond to the research contributions from R1 to R7.

For the traffic dynamic modeling, the whole corridor is broken down into the intersection- and corridor-level segments. An improved platoon-based hybrid model is proposed to model the traffic dynamics. At the intersection-level, a virtual cycle-based store-and-forward model (Vi-SFM) and a priority-augmented signal model are proposed to analyze traffic dynamics at a signalized intersection. The corresponding cycle length and split are estimated. Then, at the corridor-level, a dynamic parametric dispersion model and an improved link performance function, are proposed to obtain optimal offsets for the signal coordination.

Then, the proposed CV-based ASC and coordination framework is shown in Figure 3-1. Figure 3-1 shows that the connected vehicle sends real-time BSM data, including trajectories and motion data, to the RSE. Then, the RSE operation includes the two basic components of intersection-level and corridor-level optimization. For the optimization, the common cycle length and split for

coordination phases are optimized at the first stage through an intersection-by-intersection strategy. Next, an offset optimization is used for corridor-level throughput improvements. After that, the traffic controller receives final optimization-based controller commands from the traffic controller interface, including three phasing operations, i.e., *vehicle call*, *force-off*, *omit*, and *hold-on*.

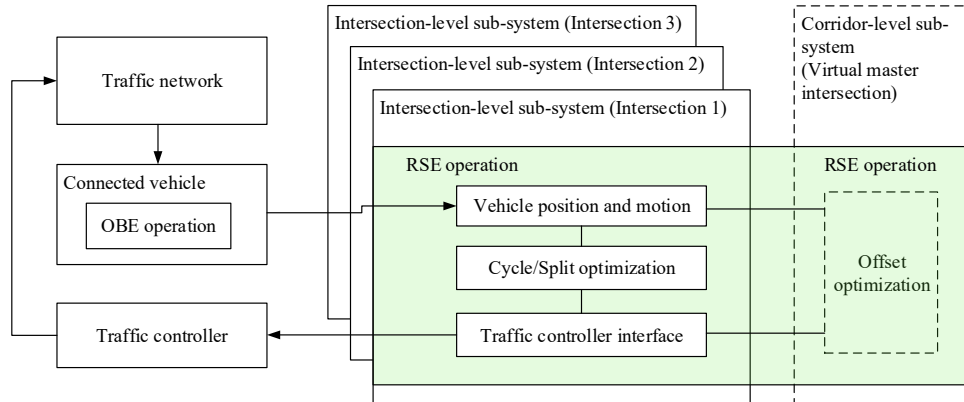


**FIGURE 3-1. Proposed CV-based adaptive signal control (CV-ASC) and coordination (CV-Coordination) framework in the CV environment.**

Finally, a summary of the contributions corresponding to three basic components is given in Table 3-1.

Component	Contributions	Chapter Index
Data	Spatial dynamic segmentation	Chapter 3.2.1
Model	Virtual cycle-based store-and-forward model, Dynamic parametric dispersion model, and Priority-augmented signal dynamic model	Chapter 3.2 & 3.3
Control strategy	CV-based MPC controller, Stabilizing scheme, and CV-centric in-the-loop experimental method	Chapter 3.4 & 3.5 Chapter 4

**TABLE 3-1. Summary of the contributions corresponding to three basic components.**

### 3.2 IMPROVED PLATOON-BASED HYBRID MODEL FOR CV-BASED TRAFFIC DYNAMIC MODELING

An improved platoon-based hybrid model is proposed consisting of two enhanced models: improved intersection-level and corridor-level dynamic models, as shown in Figure 3-2. It has two benefits. First, it can find good solutions to obtain traffic flow data through a platoon clustering method for intersection-level flow dynamics. Also, the signal dynamics are embedded in the CV environment. Second, it captures essential dispersion dynamics via the dynamic parametric dispersion model for the corridor-level flow dynamics. These two parts are introduced in detail in the following subchapters.

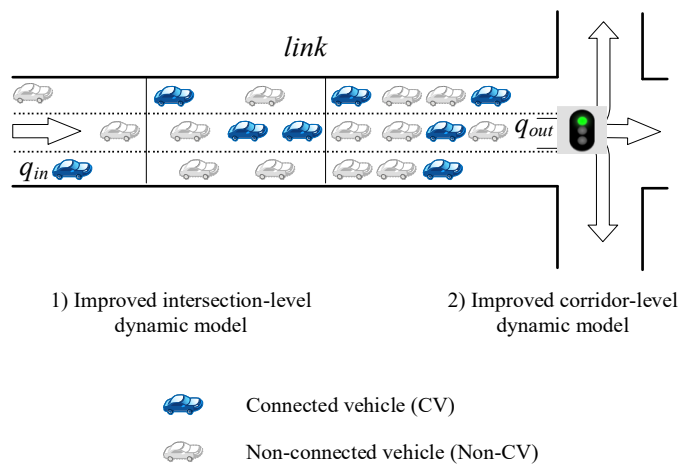
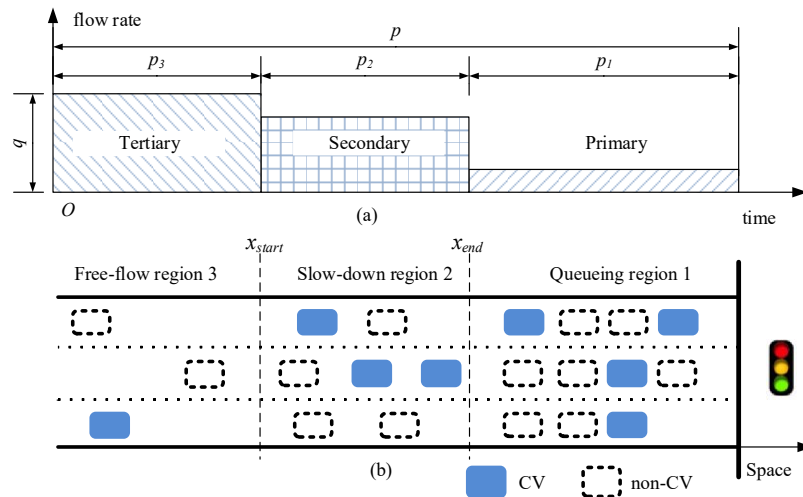


FIGURE 3-2. Dynamic segmentation-based improved hybrid traffic model.

### 3.2.1 Enhanced Platoon-based Hybrid Model via Spatial Dynamic Segmentation

The real-time CV data provides a new chance to mimic the ground truth of traffic states. Considering continuous arrivals of approaching vehicles, a dynamic segmentation approach-based enhanced platoon flow model is used to estimate dynamics and delays for vehicles, which is an extension of the previous method proposed by Feng et al. (1) and Beak et al. (19).

As shown in Figure 3-3(a), the platoon is described as a rectangular platoon model, which is constructed by length  $p$  (time, in seconds) and height  $q$  (flow rate, in veh/sec). In order to achieve the actual platoon length, the flow at the link is divided into three parts: *Primary*, *Secondary*, and *Tertiary* components. These three platoons correspond to three typical vehicle status when a coordinated vehicle stream is reaching a boundary intersection, shown in Figure 3-3(b).



**FIGURE 3-3. (a) Rectangular platoon-based hybrid model (b) Vehicle dynamic when a phase at a boundary intersection is green.**

The primary platoon component includes stopped vehicles from the stop bar in the queueing region. The secondary platoon is a vehicle platoon that is slowing down to join the primary region before the residual queue entirely dissipates. Lastly, the tertiary platoon component includes vehicles with a free-flow speed behind the secondary platoon component, but that leaves the upstream intersection before the end of the coordinated phase is green. Overall, the inputs of this modeling are the real-time CV and infrastructure data, including individual vehicle position, vehicle motion, and signal timing data. Details of these input data will be described inside each method correspondingly. Three techniques are developed here, which are 1) the dynamic segmentation method, 2) real-time state estimation, and 3) historical state estimation. They are introduced as follows.

1) *Dynamic segmentation method*. The first step is to find the positions of boundaries between any two adjacent regions to separate three regions. To find the boundaries, the start boundary (represented as  $x_{start}$ ) and end boundary (represented as  $x_{end}$ ) of the slow-down region should be calculated in Figure 3-3(b).

The slow-down region is calculated as follows,

$$l_{width} = \frac{1}{2} \frac{v_f^2}{a_{max}} \quad (3-1)$$

where  $v_f$  and  $a_{max}$  are the free-flow speed and maximum deceleration rate of the connected vehicle, respectively. Also, the length can be adjusted by the average and historical deceleration rate.

Then, the next step is to identify whether there is a CV in the slow-down region or not, which is represented by a variable  $\beta_{CViR}$ . Two conditions are used together to identify the state whether or not a vehicle is inside a slow-down region.

$$\beta_{CViR} = \begin{cases} 1, & \text{conditions} = \begin{cases} |a_t| > 0.1, & \text{condition 1} \\ v_{th1} < v_t < v_{th2}, & \text{condition 2} \end{cases} \\ 0, & \text{others} \end{cases} \quad (3-2)$$

where  $v_t$  and  $a_t$  are the current speed and deceleration rate of the connected vehicle, respectively. If both conditions are satisfied, the binary variable  $\beta_{CViR}$  is one; otherwise, its value is zero. This variable is only used in this method.

After that, how long one connected vehicle has traveled in the slow-down region is obtained as follows,

$$l_{elapsed} = v_f \cdot \frac{v_t^{cv}}{a_t^{cv}} - \frac{1}{2} \cdot a_t^{cv} \cdot \left(\frac{v_t^{cv}}{a_t^{cv}}\right)^2 \quad (3-3)$$

where  $v_t^{cv}$  and  $a_t^{cv}$  are the current speed and deceleration rate of the connected vehicle in the slow-down region, respectively.

Then, combining the previous equations, the start  $x_{start}$  and end  $x_{end}$  boundary are obtained as follows,

$$x_{start} = x_t^{cv} - l_{elapsed} \quad (3-4a)$$

$$x_{end} = x_t^{cv} + (l_{width} - l_{elapsed}) = x_{start} + l_{width} \quad (3-4b)$$

where the  $x_t^{cv}$  is the current position of the CV in the slow-down region.

2) *Real-time state estimation.* The next step is vehicle number estimation. After the boundary of each region is identified, which are used as inputs for this

method, the vehicle number within each of those regions is calculated accordingly and shown as follows,

$$N_1(t) = \text{round}\left(\frac{x_{end}}{l_{veh}}\right), \text{ for the queueing region} \quad (3-5a)$$

$$N_2(t) = l_{width} / h_{ave}, \quad \text{for the slow-down region} \quad (3-5b)$$

$$N_3(t) = \text{round}\left(\frac{N_{cv}}{P_{cv}}\right), \text{ for the free-flow region} \quad (3-5c)$$

where  $h_{ave}$  is the average space headway;  $l_{veh}$  is average vehicle length;  $N_{CV}$  is connected vehicle number;  $P_{CV}$  is the prior penetration rate of connected vehicles.

Then, the arrival flow is achieved by the above vehicle number inputs. The vehicle number of each region at time  $t$  is converted to the arrival flow  $q_{down}^{arrival}(t)$  for future signal control's performance index estimation. The derivation is shown in the following equation.

$$q_{down}^{arrival}(t) = \frac{N_1(t) + N_2(t)}{t - t_{red\_start}} \quad (3-6)$$

where  $t_{red\_start}$  is the timestamp when the signal starts red.

After that, the platoon information for each component is obtained. Then, the measured vehicle number  $N_1(t)$ ,  $N_2(t)$ , and  $N_3(t)$  is converted to each platoon length, respectively. For the low penetration condition, at least one vehicle on the road is required for the vehicle number aggregation.

The length and height of each platoon are calculated as follows. Because the uniform rectangular platoon is kept along the whole arterial, the platoon height  $q$  keeps the same for three components, which is equal to the saturation flow. This

means  $q = s$ , where  $s$  is the saturation flow. According to the conservation law, the platoon length for each component is shown as following:

$$p_1 = \frac{A(t)}{q} \quad (3-7a)$$

$$p_2 = \frac{B(t)}{q} + \frac{C(t)}{q_{turning}} \quad (3-7b)$$

$$p_3 = \left( g - \left( p_1 + p_2 - \frac{C(t)}{q_{turning}} \right) \right) \cdot \frac{f}{q} \quad (3-7c)$$

where  $A(t)$ ,  $B(t)$ , and  $C(t)$  is the total number of stopped vehicles in the queueing region, the total number of unstopped vehicles in the slow-down region, and the total number of turning vehicles from side streets merging to the slow-down region respectively;  $A(t)=N_1(t)$ ;  $B(t)=N_2(t)$ ;  $q_{turning}$  represents the flow rate of a turning flow from side streets;  $g$  denotes the green interval at the boundary intersection; and  $f$  represents the average arrival flow rate from the input link.

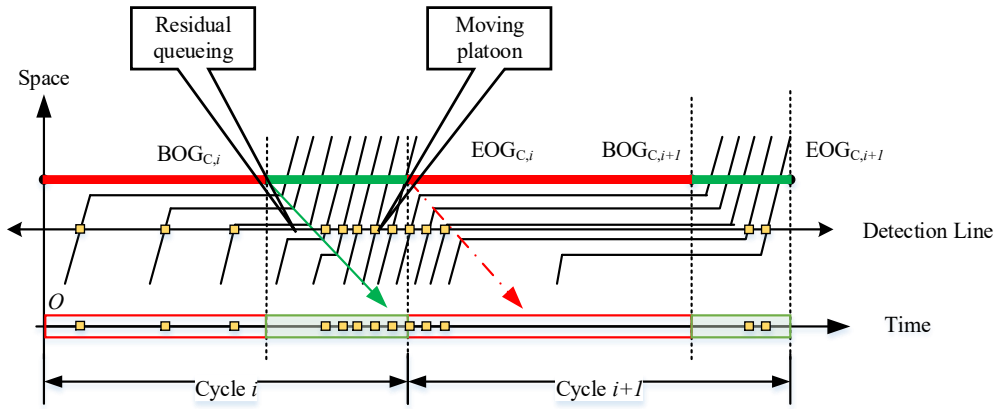
In this method, the flow conservation law is conserved for the signal control, which means that the inflows ( $N_{tot}$ ) of the total number of vehicles from both the major and the side street remains the same over the entire arterial corridor. Compared to the study in Beak et al. (19), inflows from the side street are further modeled in the flow equation.

3) *Historical state estimation.* For the historical state, a platoon-based bicyclic coordination diagram (Bi-PCD) approach <sup>1</sup> has been proposed. The extended platoon-based bicyclic coordination diagram approach is proposed,

---

<sup>1</sup> This sub-chapter includes an edited version of the article: [J5] J. Li\*, C. Qiu\*(\*co-first author), M. Seraj, L. Peng, and T. Qiu: Platoon Priority Visualization Modeling and Optimization for Signal Coordination in Connected Vehicle Environment. Transportation Research Record: Journal of the Transportation Research Board (TRR), p. 0361198119837505, 2019.

combining both the vehicle trajectories and signal timing data, to identify and estimate the platoon information.



(a) Time-space diagram and corresponding vehicle detection events

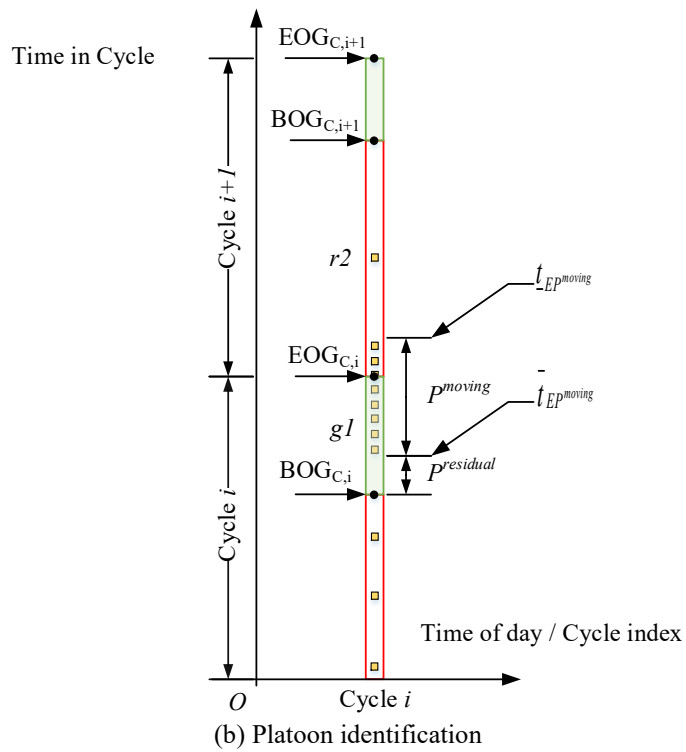


FIGURE 3-4. Platoon identification via the proposed single Bi-PCD.

As shown in Figure 3-4, the figure illustrates a time-space diagram and vehicle detection events for two consecutive cycles  $i$  and  $i+1$ , where the residual and moving platoon can be recognized. When the moving platoon departs from

upstream, the residual queuing platoon and the moving platoon are identified based on the threshold of the headway in the Bi-PCD. The headway-based method is widely justified and is usually named critical headway  $H_{critical}$  (35, 105, 133). Platoon parameters, such as the number of vehicles for the residual platoon  $N_p^{residual}$  and the moving platoon  $N_p^{moving}$ , are obtained and shown as follows:

$$N_p^{residual} = N(t_{BOG}^{detector}) - N(t_{BOR}^{detector}) \quad (3-8a)$$

$$N_p^{moving} = N_{g1+r2}^{threshold}, h_p > H_{critical} \quad (3-8b)$$

where,  $N(t_{BOG}^{detector})$  is the number of arrivals before  $t_{BOG}^{detector}$ ;  $N(t_{BOR}^{detector})$  is the number of arrivals before  $t_{BOR}^{detector}$ ;  $N_{g1+r2}^{threshold}$  is the number of arrivals during the green interval ( $g1$ ) and red interval ( $r2$ ). These numbers are calculated when the headway  $h_p$  is larger than the critical headway  $H_{critical}$ .

As shown in Equation (3-9b), the time length of the moving platoon  $EP^{moving}$ , and the estimated clearance time  $EP^{residual}$  of the residual queuing are further given as follows:

$$EP^{residual} = \min\left(\frac{N_p^{residual}}{S_{saturation}}, P^{residual}\right) \quad (3-9a)$$

$$EP^{moving} = P^{moving} = \bar{t}_{EP^{moving}} - \underline{t}_{EP^{moving}} \quad (3-9b)$$

where  $P^{moving}$  and  $P^{residual}$  are the estimated platoon length for the moving and residual queuing, respectively. Then  $\bar{t}_{EP^{moving}}$ , and  $\underline{t}_{EP^{moving}}$  are the leading and tailing vehicles' arrival time instants for the moving platoon, respectively. Furthermore, the moving platoon can be divided into a free-flow moving platoon

portion in the free-flow region and a moving platoon portion in the slow-down region. The proposed Bi-PCD utilizes minimum data during the last two cycles to estimate the platoon information.

By the above methods, the output is the real-time traffic flow of the current link. Further considerations of the platoon dispersion effects after the platoon passes the boundary intersection are described in the next sub-chapter.

### 3.2.2 Dynamic Parametric Platoon Dispersion Model in Free-flow Region

After the platoon characteristics are obtained, an extended dynamic platoon dispersion effect is depicted by updating the calibrated dispersion model proposed by Yu et al. (134). The inputs of this modeling are the real-time CV and infrastructure data, including individual vehicle position, vehicle motion, and signal timing data. The extended dynamic platoon dispersion model has the following mathematical formats:

$$q_{down}(t) = (1 - F) \cdot q_{down}(t-1) + F \cdot q_{up}(t-T) \quad (3-10)$$

$$F(t) = \frac{1}{1 + \alpha \cdot \beta \cdot t_a(t)} \quad (3-11)$$

where

$q_{down}(t)$  = downstream arrival flow rate for time interval  $t$ ,

$q_{up}(t)$  = upstream departure flow rate for time interval  $t$ ,

$T$  = lag time (i.e.,  $\beta \cdot t_a(t)$ ),

$F(t)$  = time-dependent smoothing parameter,

$\alpha$  = dispersion parameter,

$\beta$  = link travel time parameter,

$t_a(t)$  = time-dependent free-flow link travel time with respect to time  $t$ ,

These parameters are time-dependent variables, e.g.,  $F(t)$  and  $t_a(t)$ .

Compared to the previous platoon dispersion model proposed by Yu et al. (134), these time-dependent parameters better describe the dynamic platoon dispersion effects.

Equation (3-10) reveals that the traffic flow  $q_{down}(t)$  ( i.e.,  $q_{down}(t)=q_{down}^{arrival}(t)$  ), which is the arrival platoon at a given time interval  $t$ , is a weighted function of the downstream's arrival platoon during the last time interval  $t-1$  ( i.e.,  $q_{down}(t-1)$  ) and the upstream's departure platoon  $T$  seconds ago ( i.e.,  $q_{up}(t-T)$  ). Then, it is important to get the calibration of the basic parameters of  $\alpha$  ,  $\beta$  , and  $F(t)$ . These parameters are obtained by the CV data.

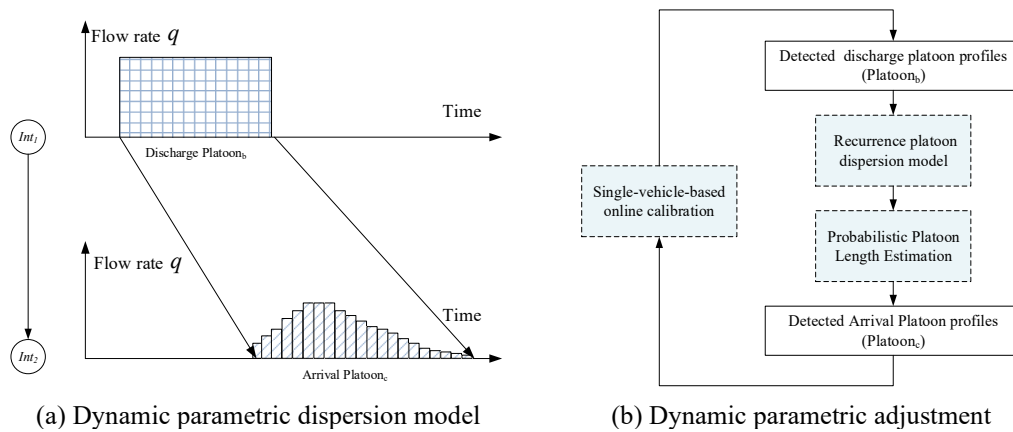


**FIGURE 3-5. Dynamic parametric platoon dispersion model.**

From the above process, the online calibration works accommodating data from a single CV. At the same time, the case with only a single CV is the worst case of the low penetration conditions. Also, unlike the work of Beak et al. (19), the platoon dispersion model is calibrated using real-time CV data rather than solely

reliance on historical travel time statistics. Thus, real-time performance is improved. As such, the proposed dynamic parametric dispersion model has the potential to perform well in both real-time and low penetration conditions. The outputs of the method are the adjusted vehicle platoon lengths and flow rates.

After that, the adjusted vehicle platoon lengths and flow rates are used as inputs for the link performance estimation in the next section.

### 3.2.3 Updated Merging Process in Slow-down Region via the Real-time Priority Request

When arriving at the slow-region area, vehicles may change their current lanes then merge into different groups in the slow-down and the queueing regions, with the merging behaviours mostly dependent on drivers' destinations. The inputs of this modeling are the real-time CV and infrastructure data, including signal priority data. The merging flow into lane group  $k$  at time step  $t_i$ , can be approximated as follows:

$$q_{merge}(t_i) = \beta_{turn}^{SRM}(k) \cdot q_{free-flow}^{up} \quad (3-12)$$

where  $q_{merge}(t_i)$  is the merging flow,  $q_{free-flow}^{up}$  is the upstream flow in the free-flow region ( i.e.,  $q_{free-flow}^{up} = q_{up}(t)$  ), and  $\beta_{turn}^{SRM}(k)$  is the dynamic turning ratio for each lane group, which is dynamically estimated by the signal priority request in the CV environment. In this section, two assisted techniques are used for estimating the dynamic turning ratio for each lane group. One is the signal priority request-based control, and the other is the lane-level positioning approach for estimating vehicles' lane groups. First is the priority request-based control <sup>2</sup>. A signal priority request-based cooperative control for emergency vehicles has been proposed in the CV environment. The signal priority requests an approaching phase by the standard J2735 message. Second is the lane-level positioning approach <sup>3</sup>. A RSE-assisted

---

<sup>2</sup> This sub-chapter includes an edited version of the article: [J3] J. Li, C. Qiu, L. Peng, and T. Qiu: Signal Priority Request Delay Modeling and Mitigation for Emergency Vehicles in Connected Vehicle Environment. Transportation Research Record: Journal of the Transportation Research Board (TRR), p. 0361198118774184, 2018.

<sup>3</sup> This sub-chapter includes an edited version of the article: [J4] J. Li, Jie. Gao, H. Zhang, and T. Qiu: RSE-Assisted Lane-Level Positioning Method for a Connected Vehicle Environment. IEEE Transactions on Intelligent Transportation Systems (IEEE T-ITS), 2019.

lane-level positioning method has also been proposed recently by us to obtain the lane number of one moving target vehicle. With the help of the lane-level positioning approach, the target vehicle should trigger the correct priority requests according to its current lane number. With the help of these two proposed techniques, the turning rate is more accurate than that offered in other existing studies (107). The output data is the turning rate data.

### 3.2.4 State Evolution in the CV Environment

Considering the flow conservation for traffic states, the state evolution of vehicle dynamics for current link  $z$  is derived as follows. The inputs are the traffic flows and signal status on the link and of the approaching intersection, respectively.

$$n(t+1) = n(t) + \Delta T_{step} \cdot [q_{up,z}^{in}(t) - q_{down,z}^{out}(t) + e_z(t)] \quad (3-13a)$$

$$n(t) = N_1^{queueing}(t) + N_2^{slow-down}(t) + N_3^{free-flow}(t) \quad (3-13b)$$

$$q_{up,z}^{in}(t) = N_{up,z}^{in}(t) / \Delta T_{step} \quad (3-13c)$$

$$q_{down,z}^{out}(t) = N_{down,z}^{out}(t) / \Delta T_{step} \quad (3-13d)$$

$$e_z(t) = d_{inter}^{demand}(t) - e_{inter}^{exit}(t) \quad (3-13e)$$

where  $q_{up}^{in}(t)$  and  $q^{out}(t)$  are the external inflow and outflow of the current link  $z$ , respectively; and  $e(t)$ ,  $d^{dem}(t)$ , and  $e^{exit}(t)$  are the total disturbance, internal demand, and exit flow within the current link.  $\Delta T_{step}$  is the time length of time step.

Its value is equal to  $N_k$  times communication broadcasting interval  $T_{CV}$ , i.e.,  $\Delta T_{step} = N_k \cdot T_{CV}$ . One popular practical version that simplifies the above law for congestion conditions was proposed by Aboudolas et al. (2009) called

store-and-forward model (SFM), as introduced in the introduction section to this thesis.

In order to further model under-saturated traffic conditions, an iterative extension using the actual flow rate to calculate the outflow rate  $q^{out}(t)$  and inflow rate  $q_{up,z}^{in}(t)$  is proposed as follows.

$$q_{down,z}^{out}(t) = \hat{q}_z(t-1) \cdot g_z / C, \quad \hat{q}_z(t-1) \leq S \quad (3-14a)$$

$$q_{up,z}^{in}(t) = \sum_{w \in \mathbf{Wz}} \tau_w \cdot \hat{q}_w(t-1) \cdot g_w / C, \quad \hat{q}_w(t-1) \leq S \quad (3-14b)$$

where  $S$  is the saturation flow;  $\mathbf{Wz}$  is the set of preceding links  $w$  that transfer flows into current link  $z$ ; the average outflow of a link  $w$  during the previous time step is  $\hat{q}_w(t-1)$  and its turning rate is  $\tau_w$ ,  $\hat{q}_z(t-1)$  is the average link flow during the previous time step;  $g_w$  and  $g_z$  are the green time duration, respectively.

When the time step  $\Delta T_{step}$  is equal to the common cycle length  $C$ , the corresponding state evolution model is then renamed iterative store-and-forward model (It-SFM). The previous evolution equation is rewritten as follows:

$$n(t+1) = n(t) + \left[ \sum_{w \in \mathbf{Wz}} \tau_w \cdot \hat{q}_w(t-1) \cdot g_w - \hat{q}_z(t-1) \cdot g_z + \frac{e_z(t)}{C} \right] \quad (3-15)$$

Further, when the time step  $\Delta T_{step}$  is less than the common cycle length  $C$ , a virtual cycle length  $vc$  is introduced correspondingly that also less than the common cycle length  $C$ . Then, it is  $C = N_{vc} \cdot vc = N_{vc} \cdot \Delta T_{step}$  and  $g = N_{vc} \cdot vg$ . Thus, there is virtual split  $u_{vsplit}$  for each link,  $u_{vsplit} = g / C = vg / vc$  or called quasi split. Then

the following equations are derived,

$$q_{down,z}^{out}(t) = \hat{q}_z(t-1) \cdot \frac{vg_z}{vc}, \quad \hat{q}_z(t-1) \leq S \quad (3-16a)$$

$$q_{up,z}^{in}(t) = \sum_{w \in Wz} \tau_w \cdot \hat{q}_w(t-1) \cdot \frac{vg_w}{vc}, \quad \hat{q}_w(t-1) \leq S \quad (3-16b)$$

Then, the new extended virtual cycle based iterative SFM (Vi-SFM) is derived as follows,

$$n(t+1) = n(t) + \Delta T_{step} \left[ \sum_{w \in Wz} \tau_w \cdot \hat{q}_w(t-1) \cdot \frac{vg_w}{vc} - \hat{q}_z(t-1) \cdot \frac{vg_z}{vc} \right] + \frac{e_z(t)}{C} \quad (3-17)$$

Thus, the state evolution in the CV environment is finally obtained in this subsection. The outputs are the traffic flow states for the current and future time.

### 3.2.5 Priority-augmented Signal Dynamic Model

A priority-augmented signal time-to-change (signal-TTCH) variable, denoted as  $sTTCH$  for the ease of discussion, as shown in Figure 3-6, is proposed to present a signal dynamic model, including phasing timing and status. The inputs of this modeling are the real-time CV and infrastructure data, including signal priority and signal timing data. The proposed  $sTTCH$  extends the original signal dynamic model in standard signal phase and timing (SPaT) from an intra-phase level to an inter-phase level in actuated and adaptive signalized intersections. The additional priority information is provided by standard SRM (signal request message) and SSM (signal status message) data. The proposed  $sTTCH$ -based approach is adopted from the prior graph-based method (135).

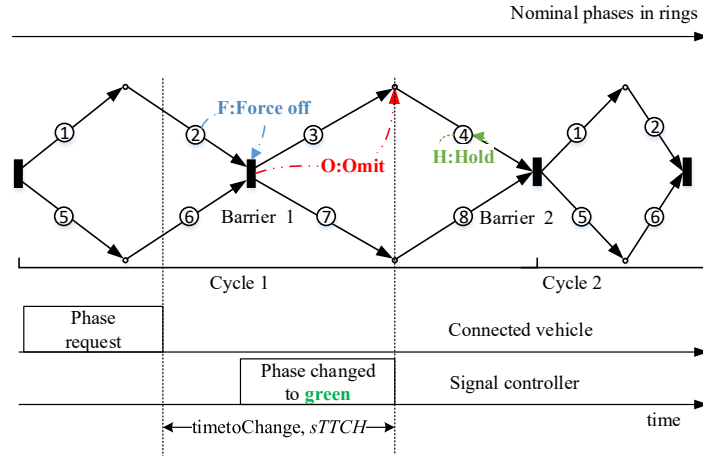


**FIGURE 3-6. Priority-augmented signal model for signal controllers in the CV environment.**

As shown in Figure 3-6, the variable  $sTTCH$  is indicating the time duration between the time instant when sending the priority request and the time instant when switching the phase status. Its mathematical format is derived as follows,

$$sTTCH = t_{\text{phase\_changed}} - t_{\text{cv,phase\_requested}} \quad (3-18)$$

where  $t_{\text{cv,phase\_requested}}$  is the initial time instant of sending the preemption priority request; and  $t_{\text{phase\_changed}}$  is the time instant of preemption phase being changed to green. What is made apparent is that the transition time between the preemption action received and activated must be considered.

Further, as shown in Figure 3-6, for the adaptive signal control in actuated signalized intersections, three phase operations are utilized: 1) *force-off*, 2) *omit*, and 3) *hold-on*. Different combinations of these three phase operations change the value of  $sTTCH$  dynamically. Without loss of generality, the standard National Electrical Manufacturers Association (NEMA) ring-and-barrier diagram (136) is applied here, while other timing planning can also be handled by proper adoptions.

Considering the minimum green duration for the pedestrian crossing and

driver expectancy, the minimum  $sTTCH$  (denoted as  $sTTCH_{min}$ ) is derived,

$$sTTCH_{grn}^{red} = timetoChange_{SPaT} \quad (3-19a)$$

$$sTTCH_{min}^{red} = \max(wk + pc, MGRN) + YEL + ALLR \quad (3-19b)$$

where  $wk$  and  $pc$  are the walking time and the clearance time for pedestrian crossing ( $Gp$ ), respectively;  $MGRN$  is the minimum green time to satisfy driver expectancy ( $Ge$ );  $YEL$  and  $ALLR$  are the yellow time and all-red time, respectively.

The signal status of the signal dynamic is quantified by a binary variable as follows,

$$\varphi = \begin{cases} \varphi_{red} = 1, & other \\ \varphi_{grn} = 0, & green \end{cases} \quad (3-20)$$

where  $\varphi$  is 0 for green status and 1 for either yellow or red status.

The output data is the priority-augmented signal time-to-change data, and it is used in the above traffic state evolution in the CV environment.

### 3.2.6 Updated Node Model based on Vacation Queueing Model

A vacation queueing model is proposed to analyze queues at a signalized intersection. Compared to existing queueing models (11, 137) and a few CV-based models (138), this proposed vacation queueing model considers more time-variant dynamics of traffic signals. The inputs of this modeling are the real-time traffic flow and signal status data.

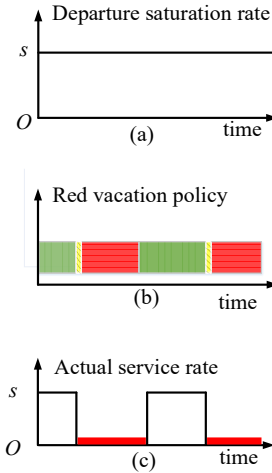


**FIGURE 3-7. The proposed vacation queueing model of a generalized intersection: (a) departure saturation rate, and (b) the red vacation policy mechanism (i.e., signal phase and timing), and its results are (c) actual service rate.**

As shown in Figure 3-7, a vacation queueing model is proposed to quantify queue analytics at the generalized intersection with a typical phase diagram. This model comprises of a traditional queueing system and a newly introduced service mechanism (i.e., *red vacation policy mechanism*). The new *red vacation policy mechanism* is used to model signal control strategies, where the intersection does not remain active for a particular time duration (i.e., the red phase) called “*on vacation*”. The vacation process prohibits vehicles from passing through the target intersection. The notation of the proposed vacation queueing model is denoted as  $M/G/1$  (*red vacation policy mechanism*). Its queue analytics is obtained by the following decomposition method (139). It has three steps, 1) decomposition, 2) traditional queueing, and 3) additional queueing modeling due to the red vacation policy mechanism.

For the  $M/G/1$  (*red vacation policy mechanism*) system, the quantitative results are given by the following Theorem (139): The stationary number of customers  $L_v$  and the stationary queue length  $Q_v$ , is made up of the sum of two

independent random variables. One of them is the queue analytic of the corresponding *traditional queueing model*, and the other is the *additional queue analytic* due to red light vacations. This decomposition method is shown as follows,

$$L_v = L + L_d \quad (3-21a)$$

$$Q_v = Q + Q_d \quad (3-21b)$$

where  $L$ , and  $Q$  are the number of customers in the system and the queue length for a *traditional queueing* system without vacations that has reached a steady state, respectively.  $L_d$ , and  $Q_d$  are the *additional* number of customers in the system and the *additional* queue length due to the vacation effect, respectively.

The traditional queueing system at a signalized intersection can be summarized as an M/G/1/FIFO system (140). That is, vehicles arrive at one intersection randomly following a homogeneous Poisson process rate  $\lambda$ . The vehicles exit the intersection following an independent general distribution with rate  $u$  (G) for each lane. This system follows the first-in, first-out (FIFO) principle. Existing studies have proposed mature analytical close-forms of queue analytics for this system without vacations when reaching a steady state (140). Defining  $\rho = \lambda / \mu$  as *traffic intensity*, average customer length  $E(L)$ , queue length  $E(Q)$ ,

and waiting time  $E(W)$  can be calculated as  $\rho + \frac{\lambda^2 \sigma^2 + \rho^2}{2(1-\rho)}$ ,  $\frac{\lambda^2 \sigma^2 + \rho^2}{2(1-\rho)}$ , and

$\frac{\lambda^2 \sigma^2 + \rho^2}{2\lambda(1-\rho)}$ , respectively.

A *red vacation policy mechanism* includes a red phase start-up rule, red phase termination rule, and timing distribution of the red phase. For the fixed-time

signal control of one approach, it is modeled as a single vacation (denoted as  $SV$ ) system where the length of each service period is limited by a given length of time  $T$  ( $T$ -limited service, denoted as  $TL$ ) and denoted as  $M/G/1(TL, SV)$ . The constant cycle length and the length of the current green phase is denoted as  $C$  and  $g$ , respectively. Accordingly, the summation of the yellow and red phase lengths is the vacation time period, which is denoted as  $R$ . From this, the additional random variable  $L_d$ , which is the additional queue length due to the vacation effect after reaching steady state, with  $E(L_d)$  in Equation (3-22) (139), can be calculated.

$$E(L_d) = \frac{\lambda^2 R^2}{2[e^{-\lambda R} + \lambda R]} \quad (3-22)$$

By that, the expected busy period (i.e., expected green interval  $E(g_k)$ ) is accommodated with the arrival flow. The output data is the performance index quantification, i.e., queue length, for further performance evaluations.

### **3.3 INTERSECTION-LEVEL PERFORMANCE FUNCTION FOR ASC AND CORRIDOR-LEVEL PERFORMANCE FUNCTION FOR COORDINATION**

Since the node model is updated based on the vacation queueing model, one can obtain the delay model to get the intersection-level performance function for CV-ASC. Also, a link model is updated by a platoon-based model, and one can obtain the extended link performance function considering tuning flows for corridor-level performance function for coordination. They are shown in the contents discussed in the subsections below.

#### **3.3.1 Extended Delay Function for the Adaptive Signal Control**

At the intersection level, a general analytic vacation queueing model is

proposed to analyze the delay performance. A *red vacation policy mechanism* includes a red phase start-up rule, red phase termination rule, and timing distribution of the red phase. For the fixed-time signal control of one approach, it is modeled as a single vacation (denoted as *SV*) system where the length of each service period is limited by a given length of time  $T$  (*T-limited service*, denoted as *TL*) and denoted as  $M/G/1(TL, SV)$ . As shown in Equation (3-22), the mean  $E(L_d)$  has been obtained. Then by Little's Law, the additional average delay due to vacations (i.e., waiting time ) is

$$E(W_v) = \frac{E(L_v) - \rho}{\lambda} = \frac{\lambda^2 \sigma^2 + \rho^2}{2\lambda(1-\rho)} + \frac{\lambda R^2}{2[e^{-\lambda R} + \lambda R]} \quad (3-23)$$

As such, the expected waiting time accommodates the arrival flow, which is the output of this function.

### 3.3.2 Extended Performance Function considering Tuning Flows for Coordination

This section explains an extended link performance function based on the previously estimated dispersed platoon. The residual queue length of the downstream intersection (denoted as  $QL_{re}$ ), is considered here to capture the unbalanced queueing clearance.

Without a proper offset setting, a leading edge of the dispersed platoon could arrive at the downstream intersection either before or after the start of the green. This arrival time of the platoon leading-edge, computed by the relative time to start of green, is denoted as  $\gamma$ . In other words, the variable  $\gamma$  is an estimated time of arrival (ETAR) relative to the start of green. Consequently, different values of  $\gamma$

generate various stopping delays since the platoon could encounter stops. These stopping delays are represented as functions of  $\gamma$  and denoted as  $d(\gamma)$ . Importantly, minimizing the stopping delay  $d(\gamma)$  is our goal here.

To obtain a minimum delay with further consideration of residual queue effects, a derivation based on a previous linearization approximation method (19) is implemented. This approximation is an extension of the method proposed by Gartner et al. (27). The minimum delay (denoted as  $d_{min}(\gamma)$ ) is determined by the approaching dispersed platoon and the effective green interval  $g$ .

The dispersion platoon length  $p_d$  can be either larger than ( $p_d > g$ ) or smaller than/equivalent to ( $p_d \leq g$ ) the green time  $g$ . These two cases are illustrated in Figure 3-8. For both cases, the delay is *minimal* when the trailing edge of the platoon arrives at the traffic light just before the traffic light turns red, and the whole platoon has cleared entirely(27). Moreover, for both cases  $p_d \leq g$  and case  $p_d > g$ , this occurs for  $\gamma$  and  $\gamma = p - g$ , respectively. The minimum delay is derived as follows:

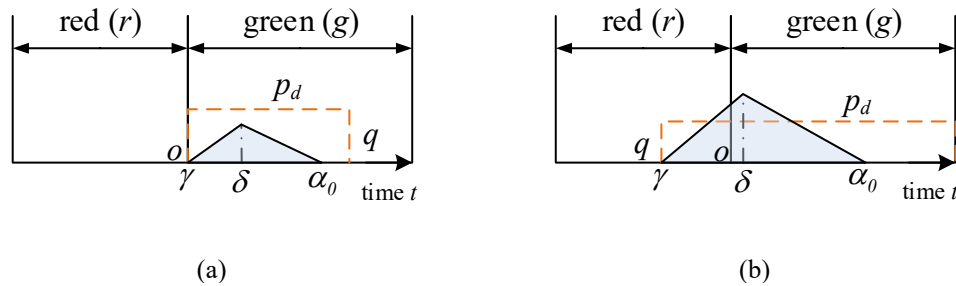


**FIGURE 3-8. Minimum platoon delay  $d_{min}(\gamma)$  when the platoon encounters residual queue where the leading edge arrives the adjacent intersection (a)  $p_d \leq g$ , the platoon length  $p_d$  is not larger than green time  $g$  (b)  $p_d > g$ , the platoon length  $p_d$  is larger than green time  $g$ . (19)**

In Figure 3-8,  $r$  is the red interval, and  $\delta$  is the residual queue clearance time.  $\delta$  is equal to the residual queue length  $QL_{re}$  divided by the saturation flow rate  $s$ , i.e.,  $\delta = QL_{re}/s$ .  $\alpha_0$  is the dissipating time during green when the stopped platoon queue disappears in Figure 3-8.

First, the simplest and ideal case is analyzed here. If the clearance of residual queue  $\delta$  ends earlier than the leading edge's arrival, i.e.,  $0 < \delta \leq \gamma$ , it leads to the minimal ZERO delay

$$d_{min}(\gamma) = 0, \quad \delta \leq \gamma \leq g - p_d \quad (3-24)$$

Further cases in Figure 3-8 show that the head of the platoon arrives  $\gamma$  earlier than the clearance time of the residual queue  $\delta$ , i.e.,  $0 < \gamma \leq \delta$ . Considering the conservation law, the inflow during the period is equal to the outflow over the period for both cases. This means  $q(\alpha_0 - \gamma) = s(\alpha_0 - \delta)$ , which leads  $\alpha_0$  as follows:

$$\alpha_0 = \frac{q\gamma - s\delta}{q - s} \quad (3-25)$$

where  $q$  is the arrival platoon flow simplified from the previous notation  $q_{down}(t)$ .

Then total minimal delay  $D_{min}(\gamma)$  for a specific  $\gamma$  is obtained by analyzing the process of the queue formulation and dissipation in a basic manner. In other words, the  $D_{min}(\gamma)$  is equal to the accumulative delay of the queue formulation from time  $\gamma$  to time  $\alpha_0$  minus the clearance time of the queue dissipation from time  $\delta$  to time  $\alpha_0$ , which is expressed as follows:

$$\begin{aligned} D_{min}(\gamma) &= \int_{\gamma}^{\alpha_0} [q(\alpha_0 - t)]dt - \int_{\delta}^{\alpha_0} [s(t - \delta)]dt \\ &= \frac{\alpha_0^2}{2}(q - s) + \alpha_0(s\delta - q\gamma) + \frac{1}{2}(q\gamma^2 - s\delta^2) \end{aligned} \quad (3-26)$$

where  $\alpha_0$  is the dissipating time calculated.

Then, denoting Equation (3-25) into (3-26), the total delay are obtained:

$$D_{min}(\gamma) = \frac{q\gamma^2 - s\delta^2}{2} - \frac{(q\gamma - s\delta)^2}{2(q-s)} = \frac{-qs(\delta - \gamma)^2}{2(q-s)} \quad (3-27)$$

Considering that the total platoon size  $N$  is equal to  $p_dq$  (i.e.,  $N=p_dq$ ), the average minimal delay for each vehicle  $d_{min}(\gamma)$  is derived in following equation,

$$d_{min}(\gamma) = \frac{D_{min}(\gamma)}{p_dq} = \frac{1}{2p_d} \frac{(\delta - \gamma)^2}{(1 - \rho)}, \rho \equiv \frac{q}{s} \quad (3-28)$$

Considering the occurring condition for both cases in Equation (3-24) and (3-28), the final minimal delay expression is derived

$$d_{min}(\gamma) = \begin{cases} 0 & , \gamma \in [\delta, g - p_d], \quad p_d \leq g, \\ \frac{(\delta - \gamma)^2}{2p_d(1 - \rho)} & , \gamma \in [0, \delta], \quad p_d \leq g, \\ \frac{(\delta - (p_d - g))^2}{2p_d(1 - \rho)} & , \gamma \in [-r, 0], \quad p_d > g. \end{cases} \quad (3-29)$$

where  $\gamma = g - p_d$  when in condition  $p_d > g$ .

Substituting Equation (3-7) into Equation (3-29), the expression of minimal delay considering the tuning flows is obtained as follows:

$$d_{min}(\gamma) = f(p_d | p_d = p_1 + p_3 + \frac{B(t)}{q} + \frac{C(t)}{q_{turning}}) \quad (3-30)$$

Thus, this method's output is the delay performance for the current link from the coordination perspective.

After the link performance results have been obtained, the offset estimation for the target link is introduced in the next sub-section.

### **3.4 MPC-BASED REAL-TIME ASC AND COORDINATION**

A framework of the MPC-based ASC and coordination is proposed to optimize the signal control for multiple intersections as well as their coordination. The proposed method will solve Questions Q5 and Q6 and correspond to the corresponding contributions R5 and R6.

#### **3.4.1 Proposed Framework of the MPC-based ASC and Coordination**

To utilize the real-time feature of the CV technology fully, a framework of the MPC-based ASC and coordination is proposed for signal controls. The structure of the proposed framework is shown in Figure 3-9. The whole framework consists of two major parts, where one is the traffic system, and the other is the MPC controller.

Traffic systems are influenced by the near-future traffic demand (  $d(t)$  ) and the optimal control inputs (i.e.,  $u^*$ , such as cycle length, split, offset). For the traffic demand, both the current and short-term data are used as the traffic system's inputs. The optimal signal control inputs are derived by the MPC controller to smooth the traffic. Then, the description of the traffic system is the traffic flow status (  $x$  ), which is measured and recorded by the CV technology.

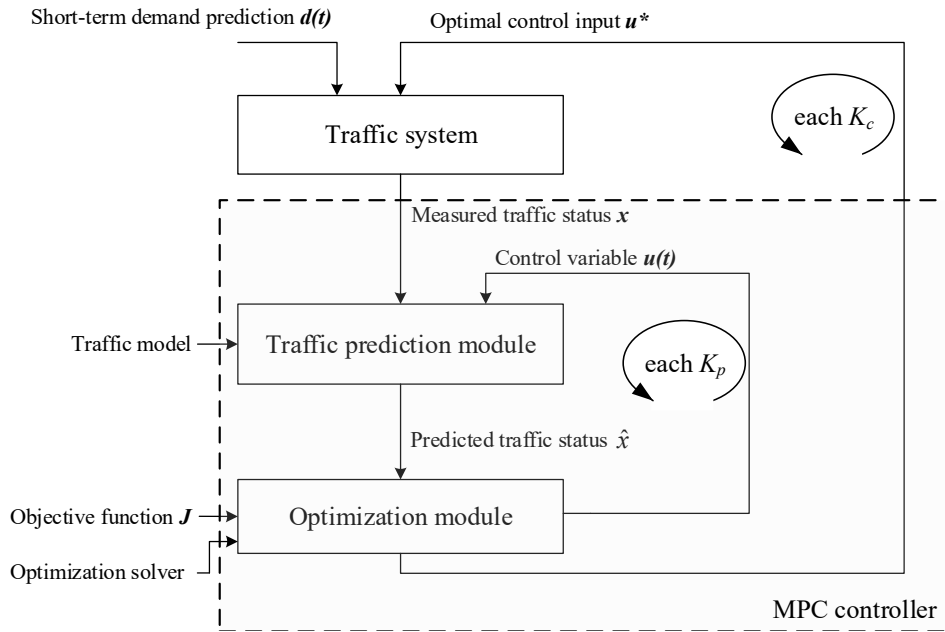


**FIGURE 3-9. Proposed framework of the basic MPC-based ASC and coordination.**

After that, the measured traffic status ( $x$ ) is input to the MPC controller as input data. The MPC controller includes three parts: 1) the traffic prediction model, 2) the optimization module, and 3) a rolling horizon scheme. In particular, for the rolling horizon scheme, the prediction module predicts future states for each  $k_p$  period, and a sequence of optimal controls is obtained over the whole  $k_p$  period. Only the first optimal action  $u^*$  is implemented. Then the whole horizon is shifted forward with one specific  $k_c$  time period. The value  $k_c$  can be either smaller, equal to or larger than the cycle length.

In the traffic prediction model, the proposed traffic models use the short-term predicted demand (marked as  $d(t)$ ), the measured traffic flow status (marked as  $x$ ), and the control variable signal inputs (marked as  $u(t)$ ) to generate predicted traffic flow status (marked as  $\hat{x}$ ). Then, the predicted traffic status is used as inputs for the enhanced optimization module to obtain optimal control variables.

In the optimization module, enhanced optimization models and improved objective functions are proposed, which will be described in the following sub-chapters.

As was introduced in previous sections, the corridor optimization is divided into intersection-level and corridor-level. The further goal here is to obtain the optimized common cycle length, split, and offset.

### 3.4.2 Cycle Length and Split Optimization Module

Within a general dual-ring signal control structure, there are  $K$  different phases ( $K \geq 1$ ) within one ring. For each phase  $k$ , the green phase interval is denoted as  $g_k$  and the red phase interval as  $R_k$ . The objective here is to get the optimal  $g_k$  and  $R_k$  for each phase  $k$ , respectively.  $E(g_k)$  is the expected green phase interval for lane group  $k$ , and it is expressed as follows:

$$E(g_k) = \frac{e^{-f\lambda_k R_k} + f\lambda_k R_k}{(fu_k) \cdot (1 - \rho_k)} \quad (3-31)$$

Accordingly, the optimal cycle length  $C^*$  can get by the sum of  $g_k$  and  $R_k$ .

The expected cycle length  $C^*$  is calculated as follows:

$$C^* = v_0 [R_k + \frac{1}{\lambda} + E(g_k)] + (1 - v_0) [R_k + E(g_k)] \quad (3-32)$$

Considering the dual-ring eight-phase signal structure, there are several equalities. In the same ring, the assigned red interval for phase  $k$  (denoted as  $R_k$ ) should be equal to the summation of other phases' expected green intervals  $E(g_h)$ . In this constraint, there are the relationships  $k, h \in \{1, \dots, K\}$  and  $k \neq h$ . This equality is shown as follows:

$$R_k = \sum_{\substack{1 \leq h \leq K \\ k \neq h}} E(g^N(h)) \quad (3-33)$$

where  $E(g^N(h))$  is the expected green phase interval for phase  $h$ . Recalling that  $E(g^N(h))$  is expressed in Equation (3-31), it is rewritten as follows:

$$g^N(h) \triangleq E(g^N(h)) = \frac{e^{-f\lambda_k R_k} + f\lambda_k R_k}{(fu_k) \cdot (1 - \rho_k)} \quad (3-34)$$

Equation (3-33) and Equation (3-34) are constraints when obtaining the nominal optimal split and cycle length. A loss function is defined as shown in the following equation:

$$J_{split} = \|\Delta g(i)\|^2 = \|g(i) - g^N(i)\|^2 \quad (3-35)$$

where  $g^N$  is the nominal green interval, i.e., the initial green interval and  $E(g_k)$  is the optimal green interval.

### 3.4.3 Common Cycle Length Calculation

Considering there are  $N$  intersections along the arterial road, the common cycle length for the whole road is needed for the signal coordination. Two strategies are considered here. One is an identical common cycle length used for all intersections, and another is that each intersection has its cycle length.

The first strategy is currently widely accepted. The cycle length is identical for all intersections, and this identical cycle length is referred to as the common cycle length. Thus, the maximum cycle length selected from all individual intersection's  $C^*$  is used, and expressed as follows:

$$C_{com}^* = \max\{C_n^*\}, \quad n \in [1, N] \quad (3-36)$$

where  $C_n^*$  is the optimal cycle length for the intersection  $n$ . Then, the coordination is applied as a fixed priority request, and the fixed request is sent periodically in

each cycle. The requested phases are the fixed coordinated phases, and the request intervals are splits of the coordinated phases (25). Thus, the optimal splits of other non-coordinated phases are finally achieved by applying the fixed-coordination setting for each intersection.

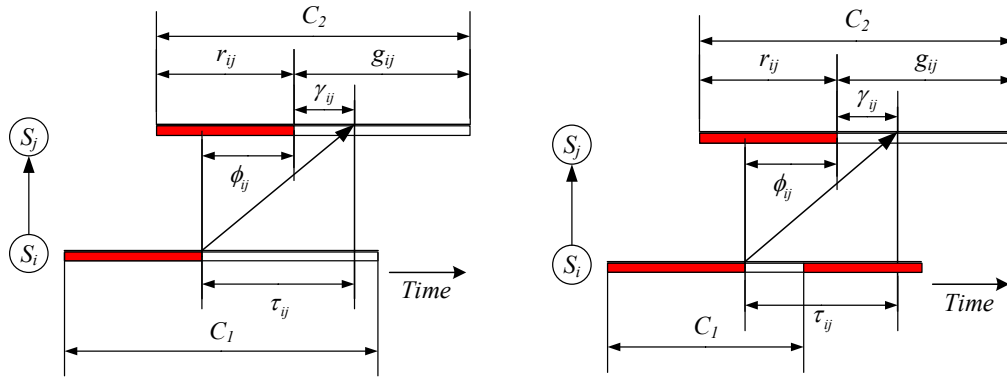
The second strategy is that each intersection has its own cycle length. Thus, the common cycle length for intersection  $n$  is equal to the optimal cycle length of the intersection  $n$ , and is expressed as follows:

$$C_{com,n}^* = C_n^*, \quad n \in [1, N] \quad (3-37)$$

where  $C_{com,n}^*$  is the common cycle length for the intersection  $n$ .

#### **3.4.4 Offset Optimization Module with and without Identical Common Cycle Length**

First, the previous notations are recalled briefly. There are  $N$  intersections along the arterial road, and intersection  $i, j$ , and  $n$  belong to these  $N$  intersections (i.e.,  $i, j, n \in \{1, \dots, N\}$ ). Figure 3-10 shows how to obtain the offset with and without an identical common cycle length.



(a) with identical common length  $C_1 = C_2 = C_{com}$  (b) without identical common length  $C_1 \neq C_2$   
**FIGURE 3-10. The offset variable between two adjacent signalized intersections. (27)**

The mathematical format is as follows,

$$\emptyset_{ij} = \tau_{ij} - \gamma_{ij} \quad (3-38)$$

where  $\tau_{ij}$  is the ideal travel time of the leading vehicle in the target platoon with a free-flow speed. The ideal travel time is obtained as  $\tau_{ij} = d_{ij} / v_f$ , where  $d_{ij}$  is a distance between two adjacent intersections and  $v_f$  is the free-flow speed. The variable  $\gamma_{ij}$  is an estimated time of arrival (ETAR) relative to the start of green. Consequently, different  $\gamma_{ij}$  cause various stopping delays because the platoon encounters stops.

Considering the minimum delay  $d_{min}(\gamma)$  of the approaching platoon from intersection  $i$  to intersection  $j$  calculated in Equation (3-26), the offset estimation  $\emptyset_{ij}$  in Equation (3-38) is converted to a minimum delay function  $d(\emptyset_{ij})$  as follows,

$$d(\emptyset_{ij}) = d(\gamma_{ij}) \quad (3-39)$$

In this equation, the  $d(\varnothing_{ij})$  depends on the *offset* for the link  $(i,j)$ . Then, the optimal offset is determined when the total delay is minimal. This leads to the following objective function (19, 27):

$$\min J_{offset} = \sum_{(i,j) \in N} f_{ij} \cdot d(\varnothing_{ij}) \quad (3-40)$$

where  $f_{ij}$  is the average flow on the link  $(i,j)$  between intersection  $i$  and intersection  $j$ . This objective function  $J_{offset}$  is separable.

Furthermore, several constraints are applied to this optimization model. First, the optimal offset  $\varnothing_{ij}^*$  remains in the interval  $[\tau_{ij} - g_{ij}, \tau_{ij} + r_{ij}]$ , which leads

$$\varnothing_{ij}^* \in [\tau_{ij} - g_{ij}, \tau_{ij} + r_{ij}] \quad (3-41)$$

Then, the sum of all offsets for one loop should be equal to an integral multiple of the cycle length  $C$ . It is shown as follows:

$$\sum_{(i,j) \in N_l} \varnothing_{ij} = n_l \cdot C \quad (3-42)$$

where  $n_l$  is an integer and  $N_l$  is a set of forward and reverse links in the loop for two opposing directions.

The aim is to minimize the delay for both ASC and signal coordination. Thus the following two optimization problems are defined as:

$$\min_{\mathbf{u}} = E[J(\mathbf{x}, \mathbf{d}(t), \mathbf{u}(t))], \quad J(\mathbf{x}, \mathbf{d}, \mathbf{u}) = \sum_{i=0}^{i=k_p-1} J_{split}(t_i) \quad (3-43a)$$

$$\min_{\mathbf{u}} = E[J(\mathbf{x}, \mathbf{d}(t), \mathbf{u}(t))], \quad J(\mathbf{x}, \mathbf{d}, \mathbf{u}) = \sum_{i=0}^{i=k_p-1} J_{offset}(t_i) \quad (3-43b)$$

subject to previous constraints. The nonlinear optimization problem is solved via a Matlab tool, e.g., successive quadratic programming algorithm (113).

### 3.5 STABILITY SYNTHESIS OF THE MPC-BASED SIGNAL CONTROL

In this subchapter, the stability synthesis of the proposed basic MPC-based signal control method is proved and demonstrated by a proposed stabilizing scheme.

#### 3.5.1 Abstract Model of the System Dynamics and the MPC Controller

For convenience, the previously proposed dynamic systems for adaptive signal control and coordination have been rewritten as an abstracted model as follows,

$$\mathbf{x}(k+1) = f(\mathbf{x}(k), \mathbf{u}(k)) \quad (3-44a)$$

$$\mathbf{y}(k+1) = g(\mathbf{x}(k)) \quad (3-44b)$$

$$\mathbf{x}(k) \in \mathbf{X} \quad (3-44c)$$

$$\mathbf{u}(k) \in \mathbf{U} \quad (3-44d)$$

where  $f(\bullet)$  is a nonlinear system state dynamic function of both the signal control input  $\mathbf{u}$  and the measurable system state  $\mathbf{x}$ ,  $g(\bullet)$  is a nonlinear system output function of state  $\mathbf{x}$ .  $k$  is the time instant. The state and control input constraint are  $\mathbf{x}(k) \in \mathbf{X}$  and  $\mathbf{u}(k) \in \mathbf{U}$ , respectively. The variable  $\mathbf{x}$ ,  $\mathbf{u}$ ,  $\mathbf{y}$  are vectors here.

Then, at each time step  $k$ , the proposed basic MPC (the basic MPC) with finite prediction horizon  $K_p$  ( $N = K_p$ ) in Figure 3-9 is rewritten as follows (141),

$$\begin{aligned}
\text{FHO:} \quad & \min J_N(k) = \sum_{i=0}^{N-1} l[\mathbf{x}(k+i), \mathbf{u}(k+i)] \\
& \text{s.t.} \\
& \mathbf{x}(k+i+1) = f(\mathbf{x}(k+i), \mathbf{u}(k+i)), \quad i = 0, \dots, N-1 \quad (3-45) \\
& \mathbf{x}(k+i) \in \mathbf{X}, \quad i = 0, \dots, N \\
& \mathbf{u}(k+i) \in \mathbf{U}, \quad i = 0, \dots, N-1 \\
& \mathbf{x}(k|k) = \mathbf{x}(k)
\end{aligned}$$

where  $l(\bullet)$  is a nonlinear performance function with a positive semi-definite value.

This MPC controller is also called finite horizon optimization (FHO) since it has a finite prediction horizon (141).

### 3.5.2 Qualitative Synthesis: Infinite Horizon Optimization (IHO)

#### Approximation

To provide a guaranteed stability for MPC controllers, qualitative synthesis is provided here by deploying a stabilizing scheme to the finite horizon optimization (FHO) in Equation (3-45) (141–143). The deployed stabilizing scheme enables the finite horizon optimization (FHO) in the MPC to approximate the infinite horizon optimization (IHO), i.e., Infinite Horizon Optimization (IHO) approximation scheme.

The infinite horizon optimization (IHO) problem is modified from the previous FHO problem; and the IHO is presented as follows,

$$\begin{aligned} \text{IHO:} \quad & \min J_{\infty}(k) = \sum_{i=0}^{\infty} l[\mathbf{x}(k+i), \mathbf{u}(k+i)] \\ \text{s.t.} \quad & \mathbf{x}(k+i+1) = f(\mathbf{x}(k+i), \mathbf{u}(k+i)), \quad i = 0, \dots \\ & \mathbf{x}(k+i) \in \mathbf{X}, \quad i = 0, \dots \\ & \mathbf{u}(k+i) \in \mathbf{U}, \quad i = 0, \dots \\ & \mathbf{x}(k|k) = \mathbf{x}(k) \end{aligned} \quad (3-46)$$

When comparing the FHO and IHO problems, the only difference between them is the prediction horizon range in the performance index, which is shown as follows,

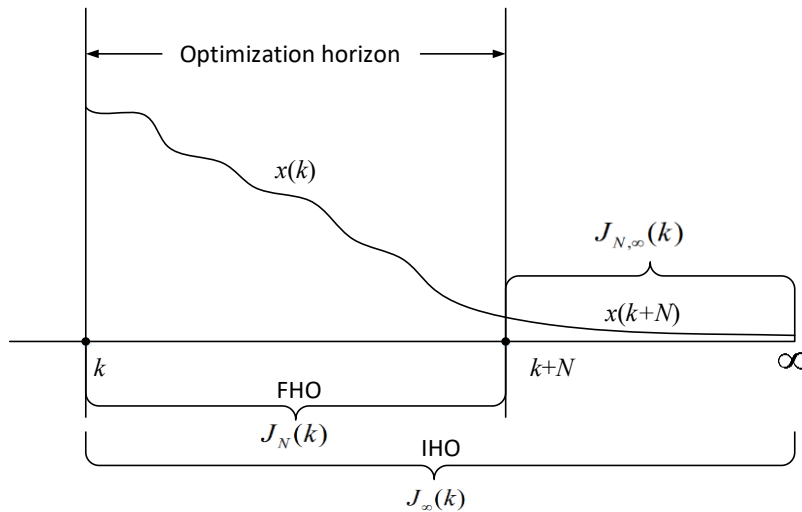


FIGURE 3-11. Different prediction horizon ranges of the FHO and IHO problems (141).

The difference that prediction horizons yields is different performance indices. Their relationship is as follows,

$$J_{\infty}(k) = J_N(k) + J_{N,\infty}(k) \quad (3-47)$$

where the difference  $J_{N,\infty}(k)$  is an additional value in IHO problem and is expressed as follows,

$$J_{N,\infty}(k) = J_{\infty}(k) - J_N(k) = \sum_{i=N}^{\infty} l[\mathbf{x}(k+i), \mathbf{u}(k+i)] \quad (3-48a)$$

$$J_{\infty}(k) = \sum_{i=0}^{\infty} l[\mathbf{x}(k+i), \mathbf{u}(k+i)] \quad (3-48b)$$

$$J_N(k) = \sum_{i=0}^{N-1} l[\mathbf{x}(k+i), \mathbf{u}(k+i)] \quad (3-48c)$$

Since the finite horizon optimization (FHO) in the MPC should approximate the infinite horizon optimization (IHO), the above Equation (3-48c) presents that the original performance function  $J_N(k)$  should be modified to compensate for the added value  $J_{N,\infty}(k)$ . The modified performance function is denoted as  $\bar{J}_N(k)$ , and the original MPC expressed in Equation (3-45) is modified accordingly.

Usually, to modify the original FHO problem approximating the IHO problem, there are many widely used strategies to impose additional terminal conditions. These strategies are briefly summarized into four categories (141–143),

- 1) adding terminal equality (zero) constraint,
- 2) adding terminal constraint set,
- 3) adding terminal cost function, and
- 4) adding both terminal constraint set and cost function.

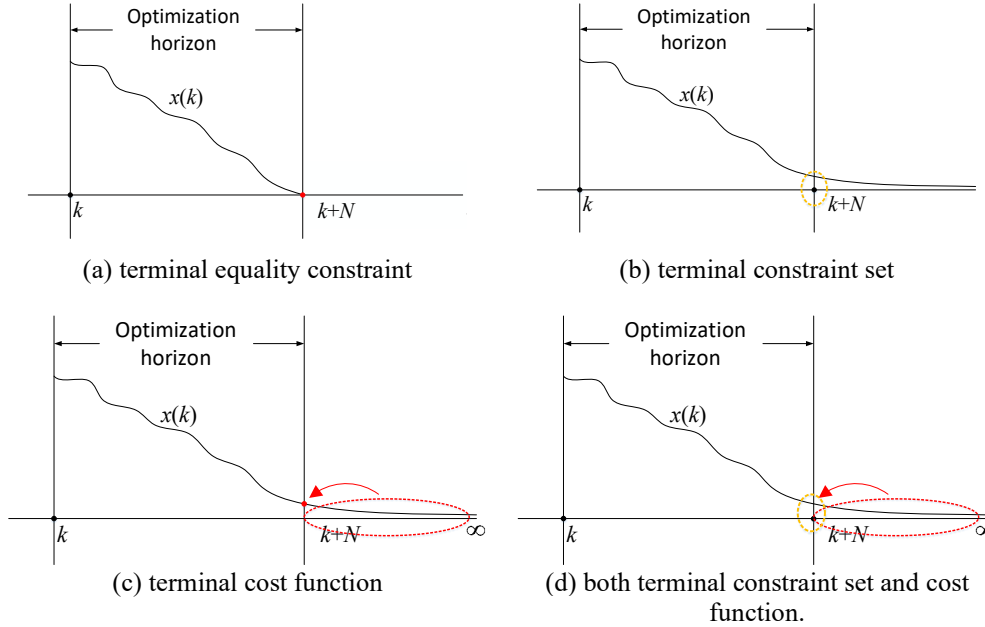


**FIGURE 3-12. Strategies for the infinite horizon optimization approximation (141, 143).**

By utilizing these strategies, the MPC with a finite horizon can be modified with guaranteed stability by the infinite horizon optimization approximation, as shown in Figure 3-12. Then, the principles of the fourth method are deployed to find a stable MPC controller.

### 3.5.3 Stabilizing Control Scheme

When applied with both terminal constraint set and cost function, the above MPC in Equation (3-45) is modified as follows,

$$\text{FHOV2 : min } \bar{J}_N(k) = \sum_{i=0}^{N-1} \left[ \|\mathbf{x}(k+i|k)\|_Q^2 + \|\mathbf{u}(k+i|k)\|_R^2 \right] \\ + F(\mathbf{x}(k+N|k))$$

$$\text{with } F(\mathbf{x}) = \mathbf{x}^T P \mathbf{x}$$

s.t.

$$\mathbf{x}(k+i+1|k) = f(\mathbf{x}(k+i|k), \mathbf{u}(k+i|k)), \quad i = 0, \dots, N-1 \quad (3-49)$$

$$\mathbf{x}(k+i|k) \in \mathbf{X}, \quad i = 0, \dots, N$$

$$\mathbf{x}(k|k) = \mathbf{x}(k)$$

$$\mathbf{u}(k+i|k) \in \mathbf{U}, \quad i = 0, \dots, N-1$$

$$\mathbf{x}(k+N|k) \in \mathbf{X}_f,$$

where a quadratic cost function is deployed, and  $\mathbf{Q}$ ,  $\mathbf{R}$  represent positive-definite, symmetric weighting matrices.  $F(\mathbf{x})$  is the terminal cost function;  $P$  is an arbitrary Hermitian, positive-definite matrix, called the terminal penalty matrix;  $\mathbf{X}_f$  is a neighborhood called terminal region. Then the terminal positive-definite, symmetric matrix  $P$  and terminal region  $\mathbf{X}_f$  together define a potential stable MPC controller. Without loss of generality, other types of cost functions could be implemented or transferred into the quadratic form.

To provide guaranteed stability of the proposed MPC controller, a stabilizing control scheme (142) is deployed to the above finite horizon optimization version two (FHO-v2) in Equation (3-49) to find both the proper terminal cost function and terminal constraint set as well as corresponding parameters. An equivalent variant for the discrete-time state-space system is briefly described in *Lemma 3-1*. Its corresponding principle is graphically presented in Figure 3-13.

---

**Lemma 3-1:** There exists a neighborhood  $X_f$  of the stabilizable origin and a unique positive-definite and symmetric matrix  $P$  to stabilize the FHO-V2 problem (3-49) when performing the following scheme (142),

---

Step 1: Obtain the Jacobian linearization of the **discrete-time** system (3-31a) inside the problem (3-36) at the stabilizable origin  $\mathbf{x}(k+i+1|k) = \mathbf{A}\mathbf{x}(k+i|k) + \mathbf{B}\mathbf{u}(k+i|k)$ , where  $\mathbf{A} = (\partial \mathbf{f} / \partial \mathbf{x})(\mathbf{0}, \mathbf{0})$  and  $\mathbf{B} = (\partial \mathbf{f} / \partial \mathbf{u})(\mathbf{0}, \mathbf{0})$ . Then the local control problem is solved to obtain a local linear controller  $\mathbf{u} = \mathbf{K}\mathbf{x}$ , where  $\mathbf{K}$  is the linear state feedback gain. Thus,  $\mathbf{A}_K = \mathbf{A} + \mathbf{B}\mathbf{K}$  is asymptotically stable.

Step 2: Select a positive constant  $\lambda$  meeting that  $\lambda > 0$ . In addition,  $\mathbf{Q}^* = \mathbf{Q} + \mathbf{K}^T \mathbf{R} \mathbf{K}$ .

Step 3: Solve the following Lyapunov equation to obtain the terminal cost matrix  $P$  for terminal cost function  $F(\mathbf{x})$ ,

$$\mathbf{A}_K^T P \mathbf{A}_K - P = -(\mathbf{Q}^* + \lambda \mathbf{Q}^*). \quad (3-50)$$

Step 4: Find the largest possible  $\alpha_1 > 0$  to obtain the neighborhood  $\Omega_1$  satisfying  $\mathbf{K}\mathbf{x} \in U, \forall \mathbf{x} \in \Omega_1$  where  $\Omega_1 = \{ \mathbf{x} \in R^n \mid F(\mathbf{x}) = \mathbf{x}^T P \mathbf{x} \leq \alpha_1 \}$ .

Step 5: Find the largest possible  $\alpha_2 \in (0, \alpha_1]$  to obtain a new neighborhood  $\Omega_2$ , where  $\alpha_2$  satisfying  $(\|P\| L_\phi^2 + 2L_\phi \|P\| \|\mathbf{A}_k\|) \|\mathbf{x}\|^2 - \lambda \mathbf{x}^T \mathbf{Q}^* \mathbf{x} \leq 0$  with  $\phi(\mathbf{x}) = f(\mathbf{x}, \mathbf{K}\mathbf{x}) - \mathbf{A}_K \mathbf{x}$ ,  $L_\phi = \sup \left\{ \frac{\|\phi(\mathbf{x})\|}{\|\mathbf{x}\|} \mid \mathbf{x} \in \Omega_1, \mathbf{x} \neq 0 \right\}$ . Thus the neighborhood  $X_f = \Omega_2$ .

Step 6: Repeat the process from step 2 to step 5 to find the largest possible  $X_f$ .

---

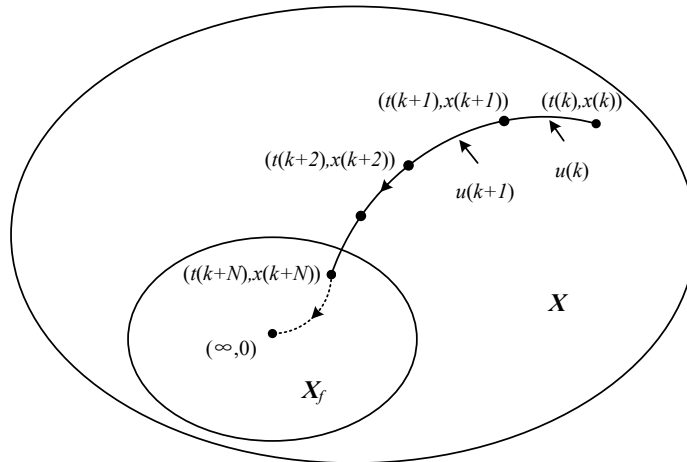


**FIGURE 3-13.** Principles of a two-step quasi-infinite horizon stabilizing scheme: the solid line is the state trajectory obtained by the finite horizon predictive control, and the dashed line is the state trajectory obtained by the local linear controller (142).

As shown in Figure 3-13, the deployed scheme has two steps. The first step is solving a finite horizon predictive control problem. This step pushes the target system model into the terminal region  $X_f$ . Then the second step stabilizes the system inside the terminal region with a local feedback controller  $\mathbf{u} = \mathbf{K}\mathbf{x}$ .

Since the finite horizon predictive control problem is solved on-line at each time, the optimal control profile is generated accordingly; while the local feedback controller is only used to find both the terminal region  $X_f$  and terminal penalty matrix  $P$  rather than to apply to the system directly. The following discussions provide the proof of the proposed stability scheme.

Proof: It will be proved that there always exists a parameter  $\alpha_2$  that can obtain a terminal cost terminal  $\Omega_2$  to ensure the stability feature.

First, a Lyapunov function  $F(x) = x^T P x$  is defined where terminal cost matrix  $P$  is the solution of the Lyapunov equation, as shown in (3-50). The difference of the Lyapunov function  $F(x)$  is written as

$$\begin{aligned}
& F(x(k+1)) - F(x(k)) \\
&= x(k+1)^T P x(k+1) - x(k)^T P x(k) \\
&= ((A+BK)x(k) + \phi(x(k)))^T P ((A+BK)x(k) + \phi(x(k))) - x(k)^T P x(k) \\
&= \phi(x(k))^T P \phi(x(k)) + 2\phi(x(k))^T P A_K x(k) + x(k)^T [A_K^T P A_K - P] x(k) \quad (3-51)
\end{aligned}$$

where  $\phi(x) = f(x, Kx) - A_K x$  and  $A_K = A + BK$ .

Substituting Equation (3-50) into Equation (3-51) becomes,

$$\begin{aligned}
& F(x(k+1)) - F(x(k)) \\
&= \phi(x(k))^T P \phi(x(k)) + 2\phi(x(k))^T P A_K x(k) - x(k)^T (Q^* + \lambda Q^*) x(k) \quad (3-52)
\end{aligned}$$

In order to ensure the inequality

$$F(x(k+1)) - F(x(k)) \leq -x(k)^T Q^* x(k) \quad (3-53)$$

to be satisfied, one must imply

$$\phi(x(k))^T P \phi(x(k)) + 2\phi(x(k))^T P A_K x(k) - \lambda x(k)^T Q^* x(k) \leq 0 \quad (3-54)$$

when  $x(t)$  is within the terminal constraint region.

The following condition is

$$\phi(x(k))^T P \phi(x(k)) + 2\phi(x(k))^T P A_K x(k) \leq (\|P\| L_\phi^2 + 2L_\phi \|P\| \|A_k\|) \|x\|^2 \quad (3-55)$$

$$\text{where } L_\phi = \sup \left\{ \frac{\|\phi(x)\|}{\|x\|} \mid x \in \Omega_1, x \neq 0 \right\}.$$

And there exists a possible  $\alpha_2 \in (0, \alpha_1]$  and  $0 < \lambda$  satisfying

$$(\|P\|L_\phi^2 + 2L_\phi \|P\| \|A_k\|) \|x\|^2 - \lambda x^T Q^* x \leq 0 \quad (3-56)$$

By combining Equations (3-55) and (3-56), the inequality (3-53) is satisfied. Thus, it is proved that the derived terminal cost matrix  $P$  and terminal cost region  $\Omega_2$  can be applied to ensure the system is asymptotically stable.

Then it is the stabilizing synthesis for the proposed SFM-based MPC framework. The stability synthesis scheme that has been introduced is further integrated with the proposed SFM-based MPC framework here. The major principles are first to obtain the terminal cost function and terminal region, and then solve the non-linear optimization problem repeatedly. The complete proposed stable MPC algorithm is described in *Algorithm 3-1*.

---

**Algorithm 3-1:** a stable SFM-based MPC algorithm

---

There exists a stable scheme for SFM-based MPC controller, and its steps are given as follows,

- 1    **Stabilization:** solve terminal cost matrix  $P$  and terminal region  $X_f$  .;
  - 2            Solve local controller with feedback gain  $K$  ,
  - 3            Obtain terminal cost matrix  $P$  ,
  - 4            Determine terminal region  $X_f$  ,
  - 5    **while** time  $K_c \geq 0$  , for each control step  $k_c$
  - 6        |    **Optimization:** solve a nonlinear optimization problem to obtain
  - 7        |    optimal control solution  $u^*$ ;
  - 8        |    **Execution:** apply the first optimal control input  $u^*(1)$  to the system.
  - 9    **end**
  - 10    Implement obtained optimal control sequence  $u^*(n)$
- 

The stability proof of the proposed algorithm is omitted since it can be simply verified by *Lemma 3-1*.

# CHAPTER 4. CONNECTED VEHICLE-BASED SIGNAL CONTROL IMPLEMENTATION AND EVALUATION PLATFORM

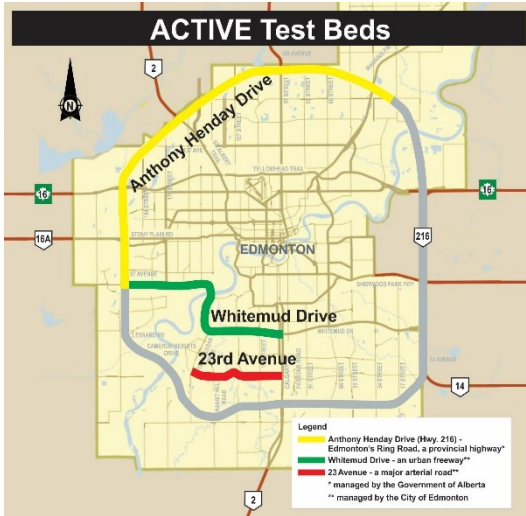
To evaluate the performances of the proposed traffic models and control methodology, both field tests and simulation evaluations have been conducted. The field tests have been conducted using the ACTIVE CV testbed in Edmonton, Alberta, Canada (144). To further investigate the comprehensive and complex scenarios that have limited scope for implementation in the field tests, simulation evaluations have been implemented by deploying a traffic simulator. The following contents describe the ACTIVE Connected Vehicle (CV) environment, on-site in-the-loop test environments, experimental prototypes, and the field CV data design and collection method, respectively.

## 4.1 ACTIVE CONNECTED VEHICLE ENVIRONMENT

The ACTIVE CV testbed network provides facilities for cutting-edge learning opportunities and hands-on experience in connected vehicle technology and applications, working towards improved safety, efficiency, and sustainability<sup>4</sup>. The testbed network includes highway, freeway, arterial road sections, and local road sections. It has more than 42 RSE units along 60 km of roadway. These testing facilities provide high-quality connectivity between infrastructure and vehicles, where its connectivity structure is shown in Figure 4-1.

---

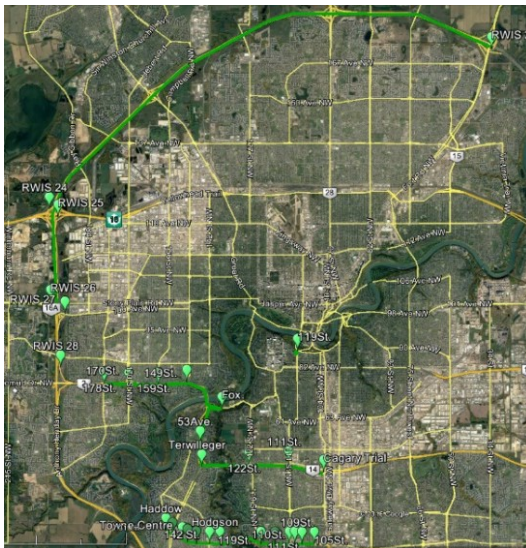
<sup>4</sup> <https://www.ualberta.ca/engineering/research/groups/smart-transportation/research/projects/connected-vehicles>



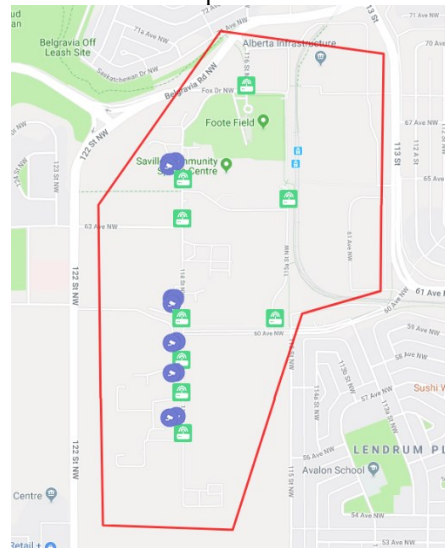
(a) the ACTIVE CV test tracks on public roads



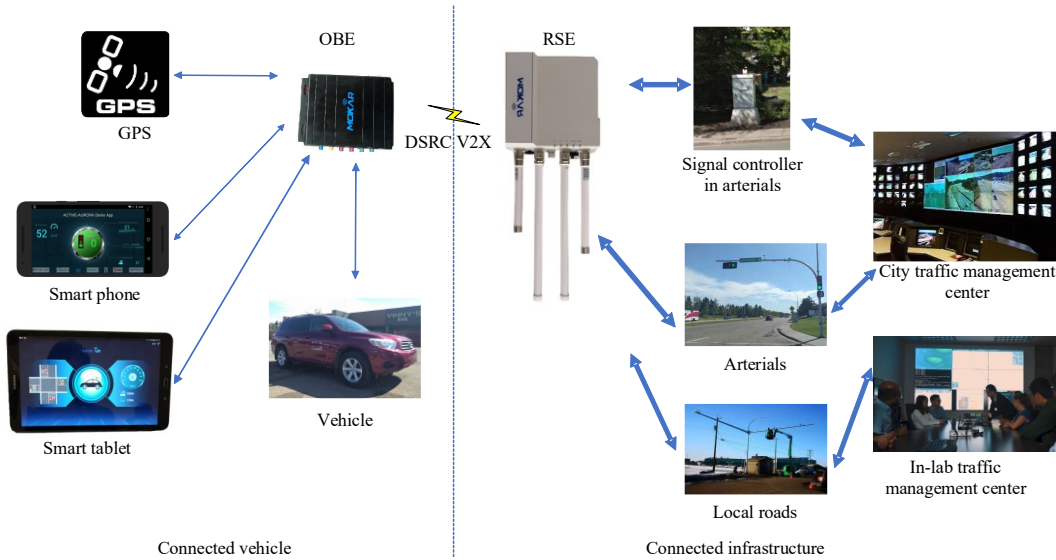
(b) the ACTIVE CV test track on private campus roads



(c) RSE locations (green pins)



(d) RSE locations (green icons)



(e) an overview of the connected vehicle environment

**FIGURE 4-1. Connected vehicle environment in the ACTIVE testbed (a-b) CV test tracks (b-c) RSE locations (e) an overview of the connected vehicle environment.**

As shown in Figures 4-1(a) and (b), both public roads and private campus roads are included in the ACTIVE CV testbed network, marked by different lines with different colors. These specific roads are portions of the University of Alberta South Campus, Anthony Henday Drive, Whitemud Drive, and 23<sup>rd</sup> Avenue in Edmonton, Alberta.

Then Figures 4-1(c) and 4-1(d) show the installation locations of RSE units for the public and private roads, respectively. There are more than 30 RSE units along the public roads and more than ten units along the private roads. They are marked by green notations in both figures. These RSE units are between 0.5 and 2 kilometers apart along each corridor, depending on the type of roadway.

Finally, the overview of the connected vehicle environment in the ACTIVE CV testbed is presented in Figure 4-1(e). The CV environment includes two fundamental components to provide advance connectivity: *connected vehicle* and

*connected infrastructure*. These two elements physically communicated with each other via two new types of devices: OBE and RSE.

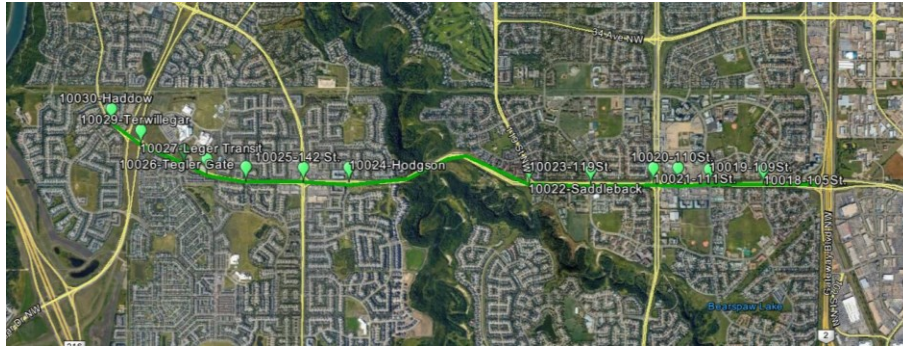
The OBE is installed inside one vehicle, connected to a built-in GPS module, and communicates using a human-machine interface (HMI), including smartphones and smart pads. Via this device, the CV can share vehicle position data, vehicle motion data, and vehicle signal request data with other CVs as well as the roadside infrastructure. The RSE is installed at each signalized intersection, connected to a nearby roadside signal controller, and communicates with a traffic management center (TMC). Then, the connected infrastructure broadcasts SPaT data, structure geometric description data, and Signal Request Status data. The OBE and RSE exchange data by dedicated short-range communication (DSRC).

In summary, the *connected vehicle* and *connected infrastructure* together in the CV environment are integrated as a closed-loop control platform to implement and evaluate the proposed CV-based signal control methods for improvements to the performance of the existing urban signal control systems.

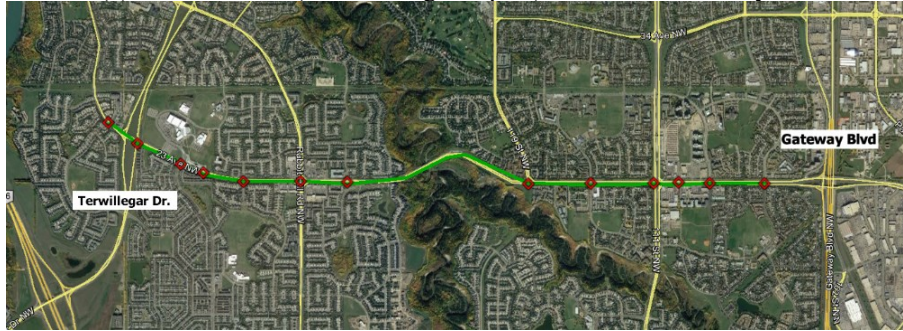
## **4.2 ON-SITE EVALUATION ENVIRONMENT FOR IN-THE-LOOP TESTS**

After the overview of the ACTIVE CV environment, two detailed on-site evaluation environments are provided for field in-the-loop tests in this sub-section. One is located along 23<sup>rd</sup> Avenue, and another is at the South Campus. These two study areas are selected because they are both major roads, where one is a major arterial road, and the other one is the major local road. For these two study areas, the locations of connected infrastructure and geographical information are presented in Figure 4-2. The connected infrastructure includes RSE and signal controllers. All of the RSE are connected to either the traffic management center (TMC) of the City of Edmonton or a traffic management server at the University of Alberta.

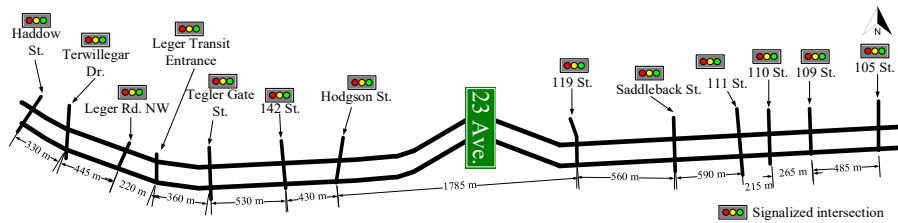
Figure 4-2(a-c) presents the location data of connected RSE and signal controllers, as well as the geographical information data of the study area along 23<sup>rd</sup> Avenue. Specifically, there are 13 traffic controllers on 23<sup>rd</sup> Avenue, which are spaced 200-500 meters apart along 23<sup>rd</sup> Avenue from 105<sup>th</sup> Street to Haddow Street. Similarly, Figure 4-2(d-f) shows the same information for study areas on South Campus. Specifically, several recently installed signal controllers were permanently connected with RSE on the private roads in the South Campus, which were spaced 50-300 meters apart.



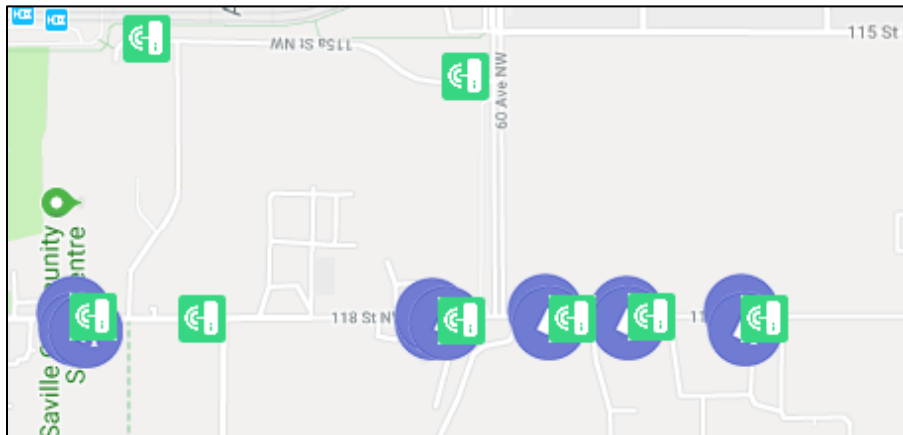
(a) RSE locations (denoted as green pins) in 23<sup>rd</sup> Avenue study area



(b) traffic controller locations (denoted as red pins) in 23<sup>rd</sup> Avenue study area



(c) detailed geometric structure of the study area in 23<sup>rd</sup> Avenue



(d) RSE locations (green icons) in the South Campus study area



(e) traffic controller locations (red icons) in the South Campus study area



(f) detailed geometric structure of the study area on the South Campus

**FIGURE 4-2. Locations of connected infrastructure ( RSE units and controllers ) along the test roads in (a-c) 23<sup>rd</sup> Avenue and (d-f) South Campus.**

RSE setups in intersections of both the 23<sup>rd</sup> Avenue and South Campus locations were already completed. Specifically, machinery and electronic installations of RSE, as well as communication connections between online controllers and RSE were already functioning. OBE setups inside vehicles were also complete.

Given the sufficiently advanced CV environment now installed on these major roads, the next step is to design efficient prototypes for in-the-loop tests to verify the proposed CV-based signal controls.

### 4.3 DESIGN AND IMPLEMENTATION OF IN-THE-LOOP TESTS

This section provides four designed prototypes for closed-loop evaluations based on in-the-loop tests. The in-the-loop test includes hardware-in-the-loop (HIL) and software-in-the-loop (SIL) tests. HIL evaluates the basic and field functioning operations of the proposed model and control strategies considering the limited deployment of CVs. SIL justifies the comprehensive functioning performance of the proposed CV-based signal control in complex conditions. All of the in-the-loop tests are in closed-loop control environments since the MPC is a closed-loop control methodology.

An overview of the in-the-loop testing platform is given first to briefly understand the in-the-loop test concept, which is then followed by different specific prototypes.

#### 4.3.1 An Overview of the In-the-loop Testing Prototypes

The overview of the in-the-loop testing framework is given in Figure 4-3.

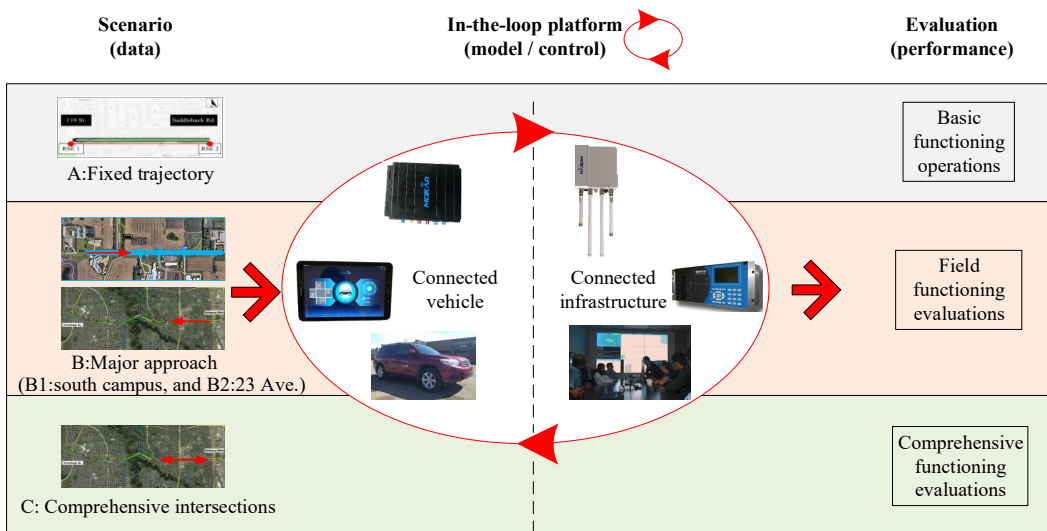


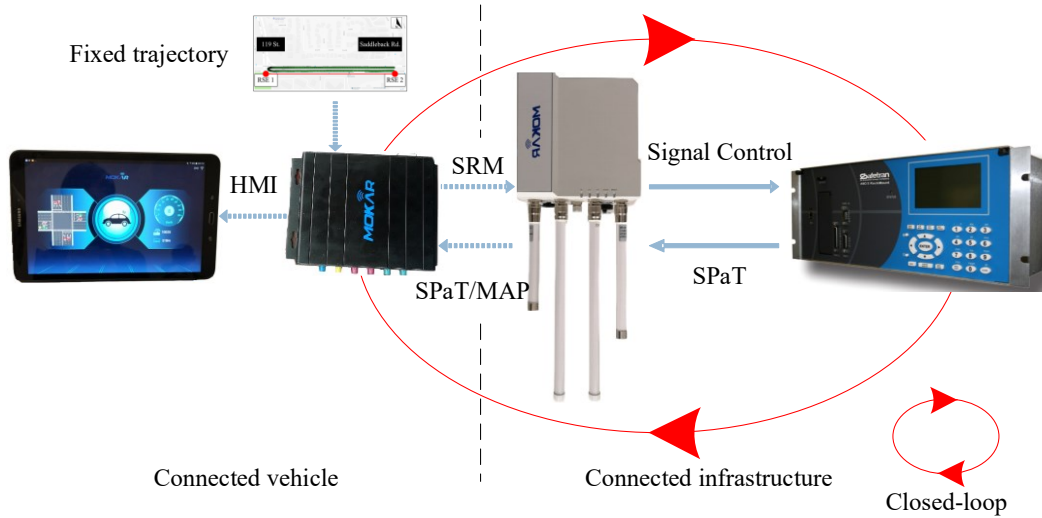
FIGURE 4-3. An overview of the in-the-loop testing prototypes in the CV environment.

As shown in Figure 4-3, the prototype includes three parts: 1) a scenario representing different data inputs, 2) an in-the-loop platform representing the model and control strategy, and 3) an evaluation purpose representing different levels of performance evaluations.

In terms of evaluation levels, the in-the-loop testing prototypes are divided into three levels using three typical types of scenarios. Test scenario A evaluates basic functioning operations using fixed trajectories captured on the road. Test scenario B evaluates typical field functioning performances for one major approach on each of the public and private roads (B1 and B2). Test scenario C evaluates the comprehensive functioning performance for complex signalized conditions on public roads. The three levels of evaluation present a fundamental step-by-step justification for the CV-based signal control methodology.

#### **4.3.2 Laboratory Hardware-in-the-loop (HIL) Platform for Basic Functioning Tests (Scenario A)**

An in-lab prototype of the real-time CV-based signal control is designed and implemented. This in-lab hardware-in-the-loop (*In-lab HIL*) prototype is used for the current basic phase operation evaluations. Only historical fixed trajectory data are used as inputs for the base functioning test. This prototype is shown in Figure 4-4.



(a) the hardware-in-the-loop (HIL) prototype



(b) SPaT, vehicle motion, and map information demonstrated by an illustrative interface prototype



(c) phase operation, e.g., green hold status in the controller interface

**FIGURE 4-4. An in-lab hardware-in-the-loop (HIL) prototype.**

As shown in Figure 4-4(a), the controller, RSE, and OBE were connected strictly according to the field installations in a lab demo. Messages such as SPaT messages, MAP messages, and Signal Request Message (SRM) messages are transmitted between devices by following the SAE J2735 message standard.

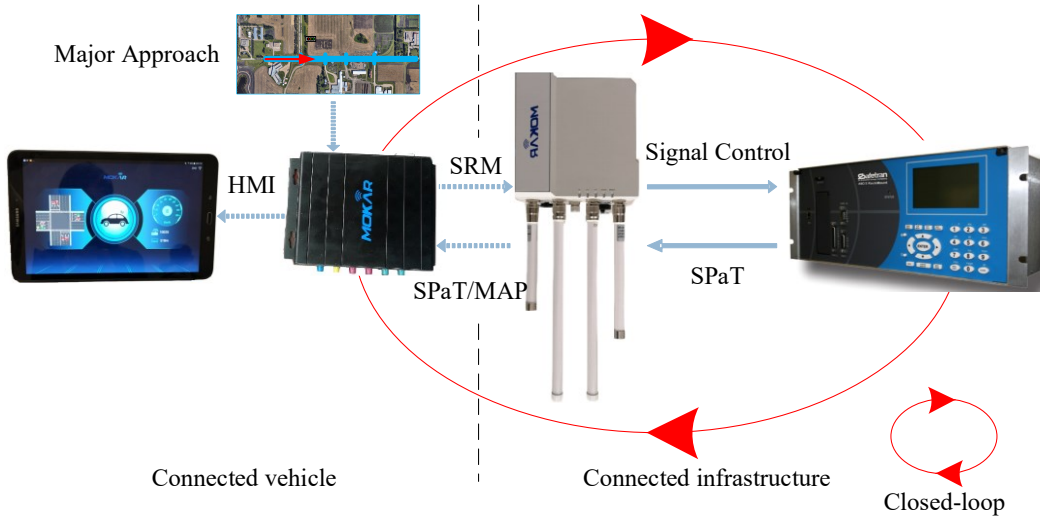
OBE reads the SPaT and Map data from the RSE. At the same time, the OBE sends visualization data to a smart pad through a Wi-Fi connection. The visualization data in the smart pad is shown in the bottom left of Figure 4-4(b).

Meanwhile, OBE sends real-time BSM data, including trajectories and motion data, to the RSE. Here, to simplify the evaluations, only historical fixed

trajectory data are used as inputs for the basic functioning test. Then, the RSE operates two primary processes, where one is the intersection-level optimization, and the other is the corridor-level optimization. After that, the traffic controller receives the final optimization-based phase operation commands from the traffic controller interface, including *vehicle call*, *force-off*, *omit*, and *hold-on*. The results of these commands are depicted in the traffic interface, and one example of these results - titling phase *hold-on* - is shown in the bottom right of Figure 4-4(c).

### **4.3.3 Field Hardware-in-the-loop (HIL) Platform for One Major Approach Tests (Scenario B)**

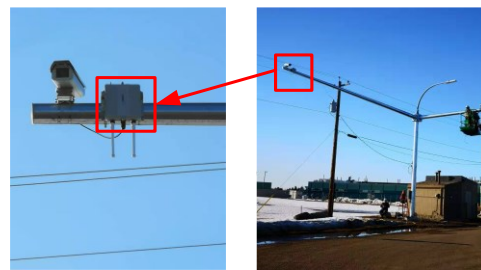
Field hardware-in-the-loop (HIL) testing prototypes are designed to test the typical field functioning performance of one major approach on public and private roads. Scenario B is further divided into two specific cases: sub-scenario B1 represents the study area along 23<sup>rd</sup> Avenue, and sub-scenario B2 represents the study area on South Campus. The details of these two sub-scenarios are shown in Figure 4-5 and Figure 4-6, respectively. Both scenarios are HIL tests but with slight differences considering the safety guarantees. The former HIL test is a full-closed-loop control environment, and the latter one is a semi-closed-loop environment.



(a) A field hardware-in-the-loop platform for closed-loop tests



(b) Test vehicle with OBE



(c) Installed RSE on the top of the traffic pole



(d) SPaT, vehicle motion, and map information demonstrated by an illustrative interface prototype



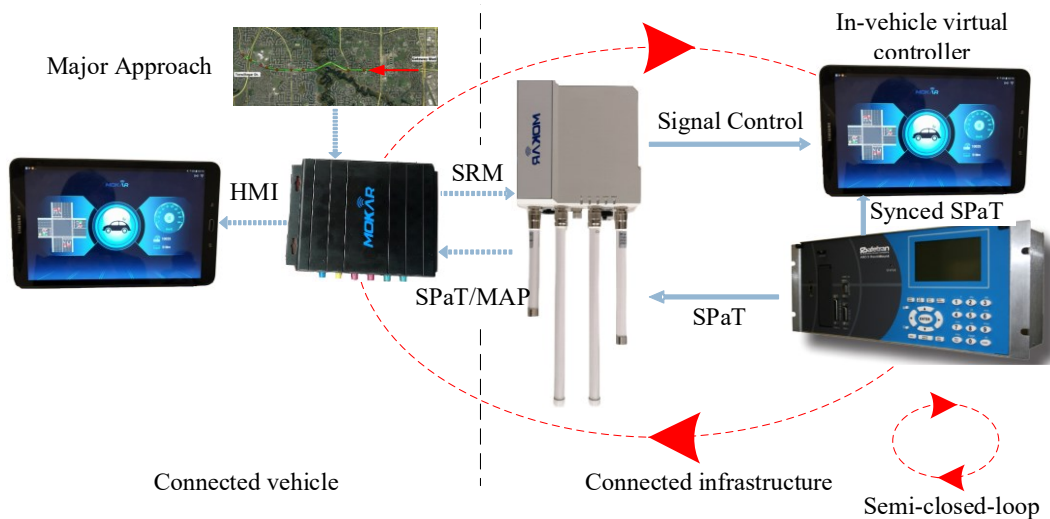
(e) Cable communication between RSE and controller via the additional switch device

**FIGURE 4-5. Field implementation and closed-loop test in South Campus (Scenario B1).**

As shown in Figure 4-5 sub-scenario B1, the control strategy is operated in a full-closed-loop control since the South Campus possesses safe, ultra-low traffic flows on the roads.

Figure 4-5(a) presents the closed-loop test procedure on one major approach on South Campus. As for the connected infrastructure, Figure 4-5(c)

shows that the RSE units are installed on the top of the traffic poles, and the connected signal controller is situated in a nearby computer room shown in Figure 4-5(e). Figure 4-5(b) shows the OBE is placed inside the test vehicle. After receiving processed visualization information from the OBE, the information is conveyed via a human interface on a smartphone ( Figure 4-5(d) ). The field tests are then conducted on one major approach in the study area on South Campus.



(a) A field hardware-in-the-loop platform for *semi-closed-loop* tests.



(b) Test vehicle with OBE



(c) Installed RSE on the top of the traffic pole



(d) SPaT, vehicle motion, and map information demonstrated by an illustrative interface prototype



(e) Cable communication between RSE and controller via the additional switch device

**FIGURE 4-6. Field implementation and semi-closed-loop test in 23<sup>rd</sup> Avenue (Scenario B2).**

As shown in Figure 4-6 sub-scenarios B2, its control environment is semi-closed-loop control due to the safety issues when testing on a public road such as 23<sup>rd</sup> Avenue. In this semi-closed-loop control, a phone-simulated controller synchronized with a real signal controller is used to implement the generated phase commands. This makes the final controlled object an online synchronized phone-simulated controller. Since the phone-simulated controller is always synchronized with the online signal controller, it is recognized as an efficient way to show the control results without disturbing the road traffic and compromising traffic safety.

Figure 4-6(a) presents the semi-closed-loop test procedure on one major approach along 23<sup>rd</sup> Avenue. As for the connected infrastructure, Figure 4-6(c) shows that the RSE units are installed on the top of the traffic poles, and the connected signal controller is situated in a roadside cabinet shown in Figure 4-6(e). Figure 4-6(b) shows the OBE is placed inside the test vehicle. After receiving processed visualization information from OBE, the information is displayed via a human interface on a smartphone ( Figure 4-6(d) ). The field tests are conducted on one major approach in the study area along 23<sup>rd</sup> Avenue.

#### 4.3.4 Complex Software-in-the-loop (SIL) Platform for Comprehensive Traffic Tests (Scenario C)

In addition to what has been just described, a complex software-in-loop (*Complex SIL*) simulation platform with both arbitrary scenarios and advanced algorithm plugins was developed, which is shown in Figure 4-7. SIL justifies the comprehensive functioning performances of the proposed CV-based signal control in complex conditions when safety concerns are a consideration. Compared with the previous simple version, this updated, complex platform includes a traffic simulator (i.e., SUMO/SUMO-GUI (145) ) and an advanced algorithm developing tool (i.e., Matlab- and Python-based tool). They are connected by the TraCI (**Traffic Control Interface**) for data exchanges. The structure between the traffic simulator and the algorithm platform is demonstrated in Figure 4-7.

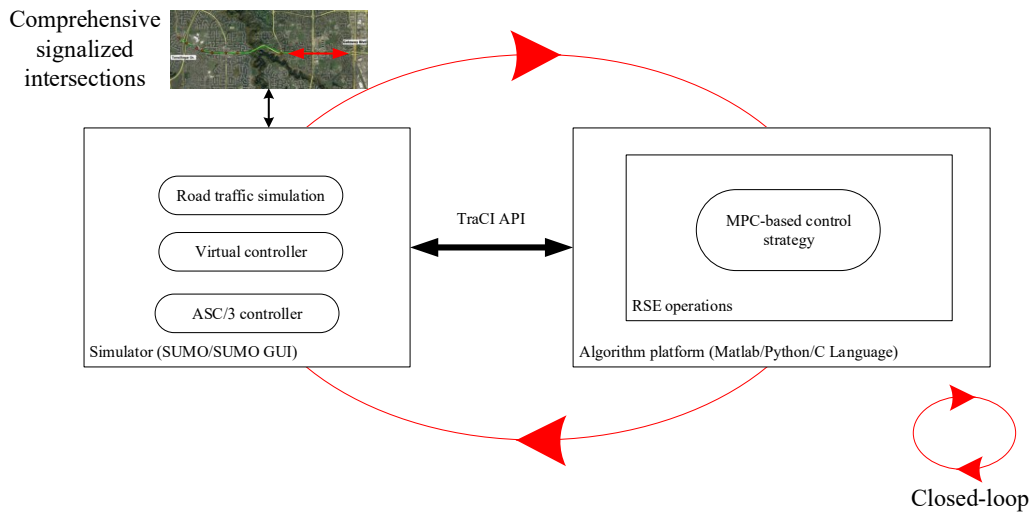
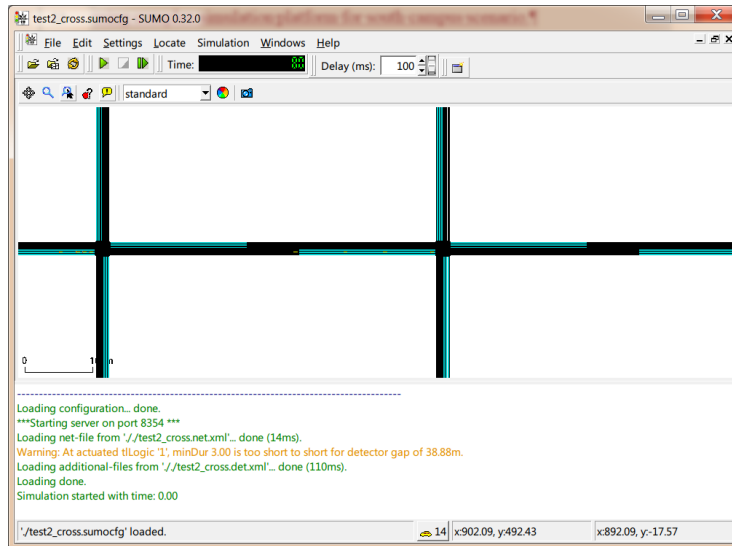


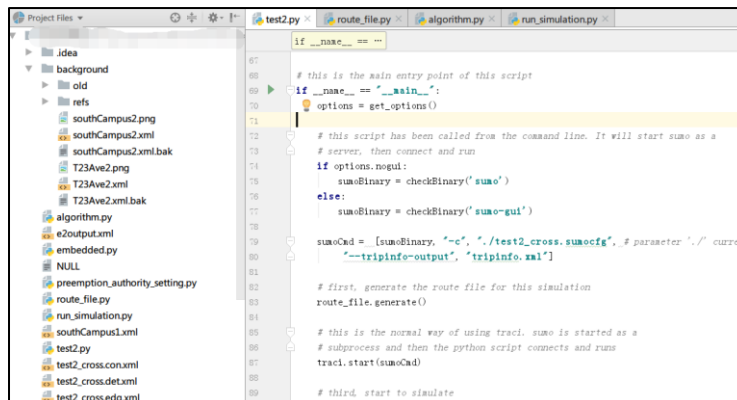
**FIGURE 4-7. Complex software-in-the-loop prototype for comprehensive traffic scenarios.**

Furthermore, the following figures demonstrate simulation designs by using the complex simulation platform in the South Campus scenario. As shown in Figure 4-8(a), two intersections in the study area are built by SUMO. This figure gives a simulation scenario with fixed demand inputs. The SUMO sends and receives SPaT

data by TraCI API. Figure 4-8(b) shows a screenshot of programming codes for the simulations. These codes are used to facilitate communication between SUMO and Matlab for state and control data exchanges.



(a) two intersections in the South Campus study area by SUMO



(b) traffic information extractions and exchange process by python

**FIGURE 4-8. Scenario design using the SIL test platform.**

## 4.4 FIELD CV DATA DESIGN AND COLLECTION

This sub-section presents the field CV data design and collection using the standard SAE J2735 message set. Then, the generation processes of boundary demand and turning rate profiles are demonstrated for practically comprehensive performance evaluations of the proposed models and control strategies on 23<sup>rd</sup> Avenue.

### 4.4.1 Standard CV exchange data design and implementation via SAE J2735

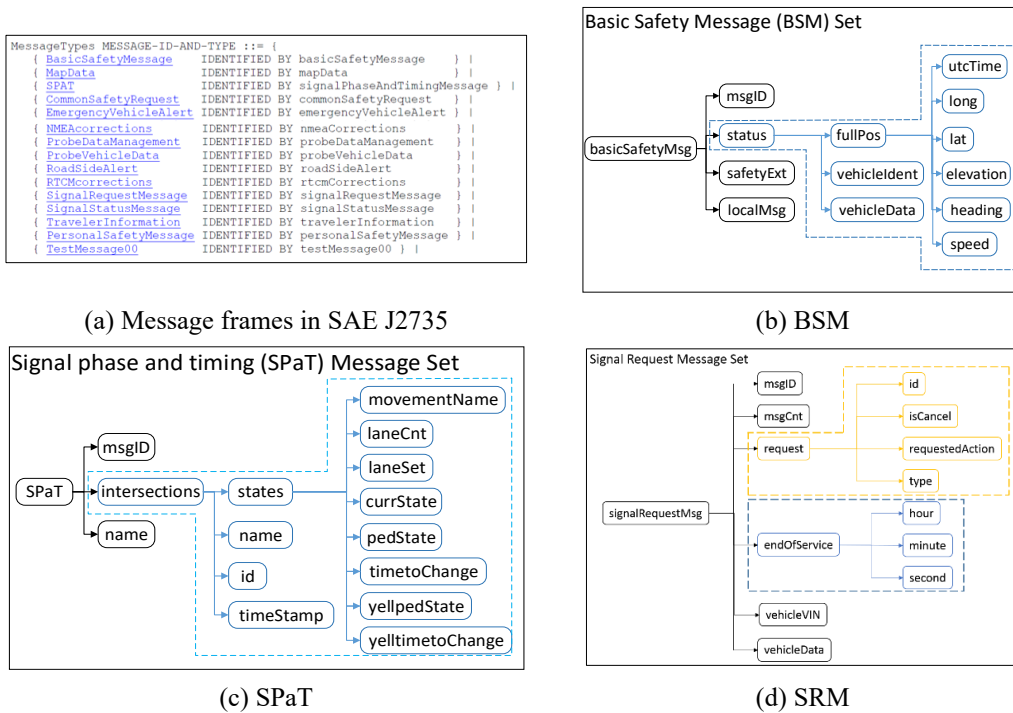


FIGURE 4-9. Standard communication message sets for field implementations (a) message frames for different standard messages in SAE J2735 (b-d) partially selected data frame's structure of implemented BSM, SPaT, and SRM message.

Firstly, a summary of the message frames in J2735 is given in Figure 4-9(a).

There are some key messages that needed to be implemented to support the

CV-based signal control in the field. Figure 4-9(b-d) presents the data frame's structures of three implemented typical message evaluated in the field (2, 146, 147), which are BSM, SPaT, and SRM, respectively. These structures described the parameters of the connected infrastructure and the CV in the control loops.

#### 4.4.2 Field CV data collection

Using test vehicles, over ten rounds of field tests were conducted in order to collect field data between the years of 2017 and 2020. During each test, BSM, SRM, and video data were collected simultaneously. There were more than 20 hours of video data, BSM message data, and SRM message data for analysis.

Continuous SPaT and offset data were possible since the RSE was connected to the online controller on 23<sup>rd</sup> Avenue. The cumulative time period of these two data types exceeds 10 months.

In summary, there were five types of data collected: 1) BSM data, 2) SRM data, 3) video data, 4) SPAT data, and 5) offset data. The final amount of each data is summarized in the following table:

Data type	Description and cumulative time period of data	
BSM data	30 times field tests with test vehicles were conducted to collect field data	40 hours
SRM data		
Video data		
SPAT data	one year	one year
Offset data		

**TABLE 4-1. Summary of the collected field data.**



# CHAPTER 5. EVALUATION RESULTS AND ANALYSIS

This section provides performance evaluations from different perspectives. At first, the results of the field CV environment and basic functioning tests in scenario A are demonstrated. Then, the field results of one major approach test in scenario B are presented considering safety and traffic demand conditions. Last, the comprehensive results and an analysis of more complex conditions are presented to provide a reliable validation of the proposed methodology.

## 5.1 RESULTS OF THE BASIC FUNCTIONING TESTS <sup>5</sup> (SCENARIO A)

First, the results of the field CV environment and basic functioning tests in scenario A are depicted in Figures 5-1, 5-2, and 5-3.



(a) RSE communication coverage of the ACTIVE CV testbed except for the South Campus area

(b) The connectivity of the target intersections in 23<sup>rd</sup> Avenue study area

**FIGURE 5-1. The connectivity performance of the study areas.**

Figures 5-1(a) and (b) depict an overview of the communication coverage over the entire ACTIVE CV testbed on open roads (except the South Campus area),

<sup>5</sup> This sub-chapter includes edited contents of the articles J6, J7, and J8.

as well as where the communication coverage was identified by the received signal strength data, extracted from standard messages. From these coverage results, it is clear that overlaps are a common phenomenon. In detail, Figure 5-1(a) depicts the detailing of signal strength distribution information over the target arterial segment, where good connectivity in the study area are clearly demonstrated and recognized. Thus, there is a solid foundation of good connectivity for promoting CV-based signal control. Similar signal strength distributions of the ACTIVE CV testbed's private roads on South Campus are also achieved in the field.

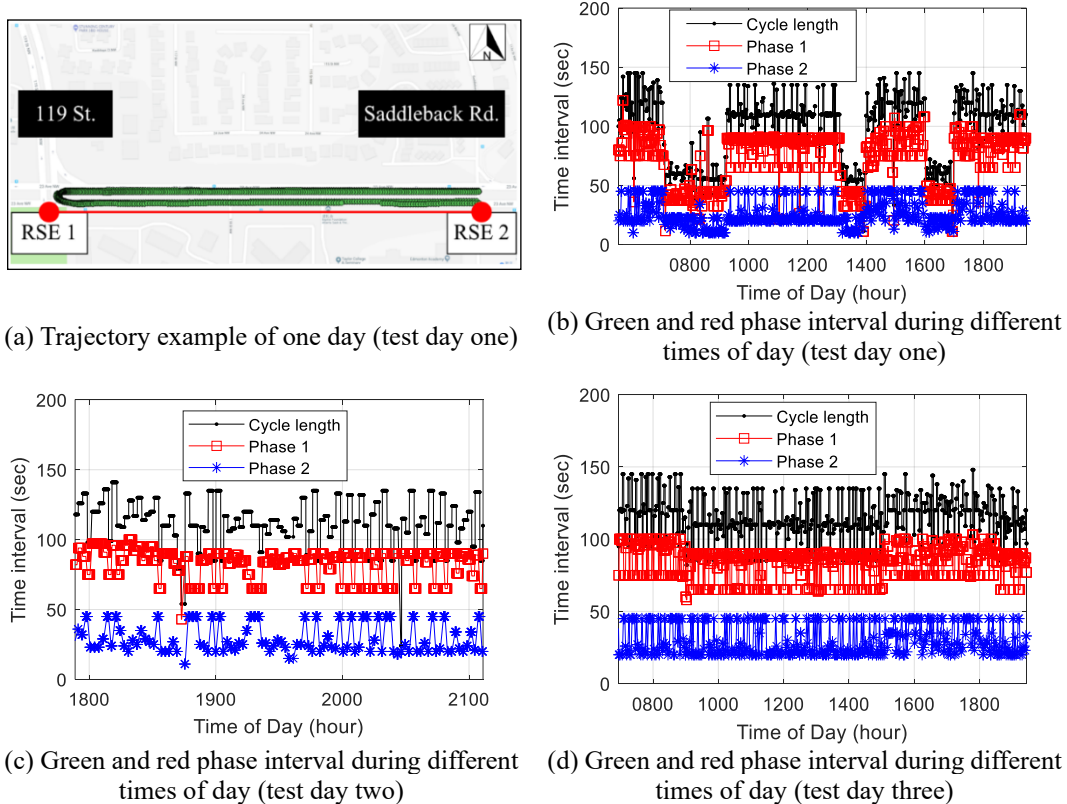


**FIGURE 5-2. Functioning results of the trajectories and phase intervals (a) one-day trajectory example from BSM data (b-d) green and red phase intervals for different days from SPaT data.**

Figure 5-2 shows the functioning vehicle trajectory and phase interval results obtained from BSM message and SPaT message data, respectively. As

shown in Figure 5-2(a), the vehicle trajectories generated from BSM data are illustrated over the study link, in which the high frequency of BSM message data leads a detailing position distribution over the study area. This dense position data offers flexibility for further vehicle detection. On the other hand, Figure 5-2(b-d) shows green intervals, red intervals, and cycle lengths during different times of the day over several days. Three test days were 16<sup>th</sup>, 18<sup>th</sup> in April and 20<sup>th</sup> in July 2018 (i.e., the test days 1, 2, and 3), respectively. These figures reflect fluctuations of signals over both different times of the day and different days.



(a) Map and vehicle motion information



(b) Signal request message (SRM, marked as a star inside the dashed box)



(c) Phase operation (e.g., green hold) status in the controller interface



(d) Phase operation (e.g., green hold) status in smartphone interface (screenshot)

**FIGURE 5-3. Basic functioning test results.**

Then, Figure 5-3 demonstrates typical basic functioning test results. Figures 5-3(a) and (b) present an illustrative graphical human-computer interface prototype. Figure 5-3(a) demonstrates that the interface can depict map and vehicle motion information. Figure 5-3(b) illustrates that the real-time SPaT and priority request, marked as a star in the dashed box, appeared when the vehicles were

approaching the target intersection. These received data, e.g., SPaT and BSM, were recorded for further quantitative analysis.

After that, Figures 5-3(c) and (d) show some results of signal phase operation examples on the signal controller and the smartphone's human interface, respectively. The traffic controller receives the final optimization-based phase operation commands from the traffic controller interface, including the aforementioned vehicle *call*, *force-off*, *omit*, and *hold-on*. The results of these commands are depicted on the traffic interface, with one example shown in the bottom right of Figure 5-3(c). At the same time, the phase operations are also shown on the smartphone human interface, as in Figure 5-3(d) that displays the result of the phase *hold-on* operation.

## 5.2 FIELD RESULTS OF ONE MAJOR APPROACH TESTS<sup>6</sup> (SCENARIO B)

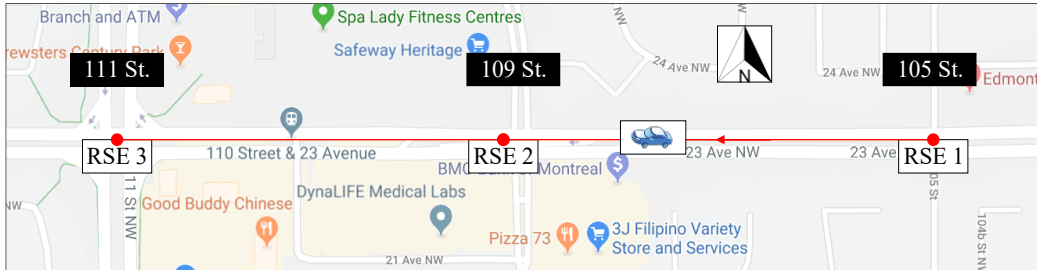
In this section, the field results of one major approach test scenario that considers safety in single-connected-vehicle conditions are presented. The field results verify and support the proposed method for one major approach conditions, named the proactive vehicle signal priority control.

First, the *field implementations* were conducted in a representative arterial scenario on the ACTIVE CV pilot testbed and on a typical local road on South Campus, in Edmonton, Canada (146, 148). Three standard message types of vehicle and infrastructure data were accessible in real-time: 1) vehicle position and motion data were transmitted via basic safety messages (BSMs), 2) signal controller status was broadcast via SPaT messages, and 3) priority request and status were exchanged by SRM and SSM. Figure 5-4 gives a summary of the field implementation and trajectory results.

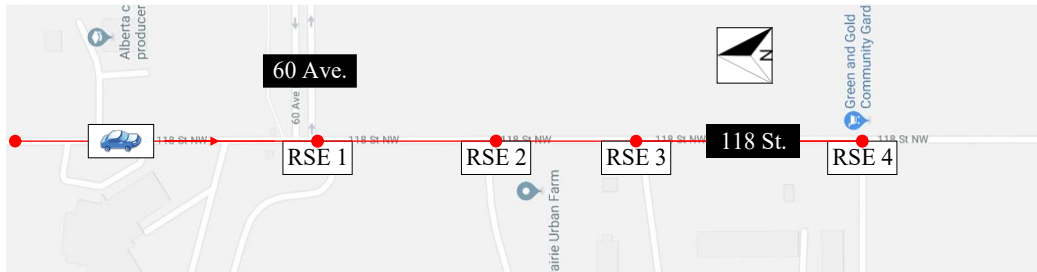
As shown in Figure 5-4(a), the field test was conducted on a major arterial segment located along 23<sup>rd</sup> Avenue NW between 105<sup>th</sup> Street and 111<sup>th</sup> Street. The corresponding vehicle trajectories during the closed-loop control are illustrated in Figure 5-4(c). Similarly, Figure 5-4(b) shows that other field tests were conducted on a typical local road on South Campus, and Figure 5-4(d) illustrates the corresponding vehicle trajectories during the closed-loop control.

---

<sup>6</sup> This sub-chapter includes edited contents of the articles J6, J7, and J8.



(a) Geometric layout of the target link and the corresponding field setup (23<sup>rd</sup> Avenue)



(b) Geometric layout of the target link and the corresponding field setup (South Campus)



(c) Vehicle trajectories during semi-closed-loop control (23<sup>rd</sup> Avenue)



(d) Vehicle trajectories during closed-loop control (South Campus)

**FIGURE 5-4. Field trajectory results ( 23<sup>rd</sup> Avenue and South Campus).**

Then, the quantitative performances of both the closed-loop and semi-closed-loop control are presented in two tables as follows.

First, the quantitative performance results of the semi-closed-loop control are presented in Table 5-1. Here, the semi-closed-loop control was introduced to verify the efficiency of the proposed method on public roads in a real-world, urban environment. In these semi-closed-loop tests, the test vehicle equipped with the OBE unit was running on the road and interacted with local signals and surrounding traffic. The OBE broadcasts the priority requests to neighboring RSE within its

communication coverage. Then, the RSE sent the received priority requests to the local signal controller. To mitigate any safety risks, the corresponding local signal controller received the priority requests but did not trigger phase operations. These phase operations were triggered and completed by a simulated signal controller inside the smartphone interface prototype application. The phone-simulated-controller synchronized its SPaT information when there were no priority requests.

Test round	Open-loop control without priority (before)		Semi-closed-loop priority (after)
	Free-flow travel time (sec)	Travel time with the local controller (sec)	Travel time with the phone-simulated-controller (sec)
Round 1	30s	79s	33s (-46s)
Round 2	30s	35s	35s (-0s)
Round 3	30s	52s	33s (-19s)
Round 4	30s	68s	36s (-32s)
Round 5	30s	44s	33s (-11s)
Average	30s	55s	34s (-21s)

**TABLE 5-1. Vehicle delay in the semi-closed-loop control ( 23<sup>rd</sup> Avenue )**

The quantitative results are outlined in Table 5-1 over the three columns. Column 1 illustrates the theoretical free-flow travel time for each round, where the speed limit is 60 km/h on the selected road segment. Column 2 presents the actual travel time with the local controller, showing that most of those times were higher than the theoretical free-flow travel times. Since the local controller did not trigger the phase operations, these results were reasonable in the open-loop control without priority. Column 3 demonstrates that travel times with the phone-simulated-controller were consistently shorter than the actual travel time with the local controller, demonstrating the reduced-delay benefits were notable.

Thus, the results demonstrate that the proposed priority control had a better delay performance during the field tests on public roads in a real-world urban environment.

Test round	Open-loop control without priority (before)		Closed-loop priority (after)
	Free-flow travel time (sec)	Travel time with the local controller (sec)	Travel time with the signal controller (sec)
Round 1	97s	119.5s	97s (-22.5s)
Round 2	97s	119.5s	97s (-22.5s)
Round 3	97s	119.5s	98s (-21.5s)
Round 4	97s	119.5s	100s (-19.5s)
Round 5	97s	119.5s	99s (-20.5s)
Average	97s	119.5s	98.2s (-21.3s)

**TABLE 5-2. Vehicle delay in the closed-loop control ( South Campus )**

Then, the quantitative performance results of the closed-loop control are presented in Table 5-2. Here, the closed-loop control was introduced to verify the efficiency of the proposed method on private local roads in a real-world, urban environment. In the closed-loop control, the signal control sends the SPaT data, and executes the signal priority commands, e.g., phase hold-on operation, simultaneously.

The quantitative results are outlined in Table 5-2 over the three columns. Column 1 illustrates the theoretical free-flow travel time for each round, where the speed limit is 30 km/h on the selected road segment. Column 2 presents the actual travel time with the local controller, showing that most of those times were higher than the theoretical free-flow travel times. Since the local controller did not trigger the phase operations, these results were reasonable in the open-loop control without

priority. Column 3 demonstrates that travel times with the real signal controller were consistently shorter than the actual travel time with the local controller. Consequently, the reduced-delay benefits were notable. The results demonstrate that the proposed proactive priority-based signal control had a better delay performance during the preliminary field tests on public roads in a real-world urban environment.

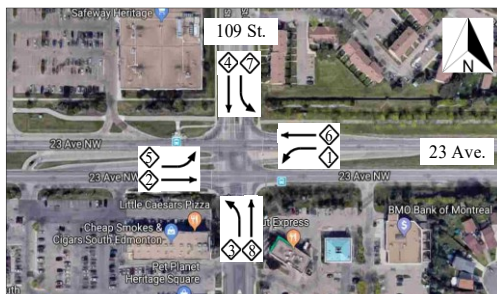
In summary, as shown in two tables, both the semi-closed loop control in 23<sup>rd</sup> Avenue (Scenario B2) and the closed-loop control in South Campus (Scenario B1) can decrease the travel times, which verifies the efficiency of the proposed CV-based signal control methods.

## 5.3 COMPREHENSIVE RESULTS OF COMPLEX CONDITIONS (SCENARIO C)

Taking safety risk and traffic demand considerations into account, only semi-closed-loop and closed-loop tests were conducted in the field with limited testing times. Thus, to further investigate the performance of the proposed method for different conditions, comprehensive simulations were implemented, and corresponding results are outlined in this sub-section. As mentioned in the previous chapter, to comprehensively verify the efficiency of the proposed algorithm, the software-in-loop (SIL) simulation platform with the selected corridor scenario and proposed advanced algorithm was designed and developed. Corresponding results are demonstrated in this chapter.

### 5.3.1 Results of the Proposed Adaptive Signal Control

This sub-section provides an account of the evaluation process coupled with a results analysis.



(a) Signal phase diagram and geometric layout of the target intersection

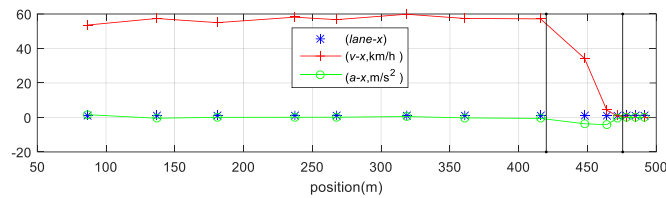


(b) RSE locations (green pins), the geometry (background picture), target intersection (dashed box), and a network representation (black lines) in SUMO traffic simulator

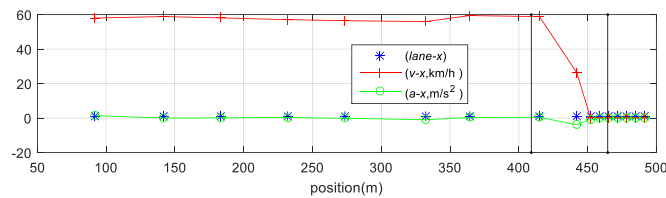
**FIGURE 5-5. Simulation setup for complex conditions: a target corridor consisting of multiple signalized intersections at the ACTIVE testbed.**

A target signalized intersection located at 109<sup>th</sup> St. and 23<sup>rd</sup> Ave. within the ACTIVE testbed (148) was selected to test the proposed algorithm, shown in Figure 5-5. Figure 5-5(a) presents the geometric layout as well as the signal phase diagram of the target intersection. As illustrated in Figure 5-5, a network representation with a built-in traffic simulator, including the corresponding components of the selected corridor, was outlined for the following simulation evaluations. The simulation platform included a traffic simulator (i.e., simulation of urban mobility - SUMO (145)) and an advanced algorithm developing tool (i.e., Matlab and Python). The SUMO traffic simulator was selected for developing and implementing the corridor scenario. At the same time, the proposed advanced algorithm, including the designed MPC controller, was developed and implemented by Matlab and Python. The simulator and algorithm tool were connected by the TraCI (traffic control interface) for essential data and parameter exchanges in real-time. To reproduce real-time exchange behavior using vehicle-to-infrastructure (V2I) communication in the CV environment, a simulated detector called e2 with a predefined length was used to cover a lane segment for capturing the vehicle motion information. The predefined length of one e2 detector was equal to the radius of the RSE communication coverage. The real-time SPaT data was obtained via the TraCI interface. Besides, to generate demand profiles, a random trip generator was applied to generate trips and corresponding routes for a given network in a defined time interval  $p$ . This means for every interval  $p$ , one vehicle drives into the network. The generated route profiles were used as demand profiles for input. For the whole

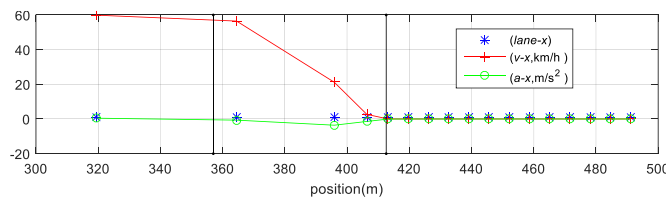
network, there were 13 input source links, where each link included three lanes. Also, the multi-entry-exit detector placed in certain areas tracked performance results of the target intersection, where both entry and exit traffic event profiles were detected. Two practical data were used, which were in-boundary flow and turning rate data from the city of Edmonton. Since the delay is widely used as a practical and significant index in transportation engineering, it is used as the major performance index in the following performance evaluations.



(a) Result at timestamp 1:  $t = t_{red1}$



(b) Result at timestamp 2:  $t = t_{red2}$

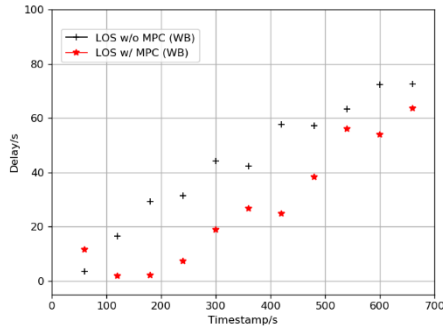


(c) Result at timestamp 3:  $t = t_{red3}$

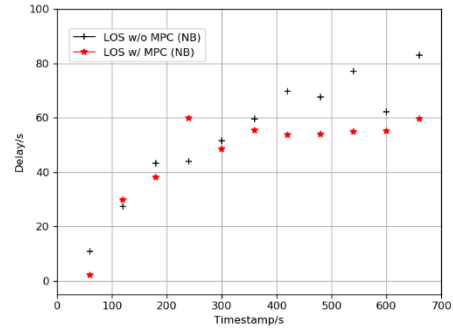
**FIGURE 5-6. Boundary estimations of the slow-down region for one approaching vehicle stream in one lane at three timestamps during a red phase.**

First, to demonstrate the efficacy of the dynamic link segmentation method, an example of the simulation results is presented in Figure 5-6. Figure 5-6 shows the estimated start and end boundary results of the slow-down region at three

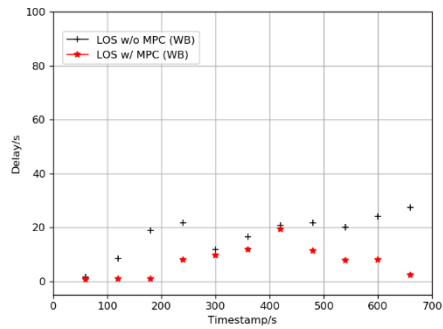
timestamps ( $t_{red1}$ ,  $t_{red2}$ ,  $t_{red3}$ ) during a red phase, where each boundary is marked as a black vertical line. The boundaries divide the approaching vehicle stream at the throughput lane into three internal regions, where the number of the throughput lane is drawn as blue star points. What is notable is that these boundaries have clear, close relationships with both the spatial-speed and spatial-deceleration diagrams. Thus, they are quantitatively identified by the proposed dynamic link segmentation method described. The spatial-speed and spatial-deceleration relationships are graphically expressed by the speed-position ( $v-x$ ) diagram and the deceleration-position ( $a-x$ ) diagram, respectively, where they are marked as red plus sign curves and green circle curves. Overall, the simulation results presented in Figure 5-6 demonstrate a good performance for the dynamic boundary segmentation. Based on this, the link state of each approach is obtained in real-time and as input for the MPC-based green split allocation within one cycle.



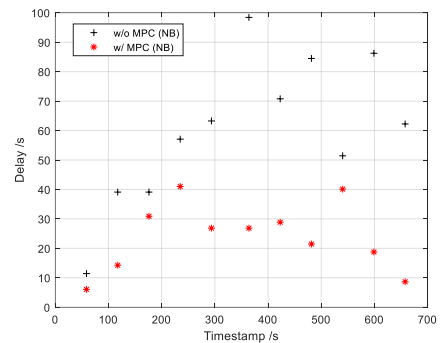
(a) delay performance of one approach of the major street (westbound, WB) in large demand condition



(b) delay performance of one approach of the minor street (northbound, NB) in large demand condition



(c) delay performance of one approach of the major street (westbound, WB) in demand level I: typical demand (small)



(d) delay performance of one approach of the minor street (northbound, NB) in demand level I: typical demand (small)

**FIGURE 5-7. Results of delay comparisons for CV-mASC (the proposed MPC-ASC with red dots, the non-MPC-method with black dots), where smaller is better.**

Figures 5-7 presents delay comparisons between the MPC-ASC and non-MPC methods for different approaches and demands from the time-dimension perspective, which are average values for five replications. As shown in two figure pairs (a)(b) and (c)(d), the proposed MPC-based ASC is more efficient with lower travel times for both major and minor approaches, when compared with the non-MPC method. Also, figure pairs (a)(c) and (b)(d) verified the efficiency of the method with lower travel times for two different traffic demands.

Following on from this, the delay performances of the target intersection with a typical demand profile are shown in Table 5-3. Column I and Column II

highlight the results of the average vehicle delays of fixed timing control and the MPC-based adaptive signal control (CV-mASC) for the westbound (WB) and northbound (NB) traffics, respectively. The prediction horizon of the MPC controller is one cycle. From the results, the MPC-based ASC (CV-mASC) method outperforms the fixed timing control for both major and minor streets. Overall, then, the MPC-based ASC (CV-mASC) method outperforms the fixed timing control for both major and minor streets for the typical demand profile with less average travel times (level of service, LOS).

<b>Control types / Delays</b>	<b>Major street (WB, sec)</b>	<b>Minor street (NB, sec)</b>	<b>Average delay (LOS, sec)</b>
Fixed timing control	53.53	70.01	35.52
Actuation control	49.55 (-4)	66.64 (-3)	30.56 (-5)
100% Pcv	18.51 (-35)	25.18 (-45)	14.78 (-21)
75% Pcv	18.71 (-35)	34.42 (-36)	17.40 (-18)
50% Pcv	18.72 (-35)	38.89 (-31)	17.53 (-18)
25% Pcv	18.97 (-35)	34.14 (-36)	17.51 (-18)
10% Pcv	19.51 (-34)	36.38 (-34)	17.62 (-18)
5% Pcv	19.52 (-34)	38.45 (-32)	17.81 (-18)
1% Pcv	25.78 (-28)	33.86 (-36)	23.42 (-12)

**TABLE 5-3. Comparison of vehicle delays for fixed timing control, actuation control, and MPC-ASC (CV-mASC) method in different penetration rate conditions, with demand type I: typical demand**

Then, the delay performance of the MPC-based ASC method is explored in different penetration rate conditions. Typical penetration rates are set at the beginning of the simulation process, drawing from 100% decreasing to 75%, 50%, 25%, 10%, 5%, and 1%. Since the CVs are randomly distributed in traffic streams, the corresponding actual penetration rates are 100%, 76%, 54%, 26%, 11%, 5%, and 1% as shown in Table 5-3 column 1. Also, since the CVs are randomly selected from the traffic streams, the simulation time horizon is extended to two-cycle lengths. When applied to the MPC-based ASC method, the average delays of the

major street, the minor street, and the whole intersection are lower than with fixed timing control (Table 5-3). Also, when the penetration rate decreases from 100% to 50%, the actual delays increase since the amount of true CV data available diminishes. The increased delays reach a peak value, and the corresponding delay benefits simultaneously achieve the minimum point. Increased delay levels mean that there are increasingly congested traffic streams. The conclusion from the results in Table 5-3, then, is that the proposed MPC-ASC demonstrates both the efficiency and sound performances in under-saturated conditions and within different penetration conditions. The average solving time is less than 0.1 seconds (i.e., around 80 *ms*), which is smaller than the typical CV communication interval.

<b>Control types / Delays</b>	<b>Major street (WB, sec)</b>	<b>Minor street (NB, sec)</b>	<b>Average delay (LOS, sec)</b>
Fixed timing control	89	123	60
Actuation control	81 (-8)	108 (-15)	53 (-7)
100% Pcv	45 (-44)	48 (-75)	26 (-34)
75% Pcv	49 (-40)	56 (-67)	30 (-30)
50% Pcv	51 (-38)	56 (-67)	30 (-30)
25% Pcv	62 (-27)	57 (-66)	36 (-24)
10% Pcv	63 (-26)	57 (-66)	36 (-24)
5% Pcv	67 (-22)	57 (-66)	38 (-22)
1% Pcv	67 (-22)	57 (-66)	38 (-22)

**TABLE 5-4. Comparison of vehicle delays for fixed timing control, actuation control, and MPC-ASC (CV-mASC) in different penetration rate conditions, with demand type II: large demand.**

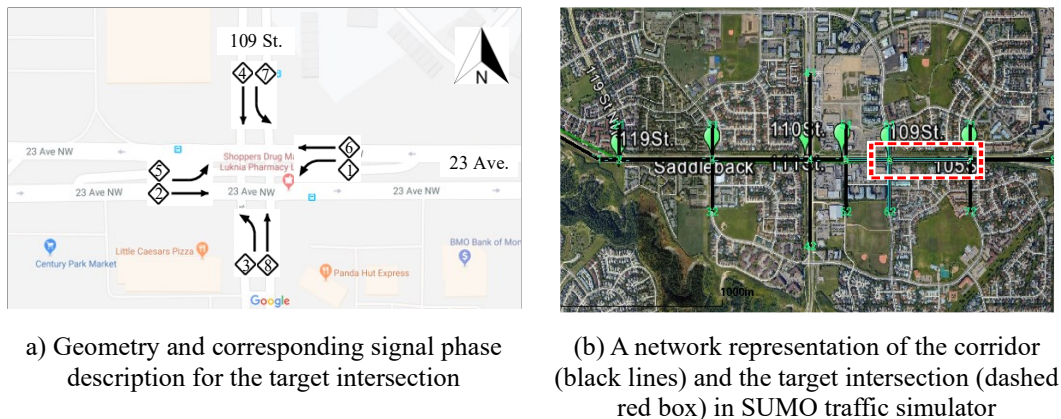
Also, this efficiency is verified for a large traffic demand, as shown in Table 5-4. The proposed CV-mASC is still efficient with lower travel times in different penetration rates in the large demand conditions.

Thus, the proposed CV-mASC is efficient for different approaches, different demands, and different penetration rates, even in a low penetration rate condition.

### 5.3.2 Results of the Proposed Signal Coordination

This section provides the simulation setup and evaluation results in different simulation scenarios, and these provided results are used to verify the efficiency of the proposed MPC-based real-time adaptive coordination control.

As shown in Figure 5-8, a signalized intersection located at 109<sup>th</sup> St. and 23<sup>rd</sup> Avenue in the ACTIVE testbed (148) was selected to evaluate the proposed method. Figure 5-8 demonstrates the geometric layout and the phase diagram of the target intersection. Further, Figure 5-8(b) presents a built network of the corridor in a traffic simulator where the relative position of the target intersection is marked by the dashed red box. The built network is used for the following simulation evaluations.



a) Geometry and corresponding signal phase description for the target intersection

(b) A network representation of the corridor (black lines) and the target intersection (dashed red box) in SUMO traffic simulator

**FIGURE 5-8. Simulation setup for the signal coordination within the ACTIVE testbed.**

Then, the performances of the target intersection via the proposed MPC-based coordination (CV-mCoordination) are presented from three different perspectives, for different approaches and with different penetration rates.

The performance for minimizing delays at the target intersection with a typical demand profile for different approaches are shown in Table 5-5. Column I and Column II present the average delays in fixed timing control and MPC-based coordination for the westbound (WB) and northbound (NB) approaches, respectively. The results show that the MPC-based coordination consistently outperformed the fixed timing control with fewer delays on the major street (i.e., WB), while it lost the reduced-delay benefits for the minor street (i.e., NB). This happened because the proposed MPC-based coordination takes greater account of the dynamic dispersion effect on the major road and minimizes its delays in the current version. Overall, the performance minimizing delays on the major street is improved by the proposed MPC-based coordination.

<b>Control types / Delays</b>	<b>Major street (WB, sec)</b>	<b>Minor street (NB, sec)</b>	<b>Average delay (LOS, sec)</b>
Fixed timing control	53.53	70.01	35.52
Actuation control	49.55 (-4)	66.64 (-3)	30.56 (-5)
100% P <sub>cv</sub>	17.76 (-36)	22.09 (-48)	15.30 (-20)
75% P <sub>cv</sub>	18.41 (-35)	23.45 (-47)	16.95 (-19)
50% P <sub>cv</sub>	18.90 (-35)	35.71 (-34)	17.67 (-18)
25% P <sub>cv</sub>	20.79 (-33)	44.70 (-25)	20.71 (-15)
10% P <sub>cv</sub>	21.18 (-32)	36.09 (-34)	21.35 (-14)
5% P <sub>cv</sub>	22.44 (-31)	41.98 (-28)	22.30 (-13)
1% P <sub>cv</sub>	31.12 (-22)	15.19 (-55)	22.32 (-13)

**TABLE 5-5. Comparison of vehicle delays for fixed timing control, actuation control, and MPC-Coordination (CV-mCoordination) in different penetration rates conditions, with demand type I: typical demand.**

Then, the performances of the target intersection with different penetration rates (denoted as  $P_{cv}$ ) via MPC-based coordination were investigated, and the results are also shown in Table 5-5. Different typical penetration rates were predefined during simulations, drawn from rates ranging from 100% and

decreasing to 75%, 50%, 25%, 10%, 5% and 1%, as shown in Table 5-5 column 1. These CVs were randomly distributed in traffic streams.

When applied with the MPC-based coordination, the average delay times of the major street, the minor street, and the whole intersection were consistently lower than with both fixed timing and actuation control, as seen in Table 5-4. When the penetration rate rose from 50% to 100%, the average delays dropped correspondingly. The average delays reached the lowest value when the penetration rate was larger than a threshold. The lowest value was stable because there were already enough CV data for MPC-based coordination. On the other hand, when the penetration rate decreased from 100% to 50%, delays increased since the effectiveness of CV data was reduced. However, even with lower CV penetration rates, it consistently outperformed both the fixed timing and actuation control. Thus, the results in Table 5-5 support the conclusion that the proposed MPC-based coordination demonstrates the good performance within different penetration rate conditions in typical demand. The average solving time is less than 0.1 seconds ( i.e., around 30 *ms* ), which is smaller than the typical CV communication interval.

<b>Control types / Delays</b>	<b>Major street (WB, sec)</b>	<b>Minor street (NB, sec)</b>	<b>Average delay (LOS, sec)</b>
Fixed timing control	89	123	60
Actuation control	81 (-8)	108 (-15)	53 (-7)
100% Pcv	27 (-62)	49 (-74)	24 (-36)
75% Pcv	27 (-62)	51 (-72)	25 (-35)
50% Pcv	27 (-62)	51 (-72)	26 (-34)
25% Pcv	31 (-58)	51 (-72)	26 (-34)
10% Pcv	61 (-28)	60 (-63)	39 (-21)
5% Pcv	61 (-28)	61 (-62)	40 (-20)
1% Pcv	65 (-23)	61 (-62)	43 (-20)

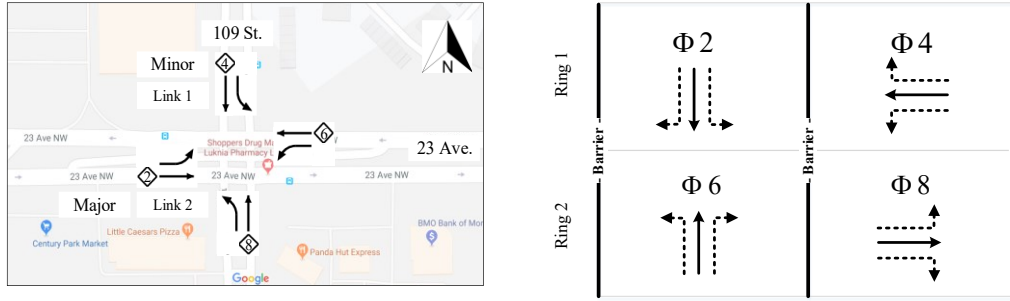
**TABLE 5-6. Comparison of vehicle delays for fixed timing control, actuation control, and MPC-Coordination (CV-mCoordination) in different penetration rates conditions, with demand type II: large demand.**

Also, this efficiency is also verified for a large traffic demand, as shown in Table 5-6. Results in Table 5-6 conclude that the proposed MPC-based coordination (CV-mCoordination) demonstrates the efficiency and good performance within different penetration rate conditions in a large demand.

In summary, the proposed CV-mCoordination is efficient for different approaches, different demands, and different penetration rates, even in a low penetration rate condition.

### 5.3.3 Stability Synthesis Results

Numerical simulations and corresponding results for the target intersection in a typical traffic scenario, i.e., intersection 109 Street at 23<sup>rd</sup> Avenue, are presented as follows.



a) Traffic movement and corresponding signal phase diagram for the target intersection: a two-dimensional moving flow

(b) The signal phasing diagram: a two-ring-four-phase diagram with the permitted left and right turn phasing

**FIGURE 5-9. The simulation scenario setup for the target intersection.**

As shown in Figure 5-9, the simulation scenario for the target intersection is abstracted as a two-dimensional traffic system with a typical phasing diagram. The traffic flow dynamics of two movements with four phases in discrete-time systems are presented as follows,

$$\begin{aligned}
 x_1(k+1) &= x_1(k) + \left(0 - \frac{s_1}{T_c} T_s\right) \cdot g_1(k) \\
 x_2(k+1) &= x_2(k) + \left(0 - \frac{s_2}{T_c} T_s\right) \cdot g_2(k) \\
 y_1(k+1) &= x_1(k) \\
 y_2(k+1) &= x_2(k)
 \end{aligned}
 \tag{5-1}$$

where  $T_c$  is the cycle length of the simple traffic system.  $T_s$  is the sampling time period;  $s_1$  and  $s_2$  are the saturation flow rates for two movements.

The state-space representation of the above flow models is as below,

$$x(k+1) = \begin{bmatrix} 1 & 0 \\ 0 & 1 \end{bmatrix} x(k) + \begin{bmatrix} -\frac{s_1}{T_c} T_s & 0 \\ 0 & -\frac{s_2}{T_c} T_s \end{bmatrix} u(k) \quad (5-2)$$

$$y(k+1) = \begin{bmatrix} 1 & 0 \\ 0 & 1 \end{bmatrix} x(k)$$

where  $A = \begin{bmatrix} 1 & 0 \\ 0 & 1 \end{bmatrix}$ ,  $B = \begin{bmatrix} -\frac{s_1}{T_c} T_s & 0 \\ 0 & -\frac{s_2}{T_c} T_s \end{bmatrix}$ ,  $C = \begin{bmatrix} 1 & 0 \\ 0 & 1 \end{bmatrix}$  are several parameters.  $x =$

$[x_1, x_2]^T$  is the queue dynamic vector, and  $u = [u_1, u_2]^T$  is the vector of the green duration or the green split.

After choosing the typical parameters, a derived state-space representation rewritten from the above flow models is presented as follows,

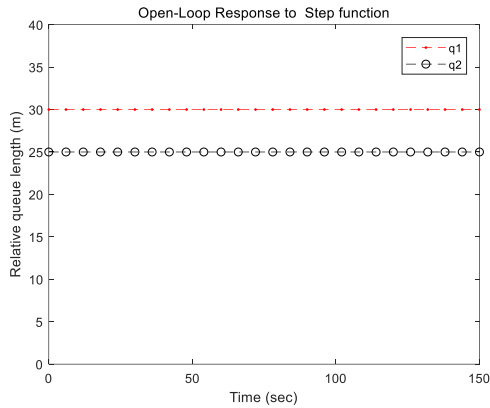
$$x(k+1) = \begin{bmatrix} 1 & 0 \\ 0 & 1 \end{bmatrix} x(k) + \begin{bmatrix} -0.48 \frac{T_s}{T_c} & 0 \\ 0 & -0.48 \frac{T_s}{T_c} \end{bmatrix} u(k) \quad (5-3a)$$

$$y(k+1) = \begin{bmatrix} 1 & 0 \\ 0 & 1 \end{bmatrix} x(k) \quad (5-3b)$$

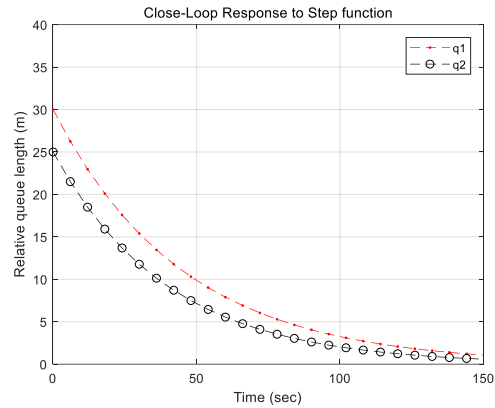
where  $s_1$  and  $s_2$  are equal to 1728 veh/hr (0.48 veh/sec). Matrix  $Q$  is determined by the maximum state value, where  $Q = \text{diag}(\frac{1}{x_1^{max}}, \frac{1}{x_2^{max}})$ . Matrix  $R$  is determined

by the control smooth level  $r$ , where  $R = rI$ .  $I$  is the identity matrix.

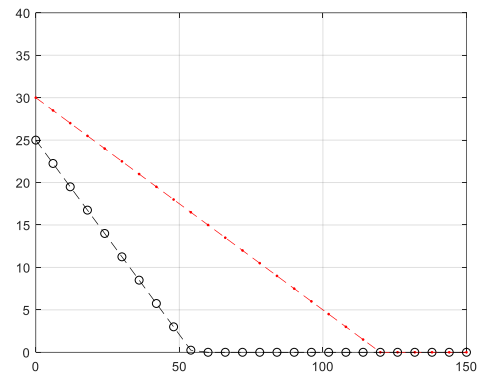
When the typical traffic scenario is applied with the proposed algorithm 3-1, the stability results are presented in the following figures.



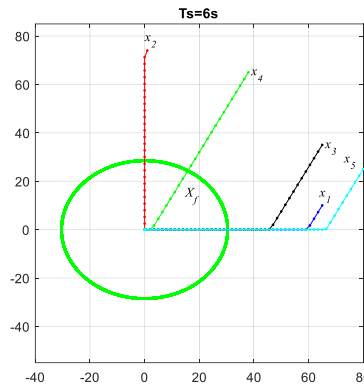
(a) Open-loop responses without a traffic control, where  $T_s = 0.1 T_c$



(b) An actuation control (the traffic-responsive urban control strategy, i.e., the TUC strategy), where  $T_s = 0.1 T_c$



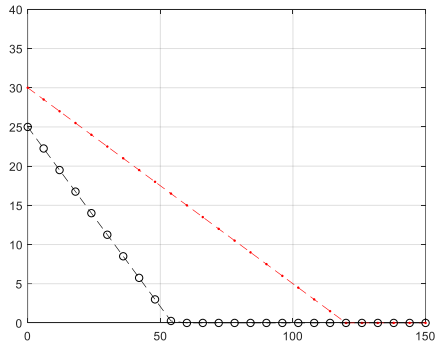
(c) Closed-loop responses via the proposed MPC control with the stable scheme, i.e., the stable MPC, where  $T_s = 0.1 T_c$



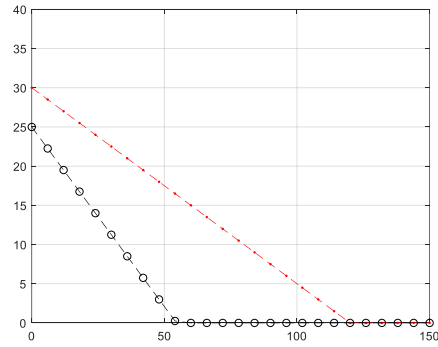
(d) Corresponding terminal regions with different state trajectories via the stable MPC, where  $T_s = 0.1 T_c$

**FIGURE 5-10. Numerical results of the stabilizing synthesis algorithm**

As shown in Figure 5-10, the closed-loop responses of the proposed MPC control with the stable scheme are symmetrically stable within a certain time.



(a) Responses of the basic MPC without the stable scheme for initial state vector  $(60, 120)$ , where  $T_s = 0.1T_c$

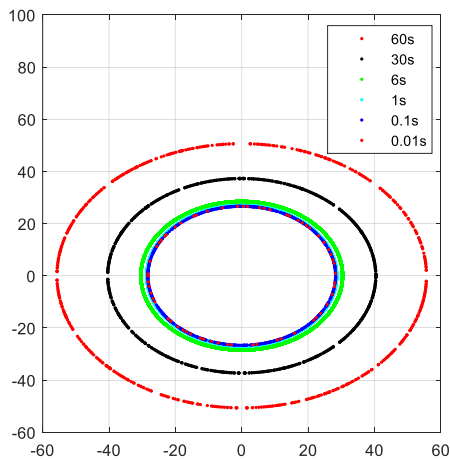


(b) Responses of the stable MPC with the stable scheme for initial state vector  $(60, 120)$ , where  $T_s = 0.1T_c$

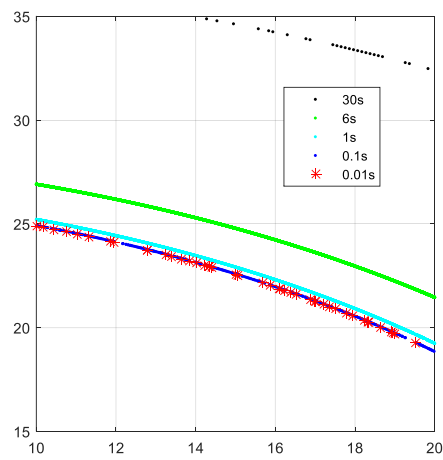
**FIGURE 5-11. Performance comparison between the basic and the stable MPC for different sampling times.**

Figure 5-11 presents the performance comparison between the basic MPC and stable MPC. This result indicates the stability scheme maintains the same performance obtained by the basic MPC in the same communication interval.

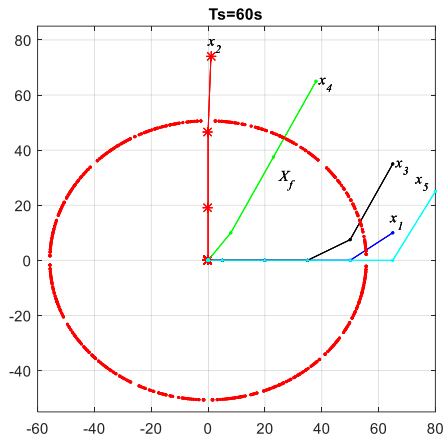
Then the performance of the proposed table MPC in different high-frequency communication sampling times are presented further.



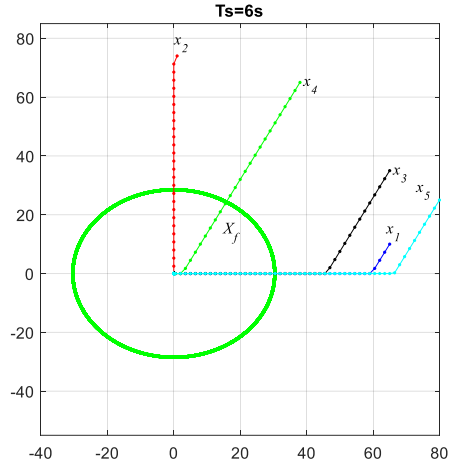
(a) Terminal regions  $X_f$  for different communication intervals



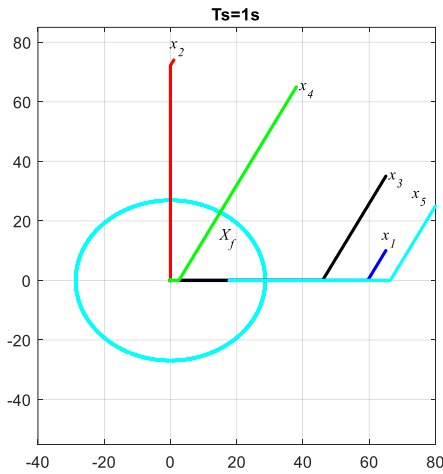
(b) Sectional details of terminal regions  $X_f$  for different communication intervals



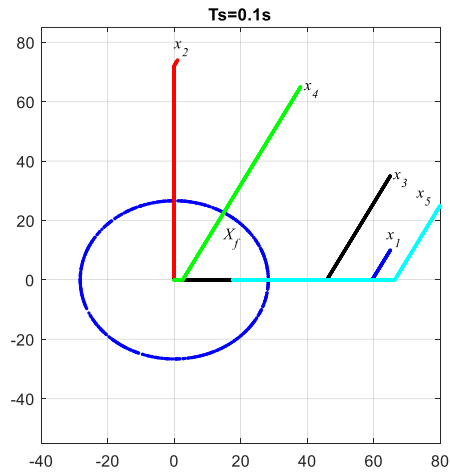
(c) Terminal region result  $X_f = (7.3, 7.9)$ , where  $T_s = T_c = 60s$



(d) Terminal region result  $X_f = (3.1, 3.16)$ , where  $T_s = 0.1T_c = 6s$



(e) Terminal region result  $X_f = (1.3, 1.4)$ , where  $T_s = 1s$

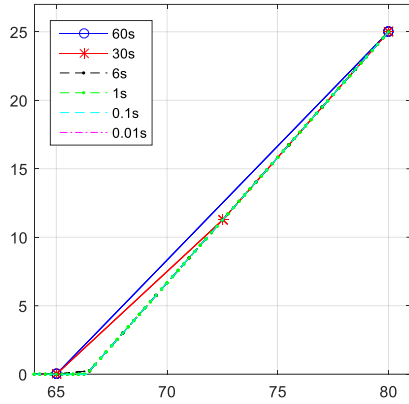


(f) Terminal region result  $X_f = (0.5, 0.5)$ , where  $T_s = 100ms$

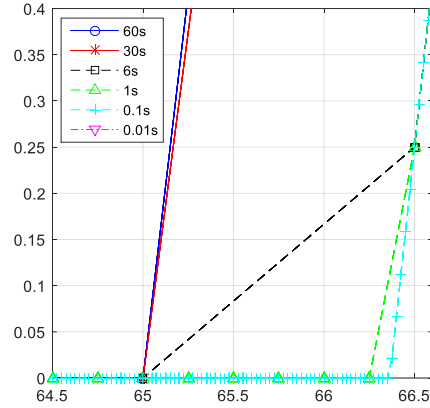
**FIGURE 5-12. Terminal regions  $X_f$  and corresponding state trajectories for different sampling times.**

Figure 5-12 demonstrates the terminal region comparisons for different sampling times. As shown in Figure 5-12, the controller is always stable inside a given stability terminal region under different sampling times. The stability terminal region finally converges to a constant region when the sampling time is around 100 ms, which is equivalent to the typical DSRC-based CV communication

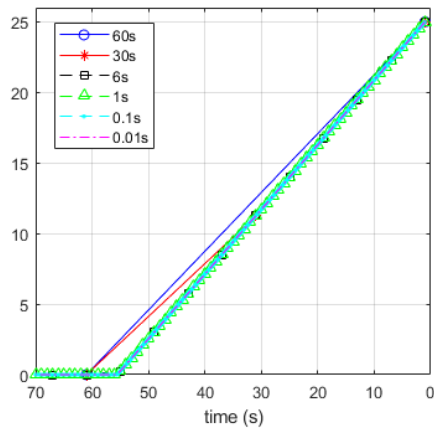
time. Thus, the proposed stable MPC always demonstrates an acceptable stability performance under different short communication intervals in the CV environment.



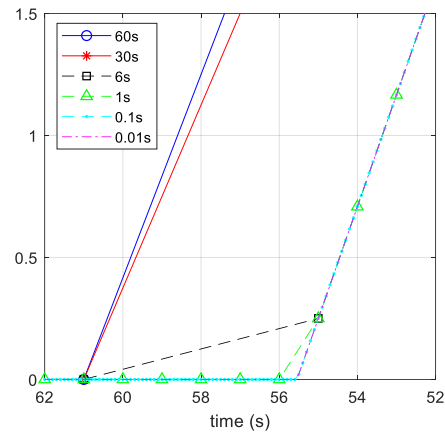
(a) State trajectories for initial state  $x_5$  in a two-dimension perspective



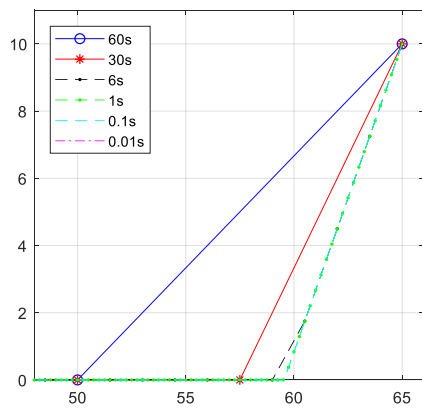
(b) Sectional details of the trajectories in a two-dimension perspective



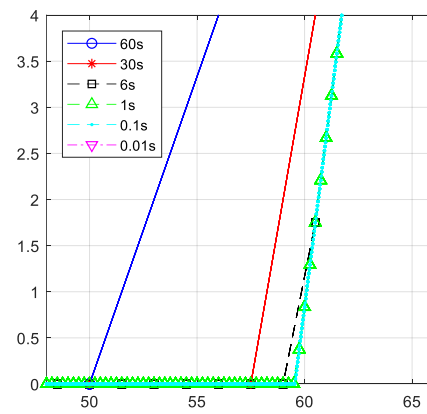
(c) Selected state trajectories for initial state  $x_5$  in one-dimension with respect to time



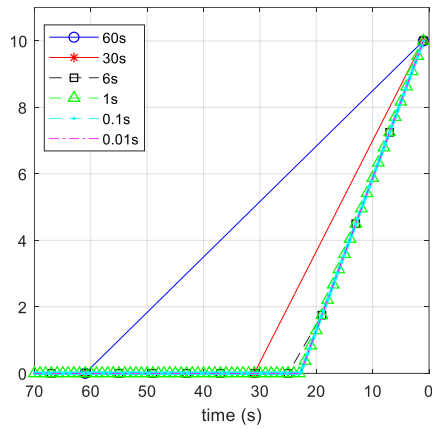
(d) Sectional details of trajectories in one-dimension with respect to time



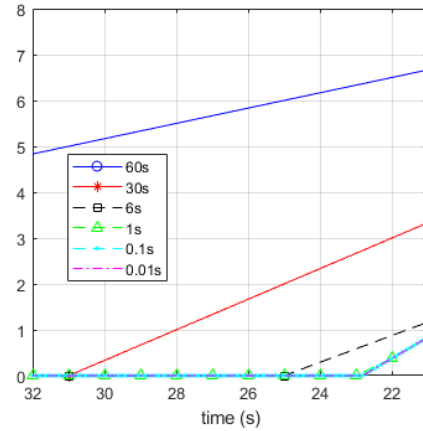
(e) State trajectories for initial state  $x_7$  in two-dimension perspective



(f) Sectional details of trajectories in two-dimension perspective



(g) Selected state trajectory for initial state  $x_l$  in one-dimension with respect to time



(h) Sectional details of trajectories in one-dimension with respect to time

**FIGURE 5-13. The faster convergence results enabled by the faster sampling frequency (a-d) trajectory  $x_5$  (e-h) trajectory  $x_l$ .**

Then, the benefit of the faster sampling frequency, being equivalent to the smaller sampling time interval, is demonstrated in Figure 5-13. As presented in Figures 5-13(b) and 5-13(d), the larger sampling frequency enables the faster convergence of the state trajectory. This indicates that the high communication frequency helps facilitates stability more efficiently for the MPC controller.

In summary, the proposed stable scheme is always with an acceptable stability performance under different short communication intervals. Further, the high-frequency communication helps the MPC be more efficient with a faster convergence speed.

# CHAPTER 6. CONCLUSION AND FUTURE WORKS

Last, this chapter demonstrates the contributions, conclusions, limitations, and future works of the current research works.

## 6.1 CONCLUSION

The research contributions as well as corresponding conclusions of the thesis, are shown as follows.

For the *data quality*, an enhanced dynamic link segmentation-based link model is proposed for accurate link state estimation. An enhanced dynamic segmentation approach in the low penetration rate conditions has been developed by dividing the current approaching roadway into different smaller stretches. This approach helps to estimate the arrival flow pattern accurately and efficiently.

Then, for the *traffic model*, this thesis proposes an improved hybrid model to increase the availability of signal dynamics in the CV environment. Specifically, a virtual cycle based store-and-forward model (Vi-SFM) is proposed for the link state evolution that is compatible with the high-frequency data exchange in the CV environment. Moreover, a dynamic parametric platoon dispersion model is presented to model the dispersion impact by utilizing the potential of a single vehicle's position and trajectory information in the low penetration rate condition in the CV environment.

Moreover, for the *control strategy*, a MPC-based adaptive signal control (CV-mASC) and coordination (CV-mCoordination) framework embedding the proposed traffic models are developed to have good scalable capability and performances. The proposed framework of MPC-based adaptive signal control and coordination is used to optimize the signal control for multiple intersections. The common cycle length and split for both non-coordinated and coordination phases are optimized initially. Next, an offset optimization is used to give optimal offset for the corridor-level's performance improvements. Also, a stabilizing scheme is proposed to achieve a stable performance for the MPC framework.

Last, this thesis proposes a CV-centric in-the-loop experimental framework to implement and validate the efficiency of the proposed methods in the CV environment. The connected vehicle sends real-time CV data, including the trajectories and motion data, to the RSE. Then, the connected RSE conducts the intersection-level and corridor-level signal controls.

Both field and simulation results from implemented CV-centric in-the-loop testing validated the efficiency of these proposed methods in the CV environment. From the field test results, both the semi-closed loop control in 23<sup>rd</sup> Avenue and the closed-loop control in the South Campus can decrease the travel times, which verifies the efficiency of the proposed CV-based signal control methods. Furthermore, from the simulation results, both proposed CV-mASC and CV-mCoordination have shorter travel times than either fixed timing or actuated control for different approaches, different demands, and different penetration rates, even in a low penetration rate condition. Besides, simulation results of the proposed

stable method indicate that high-frequency communication helps the MPC controller be more efficient with a faster convergency speed.

## **6.2 FUTURE WORKS**

On the other hand, there are some limitations and boundaries of the current works for fast-developing connected vehicle-based adaptive signal control and coordination. These limitations are listed as follows.

For the CV-based traffic dynamic modeling, even connected vehicle priority is widely used and associated three standard phase operations are modeled, other traditional phase operations, like phase sequence and pedestrian phase, are not fully considered. The complexity of the traditional phase operations may impact the potential performance improvements of the priority-augmented signal control in the CV environment.

In the proposed MPC-based ASC and coordination, they optimize the split and offset decision variables with their own constraints and objectives other than a joint optimization. The proposed CV-mASC and CV-mCoordination may impact each other further considering the spatial coupling demand impacts of the approach with two adjacent intersections in the urban arterials.

For the software-in-the-loop prototype's scenarios and control applications, individual CV data are utilized for the traffic flow generation, where demand profiles are majorly typical average values, which are acquired from average weekday traffic on an urban arterial road. However, the proposed segmentation method may degrade its performances, considering potential micro-level human behaviors of different demand profiles in different traffic conditions and modes.

Besides, considering the controlling limitations of the signal controller on the open urban arterial road, on-site scenarios with a closed-loop control environment in the field are not thoroughly investigated to explore the potential field performances of the proposed MPC-based ASC and coordination in the CV environment.

Thus, in the future, several works could be further explored, considering the limitations of the current research works.

For the traffic modeling, more flexible practical phasing techniques like dynamic phase sequence and phase switching methods could be further implemented and considered to integrate the capability of the field signal controllers.

Also, considering the spatial coupling impact between two adjacent intersections, other spatial division modeling methods, other than the existing three-region division model, could be explored for the adaptive signal control and coordination in the urban traffic control systems.

For evaluations, more complex scenarios, such as multi-modal and multi-priority traffic signal controls, could be further investigated for practical implementation purposes.

Also, for transportation engineering, the continuous research of these complex scenarios within a closed-loop control environment in the field is always essential, and will be further studied in the ACTIVE CV testbed to provide real-world testing and results.

# REFERENCES

1. Feng, Y., K. L. Head, S. Khoshmaghani, and M. Zamanipour. A Real-Time Adaptive Signal Control in a Connected Vehicle Environment. *Transportation Research Part C: Emerging Technologies*, Vol. 55, 2015, pp. 460–473. <https://doi.org/10.1016/j.trc.2015.01.007>.
2. Hartenstein, H., and K. Laberteaux, Eds. *VANET: Vehicular Applications and Inter-Networking Technologies*. Wiley, Chichester, U.K, 2010.
3. Kenney, J. B. Dedicated Short-Range Communications (DSRC) Standards in the United States. *Proceedings of the IEEE*, Vol. 99, No. 7, 2011, pp. 1162–1182. <https://doi.org/10.1109/JPROC.2011.2132790>.
4. He, S., J. Li, and T. Z. Qiu. Vehicle-to-Pedestrian Communication Modeling and Collision Avoiding Method in Connected Vehicle Environment. *Transportation Research Record: Journal of the Transportation Research Board*, Vol. 2621, 2017, pp. 21–30. <https://doi.org/10.3141/2621-03>.
5. Wan, N., A. Vahidi, and A. Luckow. Optimal Speed Advisory for Connected Vehicles in Arterial Roads and the Impact on Mixed Traffic. *Transportation Research Part C: Emerging Technologies*, Vol. 69, 2016, pp. 548–563. <https://doi.org/10.1016/j.trc.2016.01.011>.
6. He, X., H. X. Liu, and X. Liu. Optimal Vehicle Speed Trajectory on a Signalized Arterial with Consideration of Queue. *Transportation Research Part C: Emerging Technologies*, Vol. 61, 2015, pp. 106–120. <https://doi.org/10/f74mnd>.
7. Ubiergo, G. A., and W.-L. Jin. Mobility and Environment Improvement of Signalized Networks through Vehicle-to-Infrastructure (V2I) Communications. *Transportation Research Part C: Emerging Technologies*, Vol. 68, 2016, pp. 70–82. <https://doi.org/10.1016/j.trc.2016.03.010>.
8. Yang, H., and W.-L. Jin. A Control Theoretic Formulation of Green Driving Strategies Based on Inter-Vehicle Communications. *Transportation Research Part C: Emerging Technologies*, Vol. 41, 2014, pp. 48–60. <https://doi.org/10.1016/j.trc.2014.01.016>.
9. Kamalanathsharma, R. K., H. A. Rakha, and H. Yang. Networkwide Impacts of Vehicle Ecospeed Control in the Vicinity of Traffic Signalized Intersections. *Transportation Research Record: Journal of the Transportation Research Board*, Vol. 2503, 2015, pp. 91–99. <https://doi.org/10.3141/2503-10>.
10. Yuan, Q., Z. Liu, J. Li, J. Zhang, and F. Yang. A Traffic Congestion Detection and Information Dissemination Scheme for Urban Expressways Using Vehicular Networks. *Transportation Research Part C: Emerging Technologies*, Vol. 47, 2014, pp. 114–127. <https://doi.org/10.1016/j.trc.2014.08.001>.
11. Lioris, J., R. Pedarsani, F. Y. Tascikaraoglu, and P. Varaiya. Platoons of Connected Vehicles Can Double Throughput in Urban Roads. *Transportation Research Part C: Emerging Technologies*, Vol. 77, 2017, pp. 292–305. <https://doi.org/10.1016/j.trc.2017.01.023>.
12. Gordon, R. L., W. Tighe, and I. T. S. Siemens. *Traffic Control Systems Handbook*. United States. Federal Highway Administration. Office of Transportation Management, 2005.
13. Kell, J. H., I. J. Fullerton, and M. K. Mills. *Traffic Detector Handbook: Volume I*. 2006.
14. Klein, L. A., M. K. Mills, D. Gibson, and L. A. Klein. *Traffic Detector Handbook: Volume II*. United States. Federal Highway Administration, 2006.
15. Stevanovic, A. *Adaptive Traffic Control Systems: Domestic and Foreign State of Practice*.

- Publication Project 20-5 (Topic 40-03). Transportation research board, 2010.
16. Wang, Y., X. Yang, H. Liang, and Y. Liu. A Review of the Self-Adaptive Traffic Signal Control System Based on Future Traffic Environment. *Journal of Advanced Transportation*, 2018. <https://doi.org/10.1155/2018/1096123>.
  17. Jing, P., H. Huang, and L. Chen. An Adaptive Traffic Signal Control in a Connected Vehicle Environment: A Systematic Review. *Information*, Vol. 8, No. 3, 2017, p. 101. <https://doi.org/10.3390/info8030101>.
  18. Zheng, X., W. Recker, and L. Chu. Optimization of Control Parameters for Adaptive Traffic-Actuated Signal Control. *Journal of Intelligent Transportation Systems*, Vol. 14, No. 2, 2010, pp. 95–108. <https://doi.org/10/c672hn>.
  19. Beak, B., K. L. Head, and Y. Feng. Adaptive Coordination Based on Connected Vehicle Technology. *Transportation Research Record: Journal of the Transportation Research Board*, Vol. 2619, 2017, pp. 1–12. <https://doi.org/10/gcv66v>.
  20. Bretherton, D., K. Wood, and N. Raha. Traffic Monitoring and Congestion Management in the Scoot Urban Traffic Control System. *Transportation Research Record: Journal of the Transportation Research Board*, No. 1634, 1998, pp. 118–122. <https://doi.org/10.3141/1634-15>.
  21. Sims, A. G., and K. W. Dobinson. The Sydney Coordinated Adaptive Traffic (SCAT) System Philosophy and Benefits. *IEEE Transactions on vehicular technology*, Vol. 29, No. 2, 1980, pp. 130–137. <https://doi.org/10.1109/T-VT.1980.23833>.
  22. Gartner, N. H. OPAC: A Demand-Responsive Strategy for Traffic Signal Control. *Transportation Research Record: Journal of the Transportation Research Board*, Vol. 906, 1983, pp. 75–81.
  23. Mirchandani, P., and L. Head. A Real-Time Traffic Signal Control System: Architecture, Algorithms, and Analysis. *Transportation Research Part C: Emerging Technologies*, Vol. 9, No. 6, 2001, pp. 415–432. <https://doi.org/10/bdt6kp>.
  24. Brilon, W., and T. Wietholt. Experiences with Adaptive Signal Control in Germany. *Transportation Research Record: Journal of the Transportation Research Board*, No. 2356, 2013, pp. 9–16.
  25. Feng, Y., M. Zamanipour, K. L. Head, and S. Khoshmagham. Connected Vehicle-Based Adaptive Signal Control and Applications. *Transportation Research Record*, Vol. 2558, No. 1, 2016, pp. 11–19. <https://doi.org/10/gdm5cq>.
  26. Little, J. D. C. The Synchronization of Traffic Signals by Mixed-Integer Linear Programming. *Operations Research*, Vol. 14, No. 4, 1966, pp. 568–594. <https://doi.org/10.1287/opre.14.4.568>.
  27. Gartner, N., J. D. Little, and H. Gabbay. Optimization of Traffic Signal Settings by Mixed-Integer Linear Programming: Part I: The Network Coordination Problem. *Transportation Science*, Vol. 9, No. 4, 1975, pp. 321–343.
  28. Goodall, N., B. Smith, and B. Park. Traffic Signal Control with Connected Vehicles. *Transportation Research Record: Journal of the Transportation Research Board*, Vol. 2381, 2013, pp. 65–72. <https://doi.org/10.3141/2381-08>.
  29. Ilgin Guler, S., M. Menendez, and L. Meier. Using Connected Vehicle Technology to Improve the Efficiency of Intersections. *Transportation Research Part C: Emerging Technologies*, Vol. 46, 2014, pp. 121–131. <https://doi.org/10/f6k7xz>.
  30. Maslekar, N., J. Mouzna, M. Boussedjra, and H. Labiod. CATS: An Adaptive Traffic Signal

- System Based on Car-to-Car Communication. *Journal of Network and Computer Applications*, Vol. 36, No. 5, 2013, pp. 1308–1315. <https://doi.org/10/gcvj4g>.
31. Venkatanarayana, R., H. Park, B. L. Smith, C. Skerrit Jr, and N. W. Ruhter. Application of IntelliDrive<sup>SM</sup> to Address Oversaturated Conditions on Arterials. Presented at the Transportation Research Board 90th Annual Meeting, 2011.
  32. Liu, W., G. Qin, Y. He, and F. Jiang. Distributed Cooperative Reinforcement Learning-Based Traffic Signal Control That Integrates V2X Networks' Dynamic Clustering. *IEEE Transactions on Vehicular Technology*, Vol. 66, No. 10, 2017, pp. 8667–8681. <https://doi.org/10/gcf4c2>.
  33. Day, C. M., and D. M. Bullock. Detector-Free Signal Offset Optimization with Limited Connected Vehicle Market Penetration. *Transportation Research Record: Journal of the Transportation Research Board*, Vol. 2558, 2016, pp. 54–65. <https://doi.org/10.3141/2558-06>.
  34. Li, H., C. M. Day, and D. M. Bullock. Virtual Detection at Intersections Using Connected Vehicle Trajectory Data. Presented at the 2016 IEEE 19th International Conference on Intelligent Transportation Systems (ITSC), Rio de Janeiro, Brazil, 2016.
  35. He, Q., K. L. Head, and J. Ding. PAMSCOD: Platoon-Based Arterial Multi-Modal Signal Control with Online Data. *Transportation Research Part C: Emerging Technologies*, Vol. 20, No. 1, 2012, pp. 164–184. <https://doi.org/10.1016/j.trc.2011.05.007>.
  36. Li, J., and T. Qiu. An Extended Time-Delayed V2X-Based Bi-Directional Looking Car-Following Model and Its Linear Stability Analysis. Presented at the Transportation Research Board 97th Annual Meeting, 2018.
  37. Day, C. M., H. Li, L. M. Richardson, J. Howard, T. Platte, J. R. Sturdevant, and D. M. Bullock. Detector-Free Optimization of Traffic Signal Offsets with Connected Vehicle Data. *Transportation Research Record: Journal of the Transportation Research Board*, Vol. 2620, 2017, pp. 54–68. <https://doi.org/10.3141/2620-06>.
  38. He, Q., K. L. Head, and J. Ding. Multi-Modal Traffic Signal Control with Priority, Signal Actuation and Coordination. *Transportation Research Part C: Emerging Technologies*, Vol. 46, 2014, pp. 65–82. <https://doi.org/10.1016/j.trc.2014.05.001>.
  39. Remias, S. M., C. M. Day, J. M. Waddell, J. N. Kirsch, and T. Trepanier. Evaluating the Performance of Coordinated Signal Timing: A Comparison of Common Data Types with Connected Vehicle Data. Presented at the Transportation Research Board 97th Annual Meeting, Washington, D.C., 2018.
  40. Goodall Noah J., Park Byungkyu (Brian), and Smith Brian L. Microscopic Estimation of Arterial Vehicle Positions in a Low-Penetration-Rate Connected Vehicle Environment. *Journal of Transportation Engineering*, Vol. 140, No. 10, 2014, p. 04014047. [https://doi.org/10.1061/\(ASCE\)TE.1943-5436.0000716](https://doi.org/10.1061/(ASCE)TE.1943-5436.0000716).
  41. Mahmassani, H. S. 50th Anniversary Invited Article—Autonomous Vehicles and Connected Vehicle Systems: Flow and Operations Considerations. *Transportation Science*, 2016, pp. 1140–1162. <https://doi.org/10.1287/trsc.2016.0712>.
  42. Fountoulakis, M., N. Bekiaris-Liberis, C. Roncoli, I. Papamichail, and M. Papageorgiou. Highway Traffic State Estimation with Mixed Connected and Conventional Vehicles: Microscopic Simulation-Based Testing. *Transportation Research Part C: Emerging Technologies*, Vol. 78, 2017, pp. 13–33. <https://doi.org/10.1016/j.trc.2017.02.015>.
  43. Gradinescu, V., C. Gorgorin, R. Diaconescu, V. Cristea, and L. Iftode. Adaptive Traffic Lights

- Using Car-to-Car Communication. Presented at the 2007 IEEE 65th Vehicular Technology Conference - VTC2007-Spring, 2007.
44. Chou, L.-D., B.-T. Deng, D. C. Li, and K.-W. Kuo. A Passenger-Based Adaptive Traffic Signal Control Mechanism in Intelligent Transportation Systems. 2012.
  45. Nafi, N. S., and J. Y. Khan. A VANET Based Intelligent Road Traffic Signalling System. Presented at the Australasian Telecommunication Networks and Applications Conference (ATNAC) 2012, 2012.
  46. Chang, H.-J., and G.-T. Park. A Study on Traffic Signal Control at Signalized Intersections in Vehicular Ad Hoc Networks. *Ad Hoc Networks*, Vol. 11, No. 7, 2013, pp. 2115–2124. <https://doi.org/10/f5bz6k>.
  47. Ahmane, M., A. Abbas-Turki, F. Perronnet, J. Wu, A. E. Moudni, J. Buisson, and R. Zeo. Modeling and Controlling an Isolated Urban Intersection Based on Cooperative Vehicles. *Transportation Research Part C: Emerging Technologies*, Vol. 28, 2013, pp. 44–62. <https://doi.org/10/f4ssrs>.
  48. Cai, C., Y. Wang, and G. Geers. Vehicle-to-Infrastructure Communication-Based Adaptive Traffic Signal Control. *IET Intelligent Transport Systems*, Vol. 7, No. 3, 2013, pp. 351–360. <https://doi.org/10/f5f2cp>.
  49. Pandit, K., D. Ghosal, H. M. Zhang, and C.-N. Chuah. Adaptive Traffic Signal Control With Vehicular Ad Hoc Networks. *IEEE Transactions on Vehicular Technology*, Vol. 62, No. 4, 2013, pp. 1459–1471. <https://doi.org/10/f4xh7h>.
  50. Lee Joyoung, Park Byungkyu (Brian), and Yun Ilsoo. Cumulative Travel-Time Responsive Real-Time Intersection Control Algorithm in the Connected Vehicle Environment. *Journal of Transportation Engineering*, Vol. 139, No. 10, 2013, pp. 1020–1029. <https://doi.org/10/f5b283>.
  51. Kari, D., G. Wu, and M. J. Barth. Development of an Agent-Based Online Adaptive Signal Control Strategy Using Connected Vehicle Technology. Presented at the 17th International IEEE Conference on Intelligent Transportation Systems (ITSC), 2014.
  52. Tiaprasert, K., Y. Zhang, X. B. Wang, and X. Zeng. Queue Length Estimation Using Connected Vehicle Technology for Adaptive Signal Control. *IEEE Transactions on Intelligent Transportation Systems*, Vol. 16, No. 4, 2015, pp. 2129–2140. <https://doi.org/10.1109/TITS.2015.2401007>.
  53. Younes, M. B., and A. Boukerche. Intelligent Traffic Light Controlling Algorithms Using Vehicular Networks. *IEEE Transactions on Vehicular Technology*, Vol. 65, No. 8, 2016, pp. 5887–5899. <https://doi.org/10/f82x74>.
  54. Cheng, J., W. Wu, J. Cao, and K. Li. Fuzzy Group-Based Intersection Control via Vehicular Networks for Smart Transportations. *IEEE Transactions on Industrial Informatics*, Vol. 13, No. 2, 2017, pp. 751–758. <https://doi.org/10/f96g8s>.
  55. Feng, Y., J. Zheng, and H. X. Liu. A Real-Time Detector-Free Adaptive Signal Control with Low Penetration of Connected Vehicles Paper. Presented at the Transportation Research Board 97th Annual Meeting, 2018.
  56. Day, C. M., H. Li, L. Richardson, J. Howard, T. Platte, J. R. Sturdevant, and D. M. Bullock. Detector-Free Optimization of Traffic Signal Offsets with Connected Vehicle Data. Presented at the Transportation Research Board 96th Annual Meeting Transportation Research Board, 2017.
  57. Feng, Y. *Intelligent traffic control in a connected vehicle environment*. Ph.D. the University of

- Arizona, Arizona, USA, 2015.
58. Sen, S., and K. L. Head. Controlled Optimization of Phases at an Intersection. *Transportation Science*, Vol. 31, No. 1, 1997, pp. 5–17. <https://doi.org/10/dqr3mr>.
  59. Larry, H. K. Event—Based Short—Term Traffic Flow Prediction Model. *Transportation Research Record*, Vol. 1510, 1995, pp. 125–143.
  60. Jin, J., X. Ma, and I. Kosonen. An Intelligent Control System for Traffic Lights with Simulation-Based Evaluation. *Control Engineering Practice*, Vol. 58, 2017, pp. 24–33. <https://doi.org/10/f3tb95>.
  61. Gao, J., Y. Shen, J. Liu, M. Ito, and N. Shiratori. Adaptive Traffic Signal Control: Deep Reinforcement Learning Algorithm with Experience Replay and Target Network. *arXiv:1705.02755 [cs]*, 2017.
  62. Gartner, N. H., and C. Stamatiadis. Development of Advanced Traffic Signal Control Strategies for Intelligent Transportation Systems: Multilevel Design. *TRANSPORTATION RESEARCH RECORD*, p. 8.
  63. Luyanda, F., D. Gettman, L. Head, S. Shelby, D. Bullock, and P. Mirchandani. ACS-Lite Algorithmic Architecture: Applying Adaptive Control System Technology to Closed-Loop Traffic Signal Control Systems. *Transportation Research Record: Journal of the Transportation Research Board*, Vol. 1856, 2003, pp. 175–184. <https://doi.org/10/fn6dvs>.
  64. Morgan, J. T., and J. D. Little. Synchronizing Traffic Signals for Maximal Bandwidth. *Operations Research*, Vol. 12, No. 6, 1964, pp. 896–912.
  65. Little, J. D., M. D. Kelson, and N. H. Gartner. MAXBAND: A Versatile Program for Setting Signals on Arteries and Triangular Networks. 1981.
  66. Gartner, N. H., S. F. Assmann, F. Lasaga, and D. L. Hous. MULTIBAND—A VARIABLE-BANDWIDTH ARTERIAL PROGRESSION SCHEME. *Transportation Research Record*, No. 1287, 1990.
  67. Gartner, N. H., S. F. Assman, F. Lasaga, and D. L. Hou. A Multi-Band Approach to Arterial Traffic Signal Optimization. *Transportation Research Part B: Methodological*, Vol. 25, No. 1, 1991, pp. 55–74. [https://doi.org/10.1016/0191-2615\(91\)90013-9](https://doi.org/10.1016/0191-2615(91)90013-9).
  68. Stamatiadis, C., and N. Gartner. MULTIBAND-96: A Program for Variable-Bandwidth Progression Optimization of Multiarterial Traffic Networks. *Transportation Research Record: Journal of the Transportation Research Board*, No. 1554, 1996, pp. 9–17.
  69. Stamatiadis, C., and N. H. Gartner. Progression Optimization in Large Scale Urban Traffic Networks: A Heuristic Decomposition Approach. 1999.
  70. Gartner, N. H., and C. Stamatiadis. Arterial-Based Control of Traffic Flow in Urban Grid Networks. *Mathematical and computer modelling*, Vol. 35, No. 5–6, 2002, pp. 657–671.
  71. Gartner, N. H., and C. Stamatiadis. Progression Optimization Featuring Arterial-and Route-Based Priority Signal Networks. *Journal of Intelligent Transportation Systems*, Vol. 8, No. 2, 2004, pp. 77–86.
  72. Messer, C. J., R. H. Whitson, C. L. Dudek, and E. J. Romano. A Variable-Sequence Multiphase Progression Optimization Program. *Transportation Research Record*, No. 445, 1973, pp. 24–33.
  73. Chang, E. C., and C. J. Messer. *Arterial Signal Timing Optimization Using PASSER II-90-Program User's Manual*. 1991.
  74. Chaudhary, N. A., A. Pinnoi, and C. J. Messer. Proposed Enhancements to MAXBAND 86 Program. *Transportation Research Record*, No. 1324, 1991, pp. 98–104.

75. Chaudhary, N. A., and C. J. Messer. *PASSER IV-96, Version 2.1, User Guide*. Reference Manual, 1996.
76. Chang, E. C., S. L. Cohen, C. Liu, N. A. Chaudhary, and C. Messer. MAXBAND-86: Program for Optimizing Left-Turn Phase Sequence in Multiarterial Closed Networks. *Transportation Research Record: Journal of the Transportation Research Board*, No. 1181, 1988, pp. 61–67.
77. Zhang, C., Y. Xie, N. H. Gartner, C. Stamatidis, and T. Arsava. AM-Band: An Asymmetrical Multi-Band Model for Arterial Traffic Signal Coordination. *Transportation Research Part C: Emerging Technologies*, Vol. 58, Part C, 2015, pp. 515–531. <https://doi.org/10.1016/j.trc.2015.04.014>.
78. Köhler, E., R. H. Möhring, and G. Wünsch. Minimizing Total Delay in Fixed-Time Controlled Traffic Networks. 2005.
79. Hu, H., and H. X. Liu. Arterial Offset Optimization Using Archived High-Resolution Traffic Signal Data. *Transportation Research Part C: Emerging Technologies*, Vol. 37, 2013, pp. 131–144. <https://doi.org/10.1016/j.trc.2013.10.001>.
80. Shoup, G., and D. Bullock. Dynamic Offset Tuning Procedure Using Travel Time Data. *Transportation Research Record: Journal of the Transportation Research Board*, No. 1683, 1999, pp. 84–94.
81. Wallace, C. E., K. G. Courage, M. A. Hadi, and A. C. Gan. *TRANSYT-7F User's Guide*. Transportation Research Center, University of Florida, Gainesville, Florida, 1998.
82. Robertson, D. I. Research on the TRANSYT and SCOOT Methods of Signal Coordination. *ITE journal*, Vol. 56, No. 1, 1986.
83. Studio, S. *Synchro 8.0 User's Guide*. Trafficware, June, Sugar Land, Tex., 2013.
84. America, P. T. V. *PTV VISTRO User Manual*. PTV, Karlsruhe, Germany., 2014.
85. Islam, S. M. A. B. A., and A. Hajbabaie. Distributed Coordinated Signal Timing Optimization in Connected Transportation Networks. *Transportation Research Part C: Emerging Technologies*, Vol. 80, 2017, pp. 272–285. <https://doi.org/10/gbmjt2>.
86. Ban, X. (Jeff), and W. Li. *Connected Vehicle Based Traffic Signal Optimization*. 2018.
87. Christofa, E., J. Argote, and A. Skabardonis. Arterial Queue Spillback Detection and Signal Control Based on Connected Vehicle Technology. *Transportation Research Record: Journal of the Transportation Research Board*, Vol. 2356, 2013, pp. 61–70. <https://doi.org/10/gcvj7m>.
88. Xiang, J., and Z. Chen. An Adaptive Traffic Signal Coordination Optimization Method Based on Vehicle-to-Infrastructure Communication. *Cluster Computing*, Vol. 19, No. 3, 2016, pp. 1503–1514. <https://doi.org/10/f82wcq>.
89. Yang, K., I. Tan, and M. Menendez. A Reinforcement Learning Based Traffic Signal Control Algorithm in a Connected Vehicle Environment. Presented at the 17th Swiss Transport Research Conference (STRC 2017), 2017.
90. Zheng, J., W. Sun, S. Huang, S. Shen, C. Yu, J. Zhu, B. Liu, and H. X. Liu. Traffic Signal Optimization Using Crowdsourced Vehicle Trajectory Data. Presented at the Transportation Research Board 97th Annual Meeting Transportation Research Board, 2018.
91. Aziz, H. M. A., H. Wang, S. Young, J. Sperling, and J. Beck. *Synthesis Study on Transitions in Signal Infrastructure and Control Algorithms for Connected and Automated Transportation*. Publication ORNL/TM--2017/280, 1366412. 2017.
92. Roess, R. P., E. S. Prassas, and W. R. McShane. *Traffic Engineering*. Pearson, Upper Saddle River, NJ, 2011.

93. Gartner, N. H., C. J. Messer, and E. A. K. Rathi. Traffic Flow Theory: A State of the Art Report-Revised Monograph on Traffic Flow Theory. *Transportation Research Board, Washington, DC*, 2011.
94. Burghout, W., and J. Wahlstedt. Hybrid Traffic Simulation with Adaptive Signal Control. *Transportation Research Record*, Vol. 1999, No. 1, 2007, pp. 191–197. <https://doi.org/10/dvcfmf>.
95. Cai, C., C. K. Wong, and B. G. Heydecker. Adaptive Traffic Signal Control Using Approximate Dynamic Programming. *Transportation Research Part C: Emerging Technologies*, Vol. 17, No. 5, 2009, pp. 456–474. <https://doi.org/10/dqj2b3>.
96. Aboudolas, K., M. Papageorgiou, A. Kouvelas, and E. Kosmatopoulos. A Rolling-Horizon Quadratic-Programming Approach to the Signal Control Problem in Large-Scale Congested Urban Road Networks. *Transportation Research Part C: Emerging Technologies*, Vol. 18, No. 5, 2010, pp. 680–694. <https://doi.org/10/bq8fjq>.
97. Liu, G., and T. Z. Qiu. Multi-Objective Signal Optimization with Embedded Enhanced Store-and-Forward Model for Oversaturated Corridor. Presented at the Transportation Research Board 95th Annual Meeting, 2016.
98. Papageorgiou, M., C. Kiakaki, V. Dinopoulou, A. Kotsialos, and Yibing Wang. Review of Road Traffic Control Strategies. *Proceedings of the IEEE*, Vol. 91, No. 12, 2003, pp. 2043–2067. <https://doi.org/10/d4cvjb>.
99. Aboudolas, K., M. Papageorgiou, and E. Kosmatopoulos. Store-and-Forward Based Methods for the Signal Control Problem in Large-Scale Congested Urban Road Networks. *Transportation Research Part C: Emerging Technologies*, Vol. 17, No. 2, 2009, pp. 163–174. <https://doi.org/10/dv7df6>.
100. Burger, M., M. van den Berg, A. Hegyi, B. De Schutter, and J. Hellendoorn. Considerations for Model-Based Traffic Control. *Transportation Research Part C: Emerging Technologies*, Vol. 35, 2013, pp. 1–19. <https://doi.org/10/gfc3rr>.
101. Hao, Z., R. Boel, and Z. Li. Model Based Urban Traffic Control, Part I: Local Model and Local Model Predictive Controllers. *Transportation Research Part C: Emerging Technologies*, Vol. 97, 2018, pp. 61–81. <https://doi.org/10.1016/j.trc.2018.09.026>.
102. Hao, Z., R. Boel, and Z. Li. Model Based Urban Traffic Control, Part II: Coordinated Model Predictive Controllers. *Transportation Research Part C: Emerging Technologies*, Vol. 97, 2018, pp. 23–44. <https://doi.org/10.1016/j.trc.2018.09.025>.
103. Han, Y., A. Hegyi, Y. Yuan, C. Roncoli, and S. Hoogendoorn. An Extended Linear Quadratic Model Predictive Control Approach for Multi-Destination Urban Traffic Networks. *IEEE Transactions on Intelligent Transportation Systems*, 2018, pp. 1–14. <https://doi.org/10.1109/tits.2018.2877259>.
104. Lu, K., P. Du, J. Cao, Q. Zou, T. He, and W. Huang. A Novel Traffic Signal Split Approach Based on Explicit Model Predictive Control. *Mathematics and Computers in Simulation*, Vol. 155, 2019, pp. 105–114. <https://doi.org/10.1016/j.matcom.2017.12.004>.
105. Paul, B., M. Ramteke, B. Maitra, and S. Mitra. New Approach for Calibrating Robertson's Platoon Dispersion Model. *Journal of Transportation Engineering, Part A: Systems*, Vol. 144, No. 5, 2018, p. 04018014. <https://doi.org/10.1061/jtpebs.0000141>.
106. Day, C., and D. Bullock. Calibration of Platoon Dispersion Model with High-Resolution Signal Event Data. *Transportation Research Record: Journal of the Transportation Research Board*, Vol. 2311, 2012, pp. 16–28. <https://doi.org/10.3141/2311-02>.

107. Liu, G. *Development and Evaluation of Model-Based Adaptive Signal Control for Congested Arterial Traffic*. PhD Thesis. University of Alberta, 2015.
108. Daganzo, C. F. The Cell Transmission Model: A Dynamic Representation of Highway Traffic Consistent with the Hydrodynamic Theory. *Transportation Research Part B: Methodological*, Vol. 28, No. 4, 1994, pp. 269–287. <https://doi.org/10/bkrq3z>.
109. Maerivoet, S., and B. De Moor. Traffic Flow Theory. *arXiv:physics/0507126*, 2005.
110. Casas, J. V., A. Torday, and A. Gerodimos. Combining Mesoscopic and Microscopic Simulation in an Integrated Environment as a Hybrid Solution. *IEEE Intelligent Transportation Systems Magazine*, Vol. 2, No. 3, 2010, pp. 25–33. <https://doi.org/10/cq7k3r>.
111. Burghout, W., H. N. Koutsopoulos, and I. Andréasson. Hybrid Mesoscopic–Microscopic Traffic Simulation. *Transportation Research Record*, Vol. 1934, No. 1, 2005, pp. 218–225. <https://doi.org/10/gd53hr>.
112. Winston, W. L., and J. B. Goldberg. *Operations Research: Applications and Algorithms*. Thomson/Brooks/Cole, Belmont, CA, 2004.
113. Kouvaritakis, B., and M. Cannon. *Model Predictive Control*. Springer, 2016.
114. Chen, S., and D. J. Sun. An Improved Adaptive Signal Control Method for Isolated Signalized Intersection Based on Dynamic Programming. *IEEE Intelligent Transportation Systems Magazine*, Vol. 8, No. 4, 2016, pp. 4–14. <https://doi.org/10/f892jm>.
115. Gartner, N., and R. Deshpande. Dynamic Programming Approach for Arterial Signal Optimization. *Transportation Research Record: Journal of the Transportation Research Board*, Vol. 2356, 2013, pp. 84–91. <https://doi.org/10/gcx42d>.
116. Robertson, D. I., and R. D. Bretherton. Optimum Control of an Intersection for Any Known Sequence of Vehicle Arrivals. 1974.
117. Caceres, H., M. R. Kandukuri, Q. He, and Z. Zhang. Multi-Modal Hierarchically Responsive Signal Control with a Lexicographical Dynamic Programming Approach. Presented at the Transportation Research Board 96th Annual Meeting Transportation Research Board, 2017.
118. Jamshidnejad, A., I. Papamichail, M. Papageorgiou, and B. D. Schutter. Sustainable Model-Predictive Control in Urban Traffic Networks: Efficient Solution Based on General Smoothing Methods. *IEEE Transactions on Control Systems Technology*, Vol. 26, No. 3, 2018, pp. 813–827. <https://doi.org/10.1109/tcst.2017.2699160>.
119. Han, Y. *Fast Model Predictive Control Approaches for Road Traffic Control*. PhD Thesis. Delft University of Technology, 2017.
120. Bellemans, T. *Traffic Control on Motorways*. 2003.
121. Hegyi, A., B. De Schutter, and H. Hellendoorn. Model Predictive Control for Optimal Coordination of Ramp Metering and Variable Speed Limits. *Transportation Research Part C: Emerging Technologies*, Vol. 13, No. 3, 2005, pp. 185–209. <https://doi.org/10/dwbhfb>.
122. Han, Y., M. Ramezani, A. Hegyi, Y. Yuan, and S. Hoogendoorn. Network Fundamental Diagram for Hierarchical Ramp Metering in Freeways. Presented at the Transportation Research Board 97th Annual Meeting Transportation Research Board, 2018.
123. Han, Y., A. Hegyi, Y. Yuan, S. Hoogendoorn, M. Papageorgiou, and C. Roncoli. Resolving Freeway Jam Waves by Discrete First-Order Model-Based Predictive Control of Variable Speed Limits. *Transportation Research Part C: Emerging Technologies*, Vol. 77, 2017, pp. 405–420. <https://doi.org/10.1016/j.trc.2017.02.009>.
124. Wang, X. *Proactive Integrated Control for Relieving Freeway Congestion*. 2015.
125. Wang, X., M. Seraj, Y. Bie, T. Z. Qiu, and L. Niu. Implementation of Variable Speed Limits:

- Preliminary Test on Whitemud Drive, Edmonton, Canada. *Journal of Transportation Engineering*, Vol. 142, No. 12, 2016, p. 05016007.
126. Wang, X., T. Z. Qiu, L. Niu, R. Zhang, and L. Wang. A Micro-Simulation Study on Proactive Coordinated Ramp Metering for Relieving Freeway Congestion. *Canadian Journal of Civil Engineering*, Vol. 43, No. 7, 2016, pp. 599–608. <https://doi.org/10/f8vzs5>.
  127. Wang Xu, Yin Derek, and Qiu Tony Z. Applicability Analysis of an Extended METANET Model in Traffic-State Prediction for Congested Freeway Corridors. *Journal of Transportation Engineering, Part A: Systems*, Vol. 144, No. 9, 2018, p. 04018046. <https://doi.org/10/gffb6w>.
  128. Dotoli, M., M. P. Fanti, and C. Meloni. A Signal Timing Plan Formulation for Urban Traffic Control. *Control Engineering Practice*, Vol. 14, No. 11, 2006, pp. 1297–1311. <https://doi.org/10/dftxxj>.
  129. Lin, S., B. D. Schutter, Y. Xi, and H. Hellendoorn. Fast Model Predictive Control for Urban Road Networks via MILP. *IEEE Transactions on Intelligent Transportation Systems*, Vol. 12, No. 3, 2011, pp. 846–856. <https://doi.org/10/dzbprd>.
  130. Liu, G., X. Han, P. Li, and T. Z. Qiu. Adaptive Model-Based Offset Optimization for Congested Arterial Network. Presented at the Transportation Research Board 93rd Annual Meeting, Transportation Research Board, 2014.
  131. Baldi, S., I. Michailidis, V. Ntampasi, E. Kosmatopoulos, I. Papamichail, and M. Papageorgiou. A Simulation-Based Traffic Signal Control for Congested Urban Traffic Networks. *Transportation Science*, 2017. <https://doi.org/10.1287/trsc.2017.0754>.
  132. Priemer, C., and B. Friedrich. A Decentralized Adaptive Traffic Signal Control Using V2I Communication Data. Presented at the 2009 12th International IEEE Conference on Intelligent Transportation Systems, 2009.
  133. Jiang, Y., S. Li, and D. E. Shamo. A Platoon-Based Traffic Signal Timing Algorithm for Major–Minor Intersection Types. *Transportation Research Part B: Methodological*, Vol. 40, No. 7, 2006, pp. 543–562. <https://doi.org/10/bpn9xv>.
  134. Yu, L. Calibration of Platoon Dispersion Parameters on the Basis of Link Travel Time Statistics. *Transportation Research Record: Journal of the Transportation Research Board*, Vol. 1727, 2000, pp. 89–94. <https://doi.org/10.3141/1727-11>.
  135. Head, L., D. Gettman, D. M. Bullock, and T. Urbanik. Modeling Traffic Signal Operations with Precedence Graphs. *Transportation Research Record*, Vol. 2035, No. 1, 2007, pp. 10–18. <https://doi.org/10/cf96k4>.
  136. Urbanik, T., A. Tanaka, B. Lozner, E. Lindstrom, K. Lee, S. Quayle, S. Beaird, S. Tsoi, P. Ryus, D. Gettman, S. Sunkari, K. Balke, D. Bullock, National Cooperative Highway Research Program, Transportation Research Board, and National Academies of Sciences, Engineering, and Medicine. *Signal Timing Manual - Second Edition*. Transportation Research Board, Washington, D.C., 2015.
  137. Pacheco, A., M. L. Simões, and P. Milheiro-Oliveira. Queues with Server Vacations as a Model for Pretimed Signalized Urban Traffic. *Transportation Science*, 2017. <https://doi.org/10.1287/trsc.2016.0727>.
  138. Argote-Cabañero, J., E. Christofa, and A. Skabardonis. Connected Vehicle Penetration Rate for Estimation of Arterial Measures of Effectiveness. *Transportation Research Part C: Emerging Technologies*, Vol. 60, 2015, pp. 298–312. <https://doi.org/10.1016/j.trc.2015.08.013>.

139. Tian, N., and Z. G. Zhang. *Vacation Queueing Models: Theory and Applications*. Springer Science & Business Media, 2006.
140. Cheng, C., Y. Du, L. Sun, and Y. Ji. Review on Theoretical Delay Estimation Model for Signalized Intersections. *Transport Reviews*, Vol. 36, No. 4, 2016, pp. 479–499. <https://doi.org/10.1080/01441647.2015.1091048>.
141. Xi, Y., and D. Li. *Predictive Control: Fundamentals and Developments*. John Wiley & Sons, 2019.
142. Chen, H., and F. ALLGÖWER. A Quasi-Infinite Horizon Nonlinear Model Predictive Control Scheme with Guaranteed Stability. *Automatica*, Vol. 34, No. 10, 1998, pp. 1205–1217. <https://doi.org/10/ft9286>.
143. Mayne, D. Q., J. B. Rawlings, C. V. Rao, and P. O. M. Scokaert. Constrained Model Predictive Control: Stability and Optimality. *Automatica*, Vol. 36, No. 6, 2000, pp. 789–814. <https://doi.org/10/brxgpc>.
144. Qiu, T. ACTIVE On-Road Test Bed - Centre for Smart Transportation - University of Alberta. <http://www.transportation.ualberta.ca/Research/Facilities.aspx>. Accessed Jul. 9, 2016.
145. Krajzewicz, D., J. Erdmann, M. Behrisch, and L. Bieker. Recent Development and Applications of SUMO-Simulation of Urban MObility. *International Journal On Advances in Systems and Measurements*, Vol. 5, No. 3 & 4, 2012.
146. Li, J., C. Qiu, L. Peng, and T. Z. Qiu. Signal Priority Request Delay Modeling and Mitigation for Emergency Vehicles in Connected Vehicle Environment. *Transportation Research Record*, 2018, p. 0361198118774184. <https://doi.org/10/gd3v3m>.
147. Park, H., A. Miloslavov, J. Lee, M. Veeraraghavan, B. Park, and B. Smith. Integrated Traffic-Communication Simulation Evaluation Environment for IntelliDrive Applications Using SAE J2735 Message Sets. *Transportation Research Record: Journal of the Transportation Research Board*, Vol. 2243, 2011, pp. 117–126. <https://doi.org/10.3141/2243-14>.
148. Li, J., C. Qiu, M. Seraj, L. Peng, and T. Z. Qiu. Platoon Priority Visualization Modeling and Optimization for Signal Coordination in the Connected Vehicle Environment. *Transportation Research Record*, 2019, p. 0361198119837505. <https://doi.org/10.1177/0361198119837505>.